AFFDL-TR-77-31
VOLUME II
ADA 046 179

CHARACTERIZATION OF FATIGUE CRACK GROWTH IN BONDED STRUCTURES

VOLUME II: Analysis of Cracked Bonded Structures

NORTHROP CORPORATION, AIRCRAFT DIVISION
HAWTHORNE, CALIFORNIA 90250

JUNE 1977

FINAL REPORT JULY 1975 - FEBRUARY 1977

AIR FORCE FLIGHT DYNAMICS LABORATORY
AIR FORCE WRIGHT AERONAUTICAL LABORATORIES
AIR FORCE SYSTEMS COMMAND
WRIGHT-PATTERSON AIR FORCE BASE, OHIO 45433

NOTICE

When Government drawings, specifications, or other data are used for any purpose other than in connection with a definitely related Government procurement operation, the United States Government thereby incurs no responsibility nor any obligation whatsoever; and the fact that the Government may have formulated, furnished, or in any way supplied the said drawings, specifications, or other data, is not to be regarded by implication or otherwise as in any manner licensing the holder or any other person or corporation, or conveying any rights or permission to manufacture, use, or sell any patented invention that may in any way be related thereto.

This report has been reviewed by the Office of Information (OI) and is releasable to the National Technical Information Service (NTIS). At NTIS, it will be available to the general public, including foreign nations.

This technical report has been reviewed and is approved for publication.

JOSEPH P. GALLAGHER
Project Engineer

ROBERT M. BADER, Chief
Structural Integrity Br

FOR THE COMMANDER

HOWARD L. FARMER, Col, USAF
Chief, Structural Mechanics Division

Copies of this report should not be returned unless return is required by security considerations, contractual obligations, or notice on a specific document.

AIR FORCE/56780/25 October 1977 — 500

REPORT DOCUMENTATION PAGE

READ INSTRUCTIONS BEFORE COMPLETING FORM

1. REPORT NUMBER: AFFDL-TR-77-31, Volume II
2. GOVT ACCESSION NO.:
3. RECIPIENT'S CATALOG NUMBER:

4. TITLE (and Subtitle): Characterization of Fatigue Crack Growth in Bonded Structures. Volume II, Analysis of Cracked Bonded Structures

5. TYPE OF REPORT & PERIOD COVERED: July 1975 - February 1977 Volume II final

6. PERFORMING ORG. REPORT NUMBER: NOR 77-41

7. AUTHOR(s): M. M. Ratwani

8. CONTRACT OR GRANT NUMBER(s): F33615-75-C-3127

9. PERFORMING ORGANIZATION NAME AND ADDRESS
Northrop Corporation
Aircraft Division
3901 West Broadway
Hawthorne, CA 90250

10. PROGRAM ELEMENT, PROJECT, TASK AREA & WORK UNIT NUMBERS: 486U0210

11. CONTROLLING OFFICE NAME AND ADDRESS
Air Force Flight Dynamics Laboratory
Wright Patterson Air Force Base
Ohio 45433

12. REPORT DATE: June 1977

13. NUMBER OF PAGES: 103, Appendices - 44

14. MONITORING AGENCY NAME & ADDRESS (if different from Controlling Office):

15. SECURITY CLASS. (of this report): Unclassified

15a. DECLASSIFICATION/DOWNGRADING SCHEDULE:

16. DISTRIBUTION STATEMENT (of this Report)

Approved for public release, distribution unlimited.

17. DISTRIBUTION STATEMENT (of the abstract entered in Block 20, if different from Report)

18. SUPPLEMENTARY NOTES

19. KEY WORDS (Continue on reverse side if necessary and identify by block number)

Adhesive Bonding
Fracture Mechanics Analysis
Stress Intensity Factors
Finite Element Modeling
Cracked Element
Integral Equations
Complex Variables
Logarithmic Singularities
Numerical Analysis
Debond in Adhesive
Cracking of Sound a Layer
Weldbonding

20. ABSTRACT (Continue on reverse side if necessary and identify by block number)

Analytical techniques to analyze cracked, adhesively bonded, weldbonded and brazed multilayered structures have been developed. Two different methods of analyses, namely finite element and mathematical are outlined. In the finite element method, each layer is modeled as two dimensional structure and the adhesive is represented by shear elements.

In the mathematical method, a complex variable approach is used to reduce the problem to solution of integral equations which have logarithmic singularities in kernels. The integral equations are solved numerically. The stress intensity factors obtained by the finite element method and the mathematical method for the same problem are compared.

A new method of correction for the influence of bending, based on load transfer to cracked layer, is developed. A criterion for the cracking of the sound layer based on critical load transfer to sound layer is introduced.

The application of the analyses to multilayered adhesively bonded and various other types of bonded structures is shown.

The computer programs to solve the problems of a cracked plate with a partially debonded stringer, a cracked plate with two partially debonded stringers and two layer bonded structure with a debonding crack, are outlined. These programs compute stress intensity factors ahead of the crack tips, and shear stresses in the adhesive.

FOREWORD

This report was prepared by Northrop Corporation, Aircraft Division, Hawthorne, California, under Air Force Contract F33615-75-C-3127. The project was initiated under Project Number 486U, "Advanced Metallic Structures," Advanced Development Program. The work reported herein was administered under the direction of the Air Force Flight Dynamics Laboratory, Air Force Systems Command, Wright-Patterson Air Force Base, Ohio, by Dr. Joseph P. Gallagher (FBEC), Project Engineer.

The report is Volume II of two volumes covering the research conducted between July 1975 and February 1977, and was submitted by the author, Dr. M.M. Ratwani, March 1977.

The author wishes to acknowledge the constructive discussion regarding the development of the mathematical methods, with Professor Fazil Erdogán of Lehigh University, Bethlehem, Pennsylvania. The secretarial assistance of P.E. Barnes is also acknowledged. The aforementioned program was under the technical supervision of L. Jeans, Manager of the Structural Life Assurance Research Department.

CONTENTS

CONTENTS (continued)

ILLUSTRATIONS

ILLUSTRATIONS (continued)

ILLUSTRATIONS (continued)

TABLES

SECTION 1

INTRODUCTION

This report describes the research conducted on the characterization of fatigue crack growth in bonded structures. In this volume, analytical techniques required to predict fatigue crack growth in bonded structures are discussed. The specific problem is that of a two-ply, bonded, metallic laminate with a through-crack in one ply. The analytical techniques developed are applicable to adhesively bonded, weldbonded and brazed structures.

The first step in crack growth analysis is to obtain the stress intensity factors for the structure under consideration. Two methods for obtaining stress intensity factors for cracked bodies, namely, the finite element method and the mathematical method, are discussed in Section 2. A two-dimensional finite element model, in which plates are represented by membrane elements and the adhesive by shear elements, is developed. The finite element analysis is carried out with NASTRAN. In the mathematical method discussed in this volume, the problem of obtaining stress intensity factors for a cracked body is reduced to the solution of integral equations, using complex variables, and these integral equations are then solved numerically. The application of each method to a variety of structural problems is shown. The results obtained from each method for the same problem are compared.

In Section 3, the application of the analyses to multilayered, adhesively bonded, weldbonded, and brazed structures is shown.

In Section 4, the influence of bending caused by the presence of a crack in only one layer of a multilayered structure is discussed. A new method to correct the stress intensity factors for the influence of bending is described.

In Section 5, a criterion for the cracking of a sound layer bonded to a cracked layer is developed. The criterion is based on the load transferred to the sound layer from the cracked layer.

The propagation of a crack in an adhesively bonded structure is accompanied by the propagation of debond in the adhesive. In Section 6, a criterion for the propagation of debond is developed.

The guidelines for the application of analysis to bonded structures are outlined in Section 7.

The computer programs developed in this research program are outlined in the appendices. The computer programs developed for the mathematical method of analysis for three classes of problems are as follows:

1. A cracked sheet stiffened by a partially debonded stringer at an arbitrary location.
2. A cracked sheet with two partially debonded stringers, symmetrically located about the centerline.
3. A two-layer, adhesively bonded structure with a debonding crack in one layer.

These computer programs require the elastic properties of the adhesive, cracked layer, and sound layer as inputs and have provisions for accounting for the debond in the adhesive. The computer run times for these programs are very short compared to those for finite element analyses, hence the programs are well suited for parametric studies.

SECTION 2

ANALYSIS OF CRACKED ADHESIVELY BONDED STRUCTURES

The analysis of crack problems in adhesively bonded structures has attracted attention in recent years due to the increased application of bonding in primary aerospace structures. However, very little analytical work has been done in this field due to limited availability of analytical tools to handle the complicated problems. While one of the most common tools used for analysis of complex structures is the method of finite elements, an adhesively bonded structure is inherently three-dimensional. A three-dimensional finite element analysis of cracks in adhesively bonded structures does not seem to be feasible at this time, mainly because of a lack of suitable three-dimensional cracked elements to analyze such problems. However, a modified two-dimensional finite element analysis was used in Reference 1 to analyze a cracked sheet with a bonded stringer. A good correlation was obtained between analysis and experiments, which suggested that a modified two-dimensional finite element model can be used for analysis.

Finite element methods are very versatile tools for analyses. Various stiffener geometries, finite width effects, influences of holes, etc., can be studied by this method. The major disadvantages are: considerable time is required to model the structure, computer run times are often long, and the solutions are not closed form, thus cannot be easily generalized. If finite element techniques are used to do parametric studies of any nature, the cost would be prohibitive, hence this technique is not well suited for any parametric stress intensity factor studies.

The use of mathematical methods to study crack problems in adhesively bonded structures has been reported by several researchers. References 2 through 4 have used a complex variable formulation to reduce the problem to the solution of a set of integral equations that are solved numerically. The mathematical techniques are applicable to bonded plates that have infinite width. For bonded stringer cases, certain simplified assumptions regarding

stiffener areas are made. The advantages of the mathematical method are that the solutions are obtained by using numerical analysis, which generally requires short computer run times, and parametric variations are permitted, as well as generalized solutions. The computer programs developed in this study for mathematical analysis have the elastic properties of adhesives, adherends, and debond sizes, etc., as inputs, hence parametric studies can be easily made at a greatly reduced cost. The main disadvantages are that certain simplifying assumptions have to be made to account for stiffener area or finite boundaries, hence the results obtained must be carefully reviewed for such cases.

The principles involved in the two methods of analysis and their application, as well as the assumptions made, are discussed in the following paragraphs.

2.1 FINITE ELEMENT METHOD OF ANALYSIS

The presence of singular stresses ahead of a crack tip require special care in finite element analysis. Special elements, known as cracked elements, have been developed to account for the singularity ahead of a crack tip in a two-dimensional finite element analysis. For three-dimensional crack problems, the cracked elements are still in the development stage. The analysis of adhesively bonded structures with a three-dimensional cracked element presents a very complicated problem that appears to be beyond the scope of the present state of knowledge. Although increasing amounts of attention are being given to this problem (Reference 5). Hence, a modified finite element analysis using the available two-dimensional cracked element has been adopted in the present program. This method of modeling, along with corrections for bending (discussed in Section 4) has shown a very good correlation between analytical and experimental results.

The method of finite element analysis uses the available two-dimensional cracked element ahead of the crack tips in the cracked layer. The cracked and sound layers are modeled as two-dimensional structures. The adhesive layer is treated as a shear spring rather than as an elastic continuum. This method of treating adhesives has been used before in the analysis of bonded joints and cracked, adhesively bonded structures (References 1-4, 6). In the finite element analysis, the continuous shear spring is represented by shear elements (Reference 1). With these assumptions, it is possible to model the structure as

two-dimensional. Consider the adhesively bonded structure shown in Figure 1 where a through-crack exists in the plate, and a debond exists in the adhesive around the crack in Material 1, however there is no crack in Material 2. Although the debond may have any shape, it is assumed to be elliptical here, for convenience.

The bonded plates of both materials are modeled as rectangular or triangular elements as shown in Figure 2. The enlarged portion of Figure 3 identifies the location of a cracked element provided ahead of the crack tip in the cracked plate. The x and y coordinates of the grid points in the bonded regions of the two plates are kept the same, i.e., the finite element model in the bonded regions of the plates is identical. In the unbonded region, the finite element model of the two plates need not be the same since no connection is provided between the plates in the unbonded region. Around the periphery of the debond in the bonded region, the adhesive is subjected to high shear stresses, hence a closely spaced mesh is provided to reduce the length of the shear elements shown in Figure 3. The closely spaced shear elements will give an accurate determination of shear stresses and load transfer to the uncracked layer. Thus providing for more accurately computed stress intensity factors.

In the bonded region, the grid points of the two materials are connected by the shear elements. These shear elements have the same material properties as the adhesive. The thickness of the shear elements perpendicular to the cracked-uncracked plies is taken as the thickness of the adhesive. The shear elements have rectangular prismatic shape. If there are any partially bonded areas around the crack, they can be incorporated in the model by changing the properties of the shear elements in the partially bonded areas.

In this finite element analysis, the cracked element developed by Professor Pian, of MIT (Reference 7), has been used. This cracked element has been incorporated in NASTRAN by Northrop. Figure 4 shows the NASTRAN plot of a two-ply, adhesively bonded panel with a crack in one ply.

The adhesively bonded structures having different widths (e.g., a plate with an adhesively bonded stringer) can be modeled in the manner described above. In this case, only the bonded region of the two layers will have a similar grid point and finite element model. The NASTRAN plot of a cracked plate with an adhesively bonded stringer is shown in Figure 5.

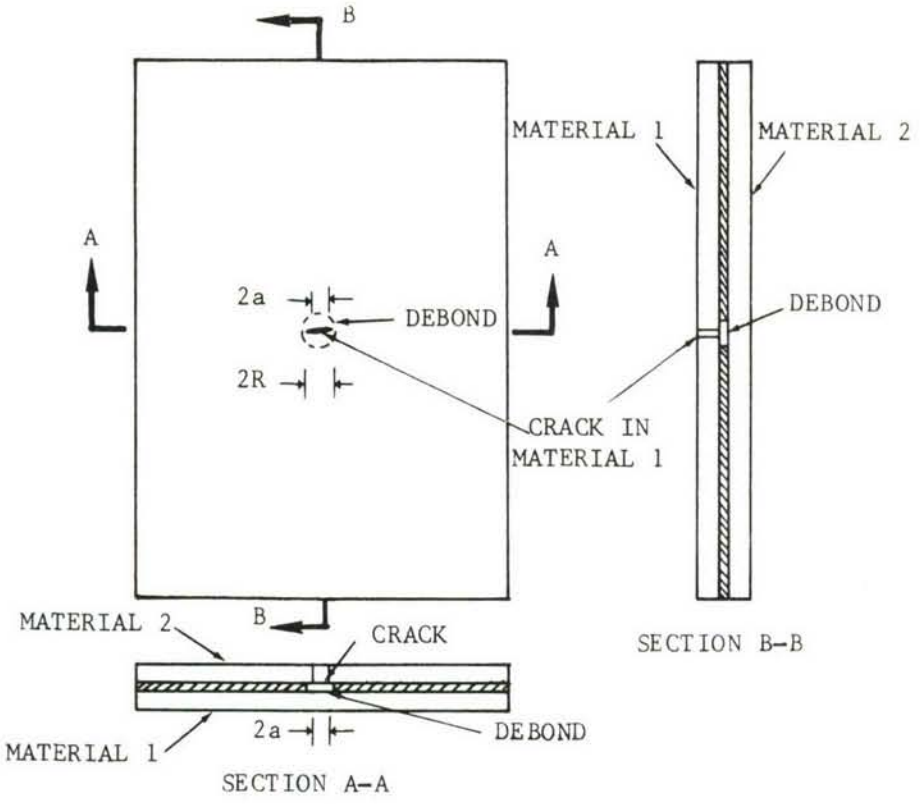

Figure 1. Adhesively Bonded Structure with a Debond and Crack

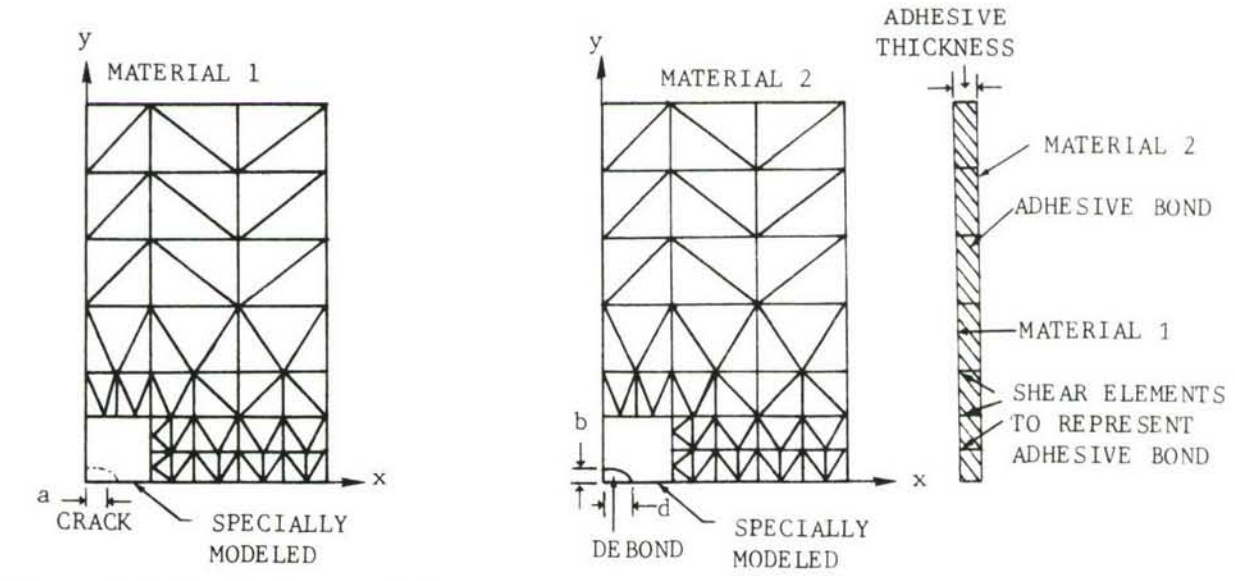

Figure 2. Finite Element Model of an Adhesively Bonded Structure (only one-quarter of plates shown)

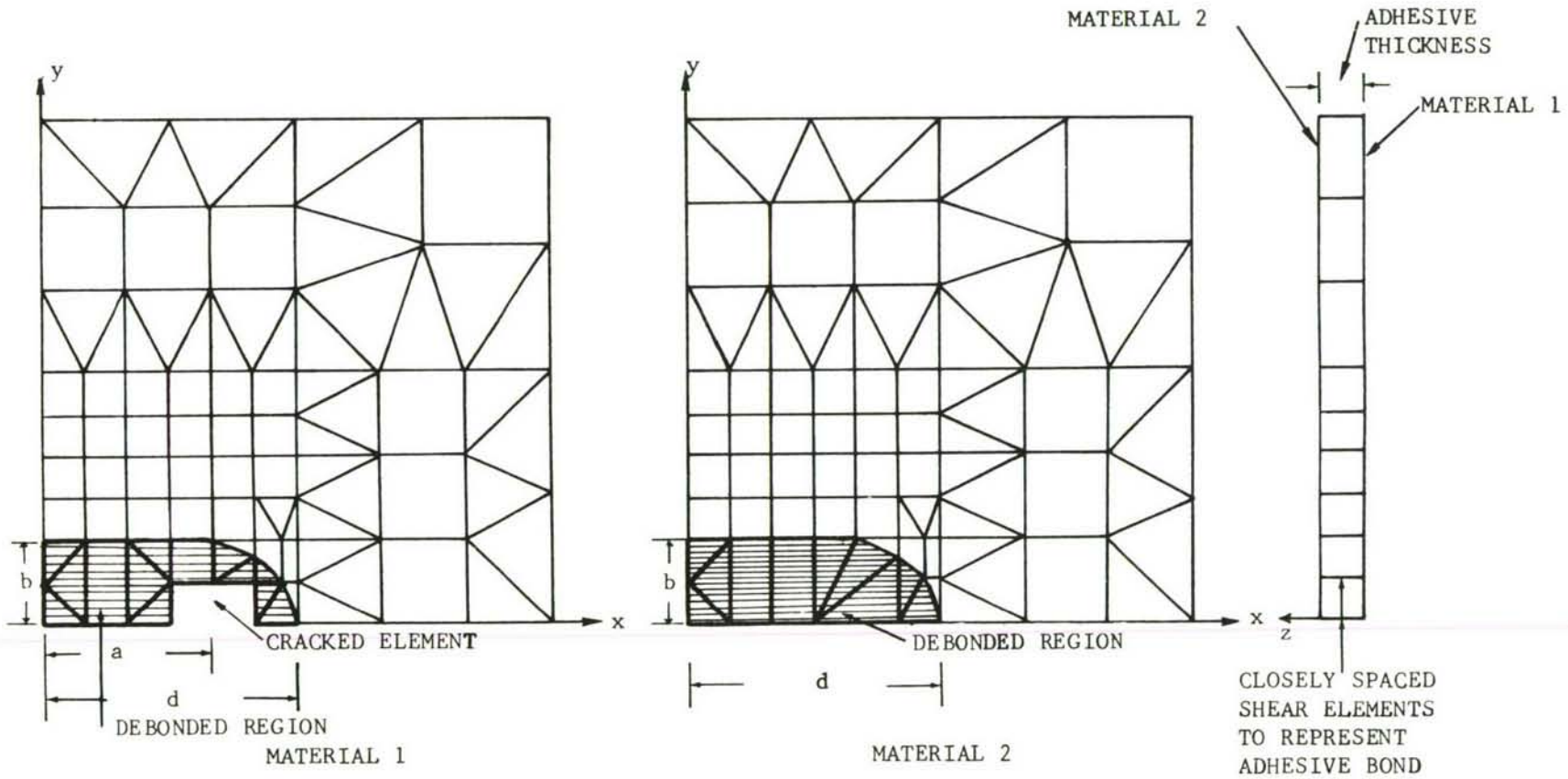

Figure 3. Cracked Element Around Crack Tip and Fine Mesh Around Debond in Finite Element Model

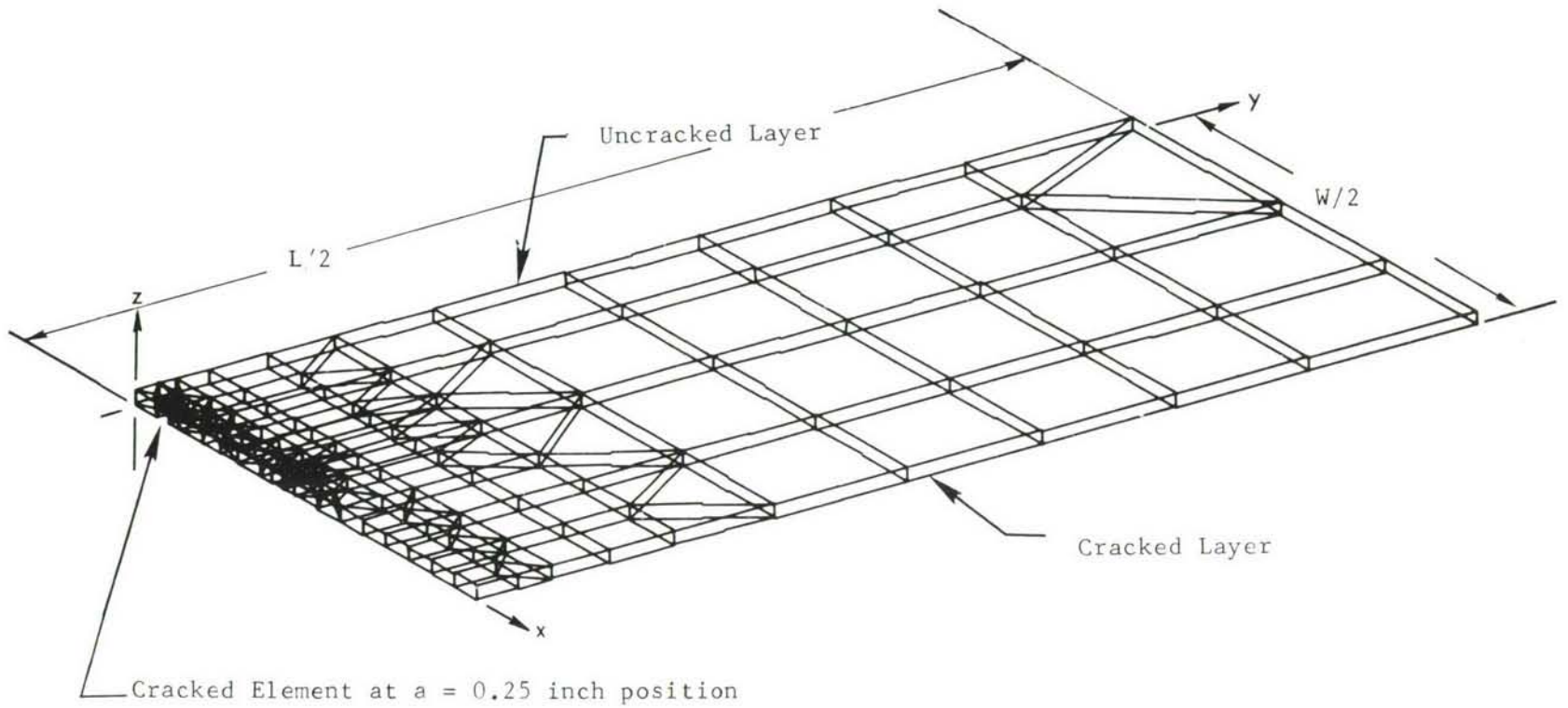

Figure 4. NASTRAN Finite Element Model of Finite Width, Center Crack Tension Bonded Panel (one-quarter of the structure shown)

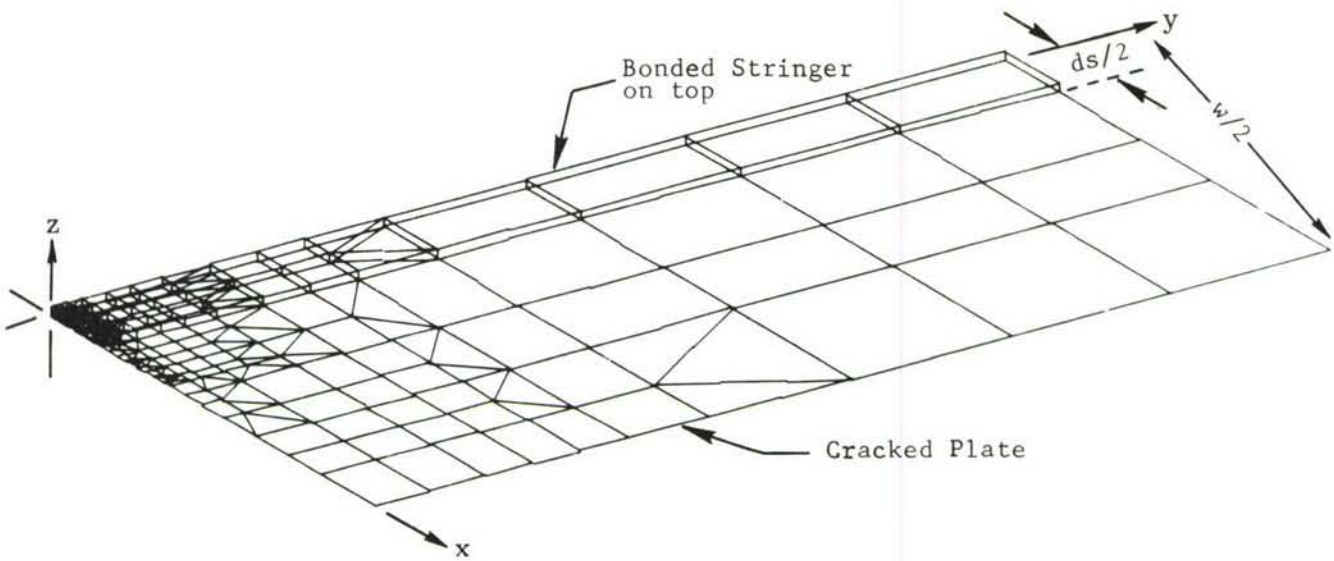

Figure 5. NASTRAN Finite Element Model of a Cracked Plate with a Bonded Stringer Geometry (one-quarter of the structure shown)

This finite element analysis can also be used for bonded structures with more than one cracked layer. In such a structure, cracked elements are provided ahead of each crack tip, in each cracked layer. The stress intensity factors for each crack are computed from displacements and stiffness matrix of each cracked element.

2.2 MATHEMATICAL METHODS OF ANALYSIS

Mathematical methods of analysis are very useful in analyzing crack problems in bonded structures. This is particularly so where boundaries are regular and the crack lengths are small compared to the dimensions of the structure. However, certain simplifying assumptions have to be made in the mathematical modeling of bonded structures (Section 2, Volume I).

A complex variable approach to reduce the problem of cracked structures to the solution of integral equations is considered convenient, and is used in these investigations. The following paragraphs describe the

mathematical formulation of three classes of structural problems: (1) a cracked plate with a partially debonded stringer, (2) a cracked plate stiffened by two partially debonded stringers and symmetrically located about the centerline, and (3) a two-layer, adhesively bonded structure with a debonding crack in one layer. The plate is assumed to have a through-the-thickness flaw and a debonding crack in the adhesive around the main crack, which propagates under fatigue loads. The debond in the adhesive also propagates as the crack in the plate propagates.

2.2.1 A Cracked Plate Stiffened by a Partially Debonded Stringer at an Arbitrary Location

The cracked plate with an adhesively bonded stringer shown in Figure 6, can be represented, due to superposition techniques, by the two problems of Figures 7a and 7b. The structure in Figure 7a has no crack, hence there are no stress singularities or shear stress in the adhesive, therefore the problem of determining stress intensity factors and shear stresses in the structure of Figure 6, reduces to analyzing the perturbation problem of Figure 7b. The solution of the problem consists of the following three steps:

1. Formulation of the problem

   The perturbation problem is formulated under the assumption of generalized plane stress. The thickness of the adhesive is assumed to be small compared to the thickness of the plate, hence the adhesive is treated as a shear spring (Reference 5). The shear stresses transmitted through the adhesive are treated as body forces in the plate analysis. The stringer transmits body forces to the crack plate, as shown in the free body diagram of Figure 8. It is further assumed that the stringer area is concentrated on one point at the centerline of the stringer. Therefore, the body forces transmitted will be concentrated along one line. Along the centerline of the stringer, the displacement continuity between sheet and stringer may be written as

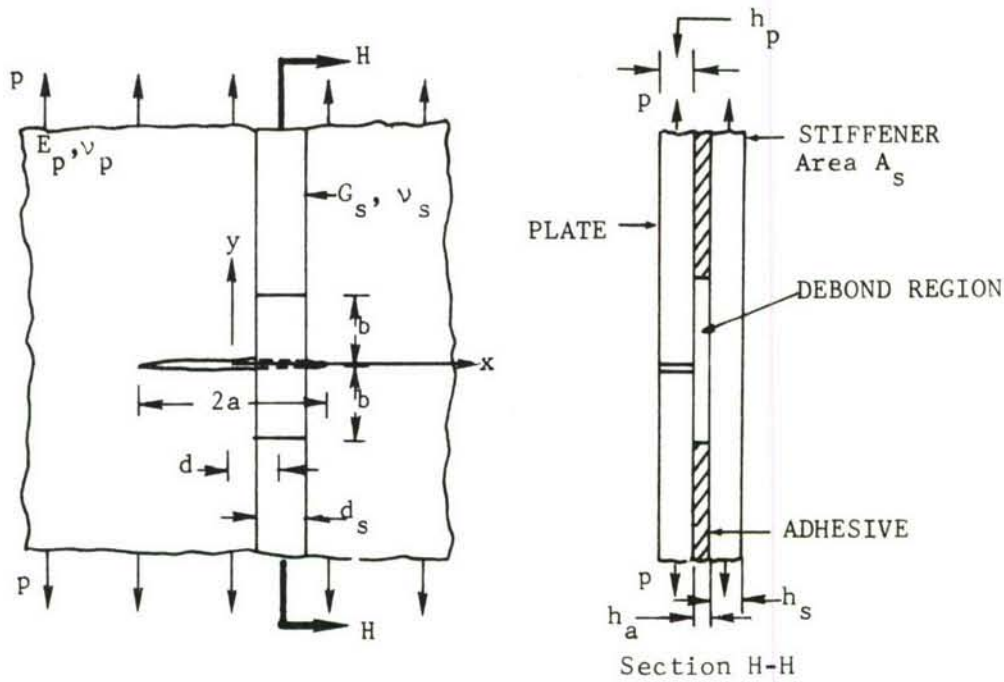

Figure 6. Cracked Plate with a Bonded Stringer

$$v_p(y) - v_s(y) = \frac{h_a}{d_s \mu_a} P(y) \quad , \qquad y \text{ on } L \tag{1}$$

where L denotes the line $x = d$, $b \le y \le \infty$, the distance between the center of the crack and the center of the stringer from b (the debond size) to ∞.

The terms $v_p(y)$ and $v_s(y)$, are displacements in the plate and stringer, respectively. μ_a is the shear modulus of the adhesive, d_s is the width of the stringer, and $P(y)$ is the contact shear force per unit length of the stringer at the y location. The displacements of the plate v_p and the stringer v_s can be written as

$$v_p(y) = p\, k_o(y) + \int_L k_p(y,y_o)\, P(y_o)\, dy_o$$

$$v_s(y) = \int_L k_s(y,y_o)\, P(y_o)\, dy_o \quad , \qquad y \text{ on } L \tag{2}$$

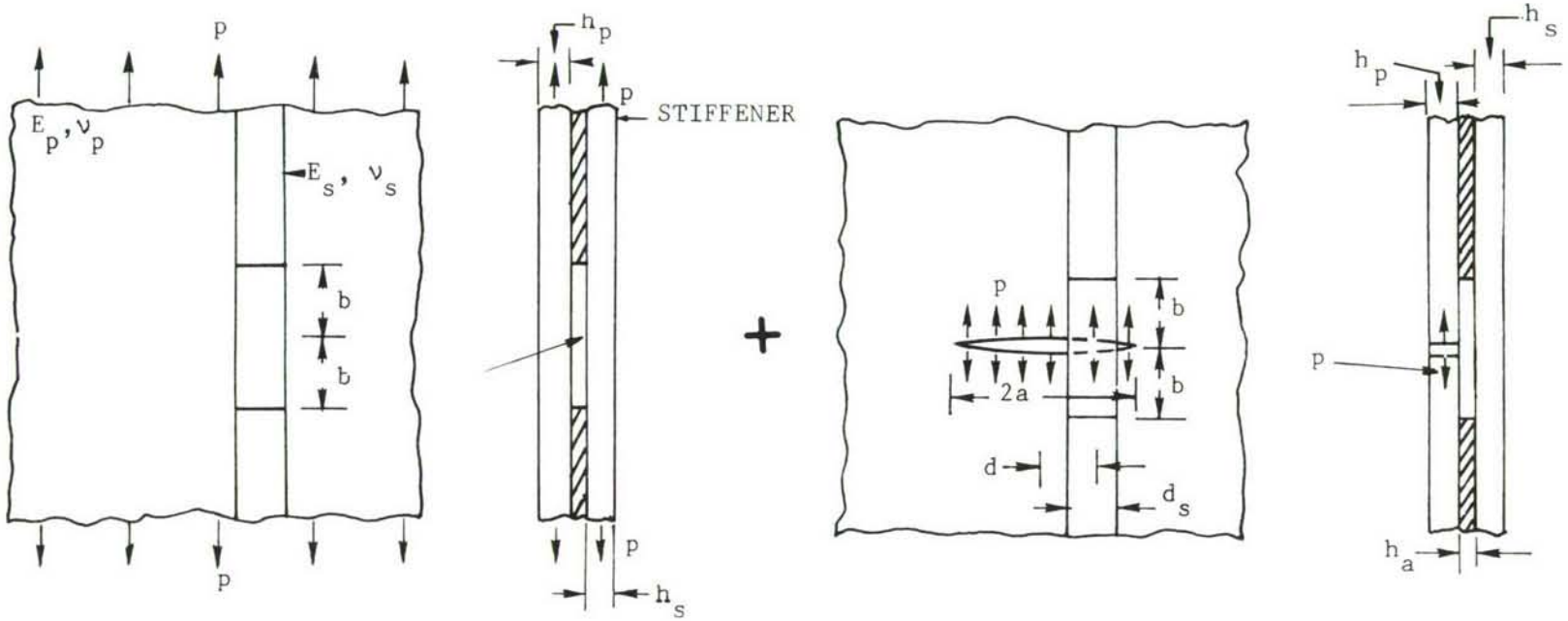

(a) Bonded plate with no crack

(b) Perturbation problem

Figure 7. Superposition Technique for a Cracked Plate with an Adhesively Bonded Stringer

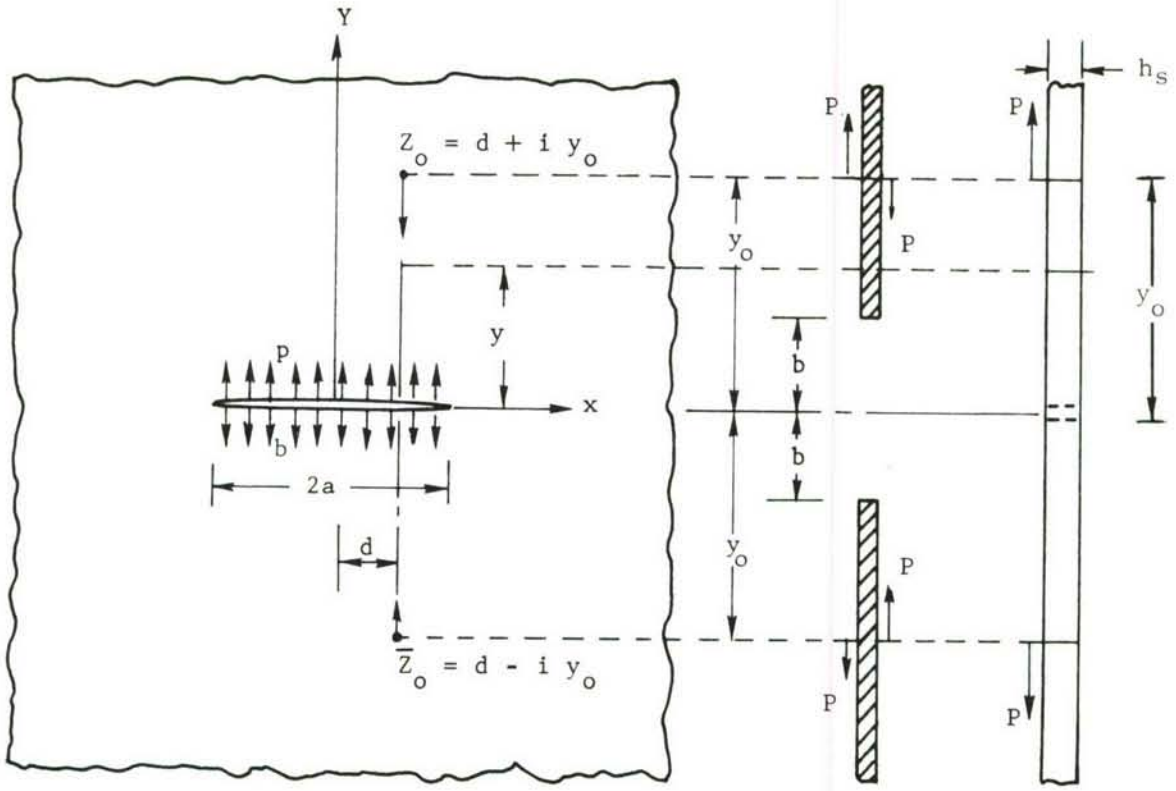

Figure 8. Free-Body Diagrams of the Plate, Adhesive, and Stringer

where $k_o(y)$ is the solution of the plate with a crack subjected to uniform unit pressure, $k_p(y,y_o)$ is Green's function for the plate with a stress-free crack, subjected to concentrated forces as shown in Figure 8, and $k_s(y,y_o)$ is the displacement at the y location (at x = d) due to the forces (P = 1) acting at y_o (Reference 4) locations.

For the stringer it is found that

$$k_s(y,y_o) = \begin{cases} \dfrac{y}{A_s E_s}, & y<y_o \\ \dfrac{y_o}{A_s E_s}, & y>y_o \end{cases}$$

$$k_s(0,y_o) = 0 \qquad (3)$$

where E_s and A_s are the elastic modulus and the cross-sectional area of the stringer, respectively.

In Equation (1), $k_o(y)$ is given by (Reference 2)

$$k_o(y) = \frac{1}{4\mu_p}\left[(\kappa + 1)\ \mathrm{Im}\sqrt{z^2 - a^2} + (1 - \kappa)y - 2y\ \mathrm{Re}\frac{z}{\sqrt{z^2 - a^2}}\right]$$

$$k_o(o) = 0 \quad , \quad |x| > a \tag{4}$$

where $\kappa = (3 - \nu_p)/(1 + \nu_p)$, μ_p and ν_p are the elastic constants for the plate, a is the half-crack length, d is the distance from the centerline stringer to the midpoint of the crack and

$$z = d + iy \quad , \quad y \text{ on } L \tag{5}$$

To obtain the kernel $k_p(y, y_o)$, the solution given in Reference 8 for a plate with a stress-free crack and subjected to concentrated forces X + iY acting a z_o is used. For a cracked plate subjected to body forces, the displacements at z are given by

$$2\mu_p(u_p + iv_p) = -\kappa S[\log(z - z_o) + \log(\bar{z} - \bar{z}_o)] + \kappa\phi_o(z) - \phi_o(\bar{z}) + \left(\frac{z - z_o}{\bar{z} - \bar{z}_o} - 1\right)\bar{S} - (z - \bar{z})\,\overline{\Phi_o(z)} + \text{rigid body displacement} \tag{6}$$

where

$$2\phi_0(z) = S\,[\log(z-z_0) - I(z_0)\,I_1(z,z_0) - I_2(z,z_0) - \kappa\log(z-\bar{z}_0) + \kappa\,I_2(z,\bar{z}_0) + \kappa\,I(\bar{z}_0)\,I_1(z,\bar{z}_0)] + (\bar{z}_0-z_0)\,\bar{S}\,[\frac{1}{z-\bar{z}_0} + I(\bar{z}_0)\,I_3(z,\bar{z}_0) + I_4(z,\bar{z}_0) + J(\bar{z}_0)\,I_1(z,\bar{z}_0)] \quad (7)$$

$$\Phi_0(z) = \frac{1}{2\sqrt{z^2-a^2}}\{\frac{S}{z-z_0}[I(z) - I(z_0)] - \frac{\kappa S}{z-\bar{z}_0}[I(z) - I(\bar{z}_0)] + (z_0-\bar{z}_0)\,\bar{S}\,[\frac{I(z) - I(\bar{z}_0)}{(z-\bar{z}_0)^2} - \frac{J(\bar{z}_0)}{z-\bar{z}_0}]\} \quad (8)$$

and

$$I_1(z,z_0) = -\frac{1}{\sqrt{z_0^2-a^2}}\log\left[\frac{z_0z - a^2 + \sqrt{z_0^2 - a^2}\,\sqrt{z^2 - a^2}}{a(z-z_0)}\right]$$

$$I_2(z,z_0) = \log\left[\frac{z}{a} + \sqrt{(z/a)^2 - 1}\right] + z_0\,I_1(z,z_0)$$

$$I_3(z,z_0) = \frac{1}{a^2-z_0^2}\left[\frac{\sqrt{z^2-a^2}}{z-z_0} + z_0\,I_1(z,z_0)\right]$$

$$I_4(z,z_0) = I_1(z,z_0) + z_0\,I_3(z,z_0) \quad (9)$$

$$I(z) = \sqrt{z^2-a^2} - z$$

$$J(z) = \frac{z}{\sqrt{z^2-a^2}} - 1$$

$$z = x + iy$$

$$z_o = x_o + iy_o$$

$$S = \frac{X + iY}{2\pi h_p(1+\kappa)} \qquad (10)$$

Combining Equations (6) through (9), the displacements u_p and v_p can be written as

$$2\mu_p(u_p+iv_p) = S \{- \kappa[\log(z-z_o) + \log(\bar{z}-\bar{z}_o)]$$

$$+ \frac{\kappa}{2} [\theta_1(z,z_o) + \theta_1(\bar{z},\bar{z}_o)] - \frac{1}{2} [\theta_1(\bar{z},z_o) + \kappa^2 \theta_1(z,\bar{z}_o)]$$

$$+ (\frac{\kappa-1}{2})[\kappa \theta_2(z) - \theta_2(\bar{z})] + (\frac{z_o-\bar{z}_o}{\bar{z}-z_o}) \theta_5(z,z_o)\}$$

$$+ \bar{S} [(\frac{z-z_o}{\bar{z}-\bar{z}_o}) - 1 + \kappa \theta_3(z,z_o) - \theta_3(\bar{z},z_o) - \theta_4(z,z_o)$$

$$+ \kappa \theta_4(z,\bar{z}_o)] + \text{rigid body displ.} \qquad (11)$$

where

$$\theta_1(z,z_o) = \log[zz_o - a^2 + \sqrt{z_o^2-a^2}\,\sqrt{z^2-a^2}\,]$$

$$\theta_2(z) = \log[z + \sqrt{z^2-a^2}\,]$$

$$\theta_3(z,z_o) = \frac{1}{2}\left(\frac{\bar{z}_o - z_o}{z-\bar{z}_o}\right)\left[1 + \frac{\sqrt{z^2-a^2}\,\sqrt{\bar{z}_o^2-a^2}}{a^2-\bar{z}_o^2}\right]$$

$$\theta_4(z,z_o) = \frac{1}{2}\left(\frac{z-\bar{z}}{\bar{z}-\bar{z}_o}\right)\left[\frac{I(\bar{z}) - I(\bar{z}_o)}{\sqrt{\bar{z}^2-a^2}}\right]$$

$$\theta_5(z,z_o) = \theta_4(z,\bar{z}_o) - \frac{1}{2}\frac{(z-\bar{z})}{\sqrt{\bar{z}^2-a^2}}\,J(z_o) \qquad (12)$$

Putting Y = 1 at $z_o = d + iy_o$ and Y = -1 at $\bar{z}_o = d - iy_o$ ($X \equiv 0$), and taking the imaginary part of the final expression to obtain $k_p(y, y_o)$ which relates a unit load (Y) located at a_o to the y direction displacement (v)

$$k_p(y,y_o) = \frac{1}{4\pi\mu_p h_p(1+\kappa)}\Big[\kappa[\log(z-z_o) + \log(\bar{z}-\bar{z}_o)]$$

$$- \kappa[\log(z-\bar{z}_o) + \log(\bar{z}-z_o)]$$

$$- \mathrm{Re}\{(\tfrac{1+\kappa}{2})[\theta_1(\bar{z},\bar{z}_o) - \theta_1(\bar{z},z_o) + \kappa\theta_1(z,z_o) - \kappa\theta_1(z,\bar{z}_o)]$$

$$+ (1+\kappa)[\theta_4(z,z_o) - \theta_4(z,\bar{z}_o)] + \kappa[\theta_3(z,\bar{z}_o) - \theta_3(z,z_o)]$$

$$+ \theta_3(\bar{z},z_o) - \theta_3(\bar{z},\bar{z}_o) + \left(\frac{z_o-\bar{z}_o}{\bar{z}-z_o}\right)\theta_5(z,z_o)$$

$$- \left(\frac{\bar{z}_o-z_o}{\bar{z}-\bar{z}_o}\right)\theta_5(z,\bar{z}_o)\}\Big] \qquad (13)$$

Thus, from Equations (1) and (2), we obtain the integral equation

$$P(y) + \int_L k(y,y_o)\, P(y_o)\, dy_o = \frac{d_s \mu_a}{h_a}\, p\, k_o(y) , \quad y \text{ on } L \tag{14}$$

where

$$k(y,y_o) = \frac{d_s \mu_a}{h_a} [k_s(y,y_o) - k_p(y,y_o)] \tag{15}$$

The kernel $k(y,y_o)$ has only logarithmic singularities and is integrable on L, Equation (14) can be treated as a Fredholm equation of the second kind.

2. Stress Intensity Factors

The stress intensity factor for the normal stress σ_y is defined as

$$k = \lim_{x \to a} [\sqrt{2(x-a)}]\, \sigma_y(x,0) \tag{16}$$

and obtained as follows (Reference 2)

$$\frac{k}{\sqrt{a}} = p + \frac{2}{a_o} \int_L \alpha(y_o')\, P(y_o)\, dy_o \tag{17}$$

where

$$\alpha(y_o) = \frac{1}{2\pi h_p (1+\kappa)}\, \mathrm{Im}\left\{ \left(\frac{\bar{z}_o - z_o}{a_o - z_o} \right) J(z_o) - \left(\frac{a_o + I(z_o)}{a_o - z_o} \right) \left[1 - \kappa + \left(\frac{\bar{z}_o - z_o}{a_o - z_o} \right) \right] \right\} \tag{18}$$

and

$$a_o = \begin{cases} a & \text{for right tip} \\ -a & \text{for left tip} \end{cases}$$

$$z_o = d + iy_o \tag{19}$$

3. Numerical Solution of Integral Equations

The Fredholm equation given in Equation (14) can be solved numerically by reducing it to a system of algebraic equations. A simple way of doing this is to replace the integral by summation, and use collocation to obtain an n x n system of equations. Hence,

$$P(y_i) + \sum_{j=1}^{N} k(y_i, y_j)\, P(y_j)\, \Delta y_j = \frac{d_s \mu_a}{h_a}\, q\, k_o(y_i), \qquad i = 1, \ldots, N \tag{20}$$

which approximately gives $P(y_j)$, $j = 1,2, \ldots, N$. Similarly, for the stress intensity factor, Equation (17) can be written as

$$\frac{k}{\sqrt{a}} = q + \frac{2}{a_o} \sum_{j=1}^{N} \alpha(y_j)\, P(y_j)\, \Delta y_j \tag{21}$$

The kernels in the integral equation, (14), have logarithmic singularities, hence the singular part of the kernel $k(y_i, y_j)$ in Equation (20) is evaluated separately as an integral along the segment Δy_i. The number of collocation points N, are chosen in such a way than an increase in N does not affect the results. The computer program for the solution of this problem is described in Appendix A.

2.2.2 A Cracked Plate Stiffened by Two Partially Debonded Stringers, Symmetrically Located About the Centerline

A cracked plate with two symmetrically located, partially debonded stringers, is shown in Figure 9a. The actual problem of determining stress intensity factors and shear stresses in the adhesive for a plate uniformly loaded far from the crack, reduces to the perturbation problem shown in Figure 9b, similar to the single-stiffener problem discussed in Paragraph 2.2.1. The free body diagram with the body forces acting on the plate is shown in Figure 10. The body forces transferred to the plate are symmetrically located as shown. Due to symmetry, the problem may be formulated for the unknown shear stresses in one stringer only.

The displacement continuity between sheet and stringer is given by Equation (1). The displacement in the stringer $v_s(y)$ is given by the second of Equations (2) and the displacement in the plate $v_p(y)$, by

$$v_p(y) = pk_o(y) + \int_{L_1} k_p(y,y_o)\, P(y_o)\, dy_o \tag{22}$$

where L_1 denotes the line $X = d$, $b \leq y < \infty$ and $x = -d$, $b \leq y < \infty$. Using the displacements given by Equation (11), the integral equation for this problem can be written as

$$P(y) + \frac{d_s \mu_a}{h_a} \int_L k_s(y,y_o)\, P(y_o) dy_o - \int_{L_1} k_p(y,y_o) P(y_o) dy_o = \frac{d_s \mu_a}{h_a}\, p\, k_o(y) \tag{23}$$

where L denotes the line $x = d$, $b \leq y < \infty$

The kernels $k_p(y,yo)$ have logarithmic singularities and are integrable on L_1. Equation (23) can be treated as the Fredholm equation of the second kind. The stress intensity factors in this case at both crack tips are equal and are given by

$$\frac{k}{\sqrt{a}} = p + \frac{2}{a} \int_L \alpha(y_o) P(y_o) dy_o \tag{24}$$

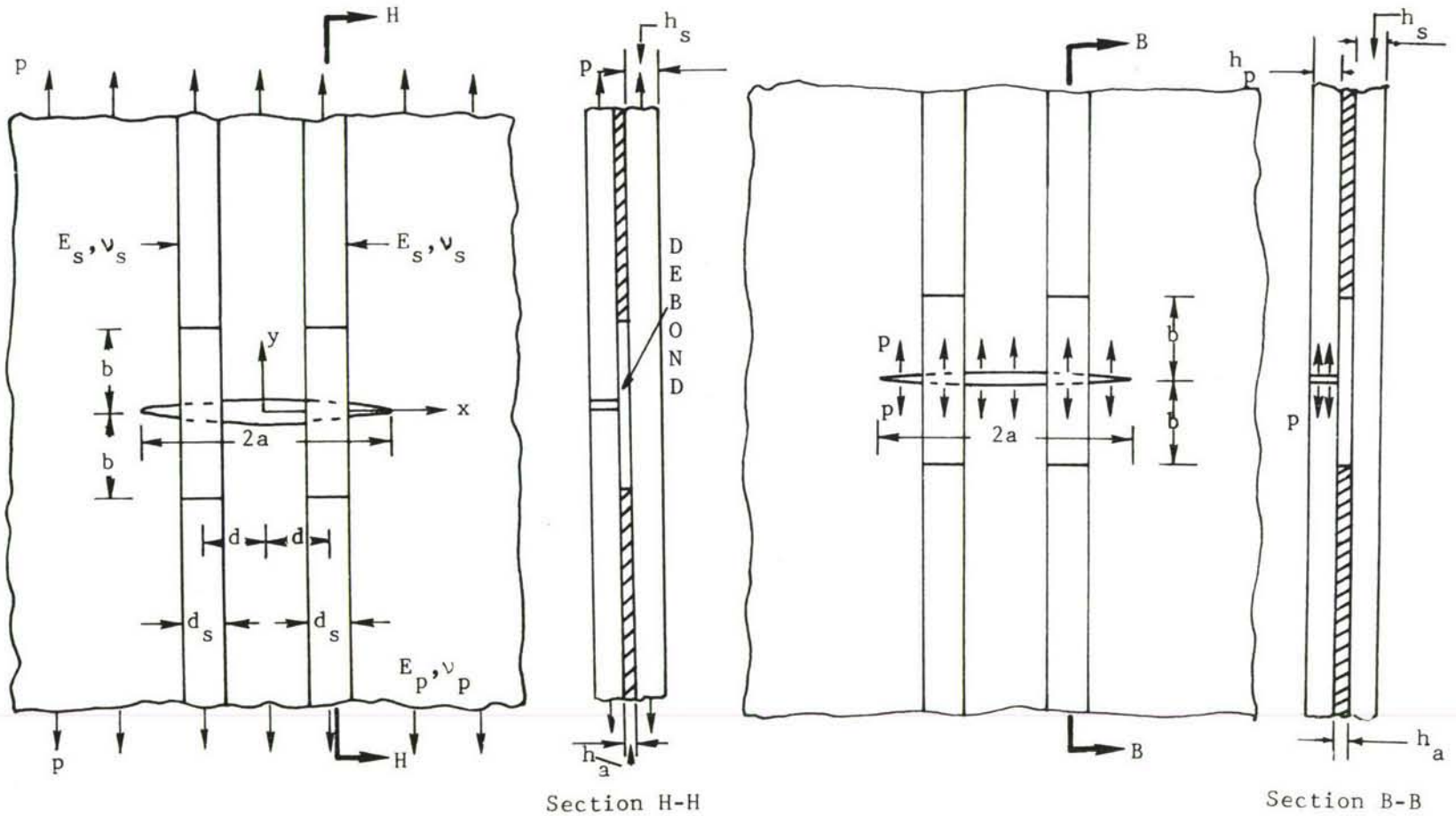

(a) Cracked plate stiffened by two bonded stringers

(b) Perturbation problem of a cracked plate stiffened by two bonded stringers

Figure 9. Cracked Plate with Two Adhesively Bonded Stringers

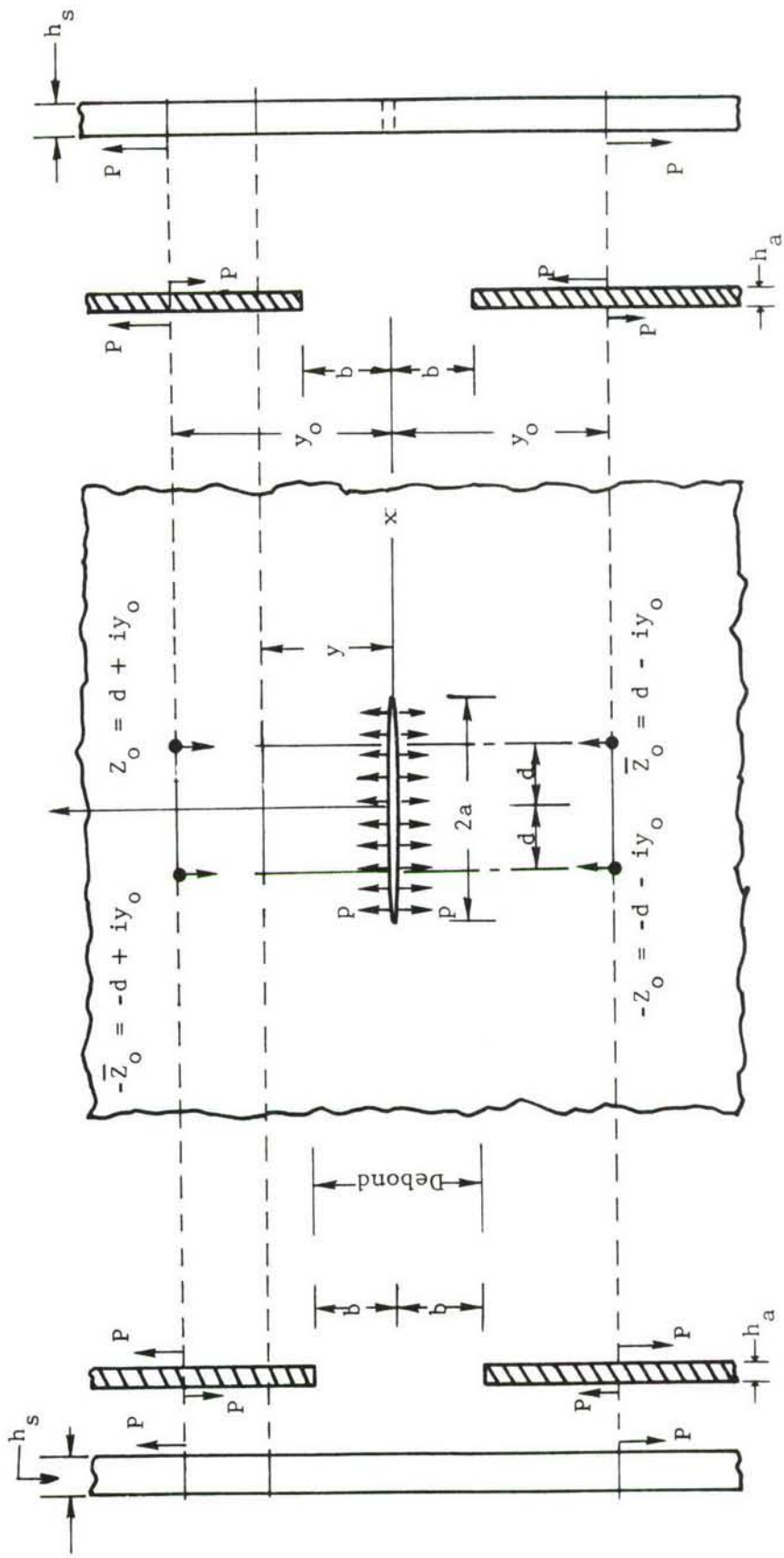

Figure 10. Free-Body Diagrams of the Plate, Adhesive, and Stringers

where $\alpha(y_o)$ is given by

$$\alpha(y_o) = \frac{i}{2\pi h_p(1+\kappa)a}\left\{-(1+\kappa)\frac{[a + I(z_o)]}{a - z_o} + (1+\kappa)\frac{[a + I(\bar{z}_o)]}{a - \bar{z}_o}\right.$$

$$+ (1+\kappa)\frac{[a + I(z_o)]}{a + z_o} - (1+\kappa)\frac{[a + I(-\bar{z}_o)]}{a + \bar{z}_o}$$

$$+ (z_o - \bar{z}_o)\left[\frac{a + I(-z_o)}{(a - z_o)^2} + \frac{J(z_o)}{a - z_o}\right]$$

$$+ (z_o - \bar{z}_o)\left[\frac{a + I(-z_o)}{(a + z_o)^2} + \frac{J(-z_o)}{a + z_o}\right]$$

$$+ (z_o - \bar{z}_o)\left[\frac{a + I(-\bar{z}_o)}{(a + \bar{z}_o)^2} + \frac{J(-\bar{z}_o)}{a + \bar{z}_o}\right]$$

$$\left.+ (z_o - \bar{z}_o)\left[\frac{a + I(\bar{z}_o)}{(a - \bar{z}_o)^2} + \frac{J(\bar{z}_o)}{a - \bar{z}_o}\right]\right\} \qquad (25)$$

where $z_o = d + iy_o$

The integral equations are solved using collocation as described in Paragraph 2.2.1, and stress intensity factors are computed.

The computer program for this problem is detailed in Appendix B.

2.2.3 Two-Layer Adhesively Bonded Structure with a Debonding Crack in One Layer

The analyses discussed in the previous two paragraphs were concerned with a cracked sheet bonded to a sound layer of small width compared to the sheet. In this problem, the cracked sheet and sound layers are of the same width, and infinitely wide.

Consider the adhesively bonded structure of Figure 11a, consisting of two plates with thicknesses h_1 and h_2, respectively, and bonded through an

adhesive layer of constant thickness h_a. The plate is subjected to forces T_x and T_y per unit length of the plate. Plate 1 is assumed to have a through-the-thickness flaw and a debonding crack in the adhesive around the main crack.

In Figure 11a, the size of the debond is shown to be the same as the length of the crack. Experiments confirm that this will generally be the case when the initial flaw has grown due to fatigue, and the edge of the debond will propagate with the crack tip. If the initial debond size in the adhesive is large, it is possible that the crack length will be shorter than the debond, however, this problem can still be formulated in the same manner as the problem of Figure 11a.

The analysis of the adhesively bonded structure in Figure 11a will be based on the following assumptions:

1. The thickness of the plates (h_1 and h_2) is small compared to the inplane dimensions so the structure may be considered to be under a generalized plane-stress loading.
2. Plates 1 and 2, and the adhesive layer, are homogeneous and linearly elastic.
3. The thickness variation of stresses in Layers 1 and 2 is neglected.
4. The thickness (h_a) of the adhesive is small compared to the thickness of the plates, therefore the adhesive may be treated as a shear spring rather than as an elastic continuum.
5. The surface shear transmitted through the adhesive acts as a body force.

Let u_1, v_1 and u_2, v_2 be the x, y components of the inplane displacement vectors in Materials 1 and 2, respectively, and τ_x and τ_y be the components of the shear stress acting on the adhesive. Assumption 4 above, gives the following continuity conditions:

$$u_1 - u_2 = \frac{h_a}{\mu_a} \tau_x \tag{26}$$

$$v_1 - v_2 = \frac{h_a}{\mu_a} \tau_y \tag{27}$$

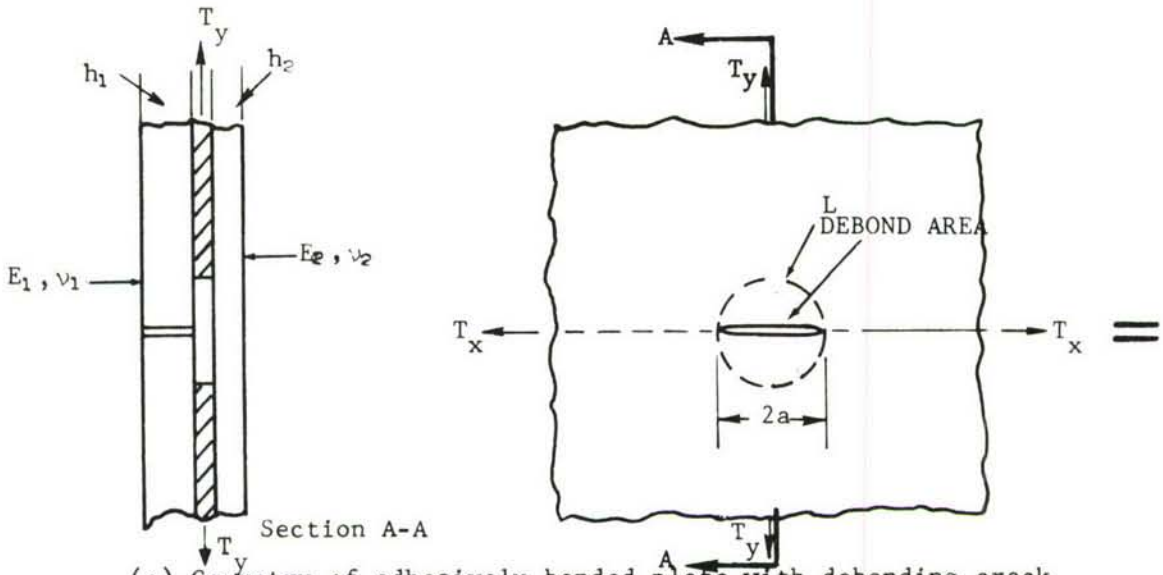

(a) Geometry of adhesively bonded plate with debonding crack

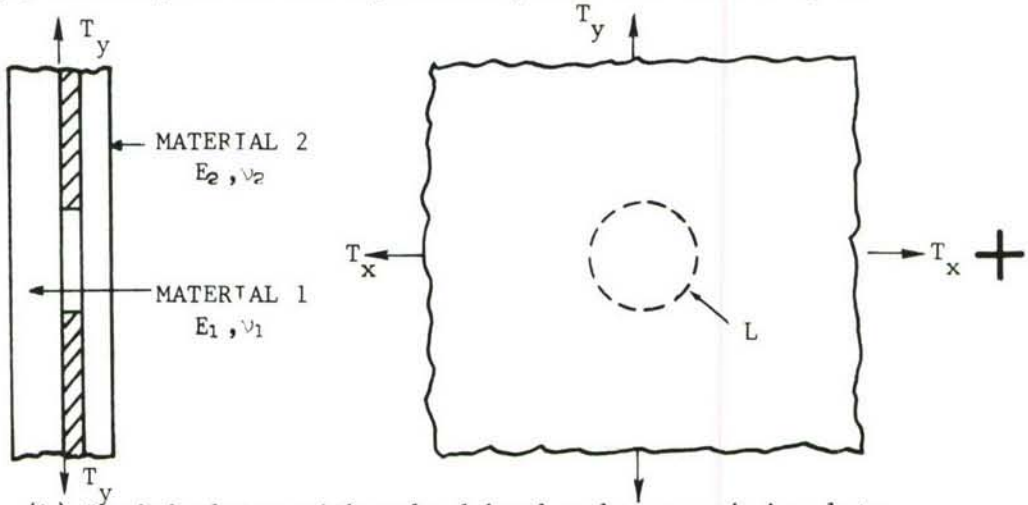

(b) Bonded plates with only debond and no crack in plate

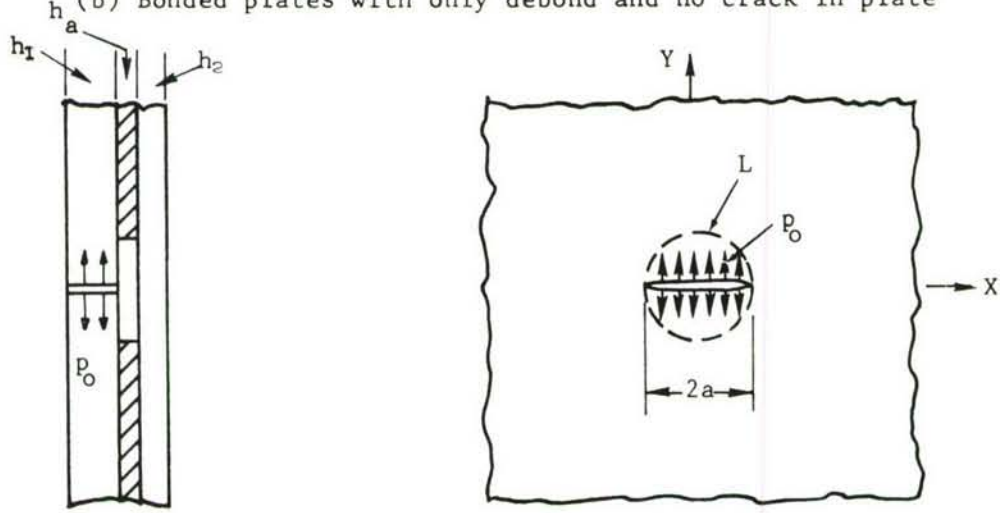

(c) Perturbation problem

Figure 11. Superposition Technique for an Adhesively Bonded Plate with a Debonding Crack

where μ_a is the shear modulus of the adhesive. The body forces acting on Plates 1 and 2 are given by

$$X_1 = -\frac{\tau_x}{h_1}, \qquad Y_1 = -\frac{\tau_y}{h_1}$$

$$X_2 = \frac{\tau_x}{h_2}, \qquad Y_2 = \frac{\tau_y}{h_2} \tag{28}$$

where X_1, Y_1 are the body forces in Plate 1, and X_2, Y_2, the body forces in Plate 2 at the point having coordinates (x,y).

The solution to the problem in Figure 11a can be obtained by superimposing the two cases shown in Figure 11b and 11c. In Figure 11b, the displacements for the two plates are such that $u_1 = u_2$, and $v_1 = v_2$ throughout the plate, hence there are no interface shear stresses or body forces in the plate. Thus, the stress intensity factors, interface stresses, and boundary of the debonding crack of Figure 11a will be given by the perturbation problem of Figure 11c. The solution to the problem of Figure 11a is carried out in the following steps.

1. Determination of Applied Crack Surface Stress

   The crack surface stress p_o to be applied to the crack surface in the perturbation problem of Figure 11c, is equal to the stress taken by the plate of Material 1 in Figure 11b. Let T_{x1} and T_{x2} be the forces per unit length in x direction, taken by plates of Materials 1 and 2, respectively. Similarly, T_{y1} and T_{y2} are the forces per unit length in y direction, taken by plates of Materials 1 and 2, respectively. The equilibrium conditions in x and y directions give

$$T_{x1} + T_{x2} = T_x \tag{29}$$

$$T_{y1} + T_{y2} = T_y \tag{30}$$

The continuity of displacement in the problem of Figure 11b, gives

$$u_1 = u_2$$

or

$$\frac{\left(T_{x1} - \nu_1 T_{y1}\right)}{h_1 E_1} = \frac{\left(T_{x2} - \nu_2 T_{y2}\right)}{h_2 E_2} \tag{31}$$

Similarly

$$\frac{\left(T_{y1} - \nu_1 T_{x1}\right)}{h_1 E_1} = \frac{\left(T_{y2} - \nu_2 T_{x2}\right)}{h_2 E_2} \tag{32}$$

Equations (29) through (32) can be solved for T_{x1}, T_{x2}, T_{y1}, and T_{y2}. The stress p_o is equal to T_{x1}/h_1 and is given by

$$p_o = \frac{\left(a_1 T_x + a_2 T_y\right)}{a_3} \tag{33}$$

where

$$a_1 = \frac{h_2}{h_1}\left(\frac{E_2}{h_1 E_1 + h_2 E_2} - \frac{\nu_1 E_2}{\nu_1 h_2 E_2 + \nu_2 h_1 E_1}\right)$$

$$a_2 = \frac{E_1 \nu_2}{h_1 E_1 + h_2 E_2} - \frac{E_1}{h_1 \nu_2 E_1 + h_2 \nu_1 E_2}$$

$$a_3 = \frac{h_1 \nu_2 E_1 + h_2 \nu_1 E_2}{h_1 E_1 + h_2 E_2} - \frac{h_1 E_1 + h_2 E_2}{h_1 \nu_2 E_1 + h_2 \nu_1 E_2} \tag{34}$$

2. Formulation of Perturbation Problem

The perturbation problem will be looked upon as consisting of Plate 2 with body forces in Region D of Figure 12a, and Plate 1 with body forces and loading on the crack surface, as shown in Figure 12b.

The stresses and displacements in terms of complex functions φ, Ω, are given by (Reference 9)

$$\sigma_x + \sigma_y = 2[\varphi(z) + \overline{\varphi(z)}] \tag{35a}$$

$$\sigma_y - \sigma_x + 2i\tau_{xy} = 2[(\bar{z} - z)\varphi'(z) - \varphi(z) + \bar{\Omega}(z)] \tag{35b}$$

$$2\mu(u + iv) = \kappa \int_0^z \varphi(z)dz - \int_0^{\bar{z}} \Omega(\bar{z})d\bar{z} - (z - \bar{z})\overline{\varphi(z)} \tag{35c}$$

a. Displacements in Uncracked Plate

For an infinite plate under the body forces X_2, Y_2, acting at at z_o (x_o, y_o), the complex functions are given by (Reference 8)

$$\varphi(z) = -\frac{S}{z - z_0}$$

$$\Omega(s) = \frac{\kappa S}{z - \bar{z}_0} + \frac{\bar{S}(\bar{z}_0 - z_0)}{(z - \bar{z}_0)^2}$$

$$S = \frac{X_2 + iY_2}{2\pi(1 + \kappa)} \tag{36}$$

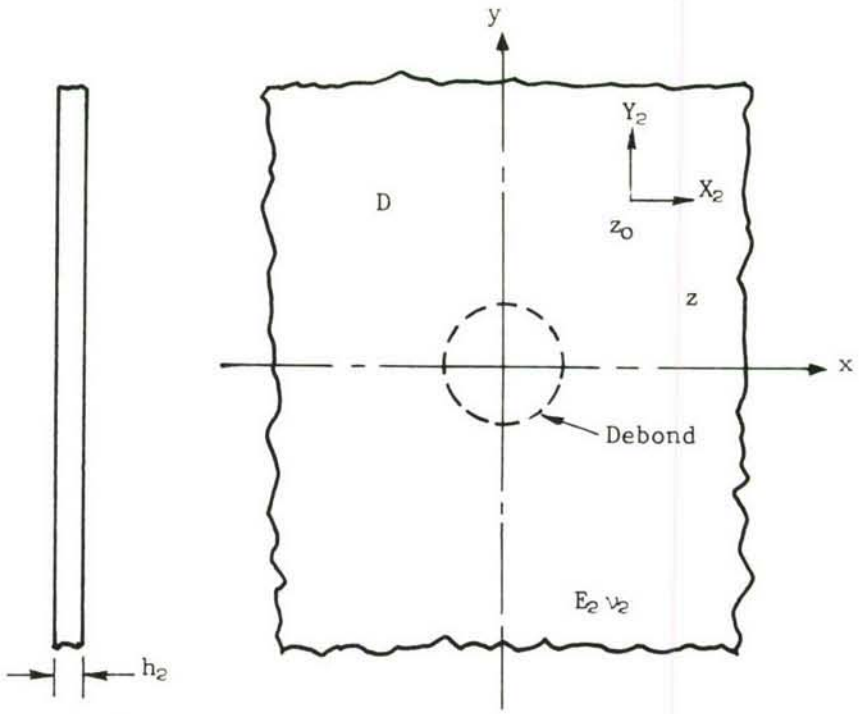

(a) Plate of Material 2 with body forces

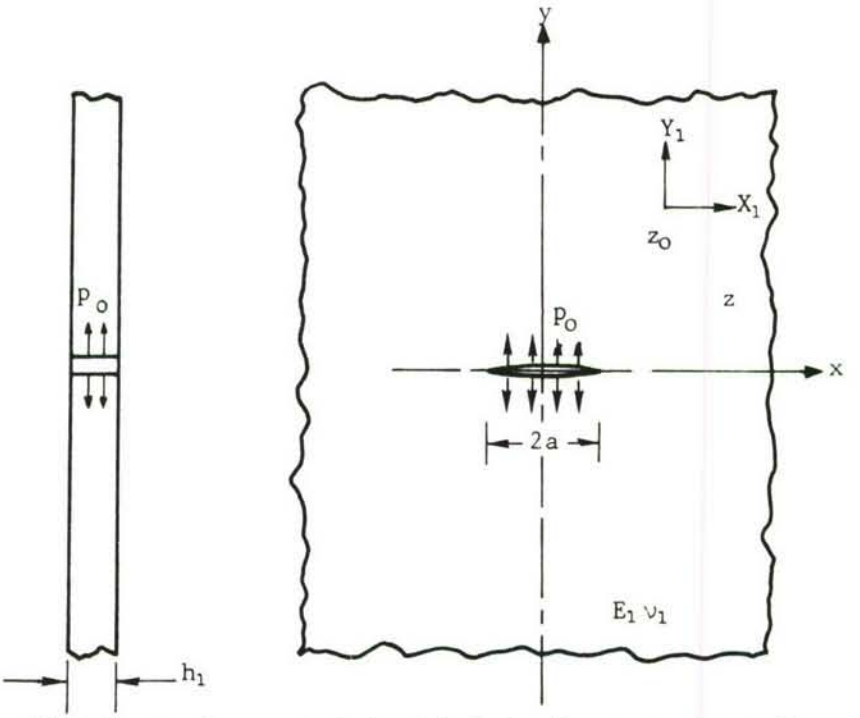

(b) Plate of Material 1 with body forces and crack surfaces loaded

Figure 12. Loadings on Plates of Materials 1 and 2 in Perturbation Problem

Substituting Equation 36 in Equation 35c, the displacements in the uncracked plate with body forces (plate of Material 2) can be obtained. These displacements are given by

$$
\begin{aligned}
2\mu_2(u_2 + iv_2) = &- \kappa S[\log(z - z_0) + \log(\bar{z} - \bar{z}_0)] \\
&+ \kappa S[\log(z + z_0) + \log(\bar{z} + \bar{z}_0)] \\
&+ S\left[\frac{z - \bar{z}_0}{\bar{z} - z_0} - 1\right] - S\left[\frac{z + \bar{z}_0}{\bar{z} + z_0} - 1\right] \\
&- \kappa\bar{S}[\log(z - \bar{z}_0) + \log(\bar{z} - z_0)] \\
&+ \kappa\bar{S}[\log(z + \bar{z}_0) + \log(\bar{z} + z_0)] \\
&+ \bar{S}\left[\frac{z - z_0}{z - \bar{z}_0} - 1\right] - \bar{S}\left[\frac{z + z_0}{\bar{z} + \bar{z}_0} - 1\right]
\end{aligned}
\tag{37}
$$

Assuming that the body forces X_2, Y_2 are continuous functions of z_0 or (x_0, y_0) as defined in region D, the displacements at point $z = x + iy$ in the plane are given by

$$
\begin{aligned}
u_2(x,y) = &\iint_D [K_{11}(x,y;x_0,y_0)X_2(x_0,y_0) \\
&+ K_{12}(x,y;x_0,y_0)Y_2(x_0,y_0)]dx_0\,dy_0 \\
v_2(x,y) = &\iint_D [K_{21}(x,y;x_0y_0)X_2(x_0,y_0) \\
&+ K_{22}(x,y;x_0y_0)Y_2(x_0,y_0)]dx_0\,dy_0
\end{aligned}
\tag{38}
$$

where the kernels $K_{ij}(i,j = 1,2)$ are given by Green's functions (Equation (37)).

b. Displacements in a Cracked Plate

The displacements in the cracked plate will consist of two components, one due to uniform applied pressure on the crack surface (Reference 9) and the other due to body forces acting on the plate surface. The displacements due to uniform applied pressure are given by

$$u_{11}(x,y) = \frac{p_0}{4\mu_1}\left\{(\kappa - 1)\mathrm{Re}\left[(z^2 - a^2)^{1/2}\right] - 2y\mathrm{Im}\left[\frac{z}{(z^2 - a^2)^{1/2}}\right] + (1 - \kappa)x\right\} = p_0 f_1(x,y)$$

$$v_{11}(x,y) = \frac{p_0}{4\mu_1}\left\{(\kappa + 1)\mathrm{Im}\left[z^2 - a^2{}^{1/2}\right] - 2y\mathrm{Re}\left[\frac{z}{(z^2 - a^2)^{1/2}}\right] + (1 - \kappa)y\right\} = p_0 f_2(x,y) \qquad (39)$$

where $\kappa = (3 - \nu_1)/(1 + \nu_1)$, μ_1 and ν_1 are elastic constants. To find the solution of the cracked plate under distributed body forces, the solution for the concentrated forces X_1, Y_1 acting at z_0 is used as Green's function. This solution is given by

$$\left.\begin{aligned}\Phi(z) &= -\frac{S}{z - z_0} + \Phi_0(z)\\ \Omega(z) &= \frac{\kappa S}{z - z_0} + \frac{(\bar{z}_0 - z_0)\bar{S}}{(z - \bar{z}_0)^2} + \Phi_0(z)\end{aligned}\right\} \qquad (40)$$

$$S = \frac{X_1 + iY_1}{2\pi(1+\kappa)}$$

$$\Phi_0(z) = \frac{1}{2\pi}\left(z^2 - a^2\right)^{-1/2}\left\{\frac{S}{z - z_0}\left[I(z) - I(z_0)\right]\right.$$

$$- \frac{\kappa S}{z - \bar{z}_0}\left[I(z) - I(\bar{z}_0)\right]$$

$$\left. + (z_0 - \bar{z}_0)\bar{S}\left[\frac{I(z) - I(\bar{z}_0)}{\left(z - \bar{z}_0\right)^2} - \frac{J(\bar{z}_0)}{z - \bar{z}_0}\right]\right\}$$

$$I(z) = \pi\left[\left(z^2 - a^2\right)^{1/2} - z\right]$$

$$J(z) = \pi\left[z\left(z^2 - a^2\right)^{-1/2} - 1\right] \qquad (41)$$

Substituting Equation (40) into (35c), the displacements are obtained. These displacements in the cracked plate due to body forces acting at an arbitrary location, are given by Equations (11) and (12). Assuming again, that the body forces X_1, Y_1 are continuous functions of $(x_0, y_0))$ defined in region D, using Equations (11) and (12) as the Green's function, the displacements in the cracked plate due to body forces X_1 and Y_1, may be expressed as

$$u_{12}(x,y) = \iint_D \left[H_{11}(x,y;x_0,y_0)X_1(x_0,y_0)\right.$$

$$\left. + H_{12}(x,y;x_0,y_0)Y_1(x_0,y_0)\right]dx_0dy_0 \qquad (42a)$$

$$v_{12}(x,y) = \int_D \int \Big[H_{21}(x,y;x_0,y_0) X_1(x_0,y_0)$$

$$+ H_{22}(x,y;x_0,y_0) Y_1(x_0,y_0) \Big] dx_0 dy_0 \qquad (42b)$$

The total displacements in the base plate of Material 1 may then then be obtained by adding Equations (39) and (42).

$$u_1(x,y) = u_{11} + u_{12}, \quad v_1(x,y) = v_{11} + v_{12} \qquad (43)$$

c. Integral Equations for τ_x, τ_y

The τ_x and τ_y are the x and y components of the shear stress on the adhesive layer. The relationship between body forces and shear stresses is given by

$$X_1 = -\frac{\tau_x}{h_1}, \quad Y_1 = -\frac{\tau_y}{h_1} \qquad (44)$$

$$X_2 = \frac{\tau_x}{h_2}, \quad Y_2 = \frac{\tau_y}{h_2}$$

Use of the displacements u_1, u_2, v_1, and v_2 in Equations (26) and (27) yields the following system of integral equations for the unknown functions τ_x and τ_y.

$$\frac{h_a}{\mu_a}\tau_x(x,y) + \iint_D \Big[k_{11}(x,y;x_0,y_0)\tau_x(x_0,y_0)$$

$$+ k_{12}(x,y;x_0y_0)\tau_y(x_0,y_0)\Big]dx_0dy_0 = p_0f_1(x,y)$$

$$\frac{h_a}{\mu_a}\tau_y(x,y) + \iint_D \Big[k_{21}(x,y;x_0,y_0)\tau_x(x_0,y_0)$$

$$+ k_{22}(x,y;x_0y_0)\tau_y(x_0,y_0)\Big]dx_0dy_0 = p_0f_2(x,y)$$

$$(x,y) \in D \qquad (45)$$

The functions f_1, f_2 are given by Equation (39) and

$$k_{11} = \frac{H_{11}}{h_1} + \frac{K_{11}}{h_2},\quad k_{12} = \frac{H_{12}}{h_1} + \frac{K_{12}}{h_2}$$

$$k_{21} = \frac{H_{21}}{h_1} + \frac{K_{21}}{h_2},\quad k_{22} = \frac{H_{22}}{h_1} + \frac{K_{22}}{h_2} \qquad (46)$$

The kernels K_{ij}, $(i,j = 1,2)$, which have logarithmic singularities, are known and are square integrable in region D.

3. The Stress Intensity Factors

In general, the stress intensity factors in plane stress problems may be expressed in terms of the Kolosov-Muskhellishvili function $\Phi(z)$ as follows (Reference 8)

$$k_1 - ik_2 = \lim_{x \to a} [2(x-a)]^{1/2} \left[\sigma_y(x,0) - i\tau_{xy}(x,0)\right]$$

$$= \lim_{z \to a} 2[2(z-a)]^{1/2} \Phi(z) \qquad (47)$$

In the problem considered here, the shear component of stress intensity factor k_2, is zero due to the symmetry in loading and geometry. The cleavage component k_1, is determined by adding the effects of the crack surface pressure p_0 and the body forces X_1 and Y_1. The stress intensity factor k_1 can be written as

$$k_1 = p_0\sqrt{a} + \iint_D \left[h_1(x_0,y_0)X_1(x_0,y_0) \right.$$

$$\left. + h_2(x_0,y_0)Y_1(x_0,y_0)\right] dx_0 dy_0 \qquad (48)$$

where $h_1(x_0,y_0)$ and $h_2(x_0,y_0)$ are the cleavage components of the stress intensity factor due to the concentrated body forces X_1 and Y_1, respectively (Figure 12) and are obtained by substituting Equation (40) into Equation (47). Substitution of Equation (40) into Equation (47) gives

$$k_1 - ik_2 = \frac{1}{\sqrt{a}}\left[- S\frac{[a + I(z_0)]}{a - z_0} + \kappa S\frac{[a + I(\bar{z}_0)]}{a - \bar{z}_0} \right.$$

$$\left. - \bar{S}(z_0 - \bar{z}_0)\frac{a + I(\bar{z}_0)}{(a - \bar{z}_0)^2} + \frac{J(\bar{z}_0)}{a - \bar{z}_0}\right] \qquad (49)$$

$h_1(x_o, y_o)$ and $h_2(x_o, y_o)$ are coefficients of X_1 and Y_1 respectively, in real part of Equation (49).

4. Solution of Integral Equations

The system of integral equations given by Equations (45), are the Fredholm type and may be solved by using the standard numerical techniques. In this case, it is done by dividing the region D into smaller cells, and unknown functions τ_x and τ_y are assumed to be constant in each cell. Thus, using a numerical integration scheme to evaluate the integrals, the integral equations are reduced to a system of algebraic equations. The kernels in the integral equations have logarithmic singularities, hence the singular part of the kernels is evaluated separately, in closed form. In the actual integration, a telescopic grid is used. A typical grid layout used in integration is shown in Figure 13, where only one-quarter of the plate is shown because of symmetry. The cell size is kept small above the crack plane for a distance of about a half-crack length, as the shear stresses are high in this region and are maximum at the boundary of debond. The cell size is progressively increased, as shown. The debonded region is approximately represented by straight lines for integration purposes. The boundary of the domain of integration goes to infinity, hence the size of Region D is restricted in numerical analysis such that the stress intensity factors are not appreciably affected.

A generalized program to obtain stress intensity factors could not be developed, as convergence of the solution is dependent on the thickness and material properties of adherends and adhesive. The convergence of the solution also depends on crack length. In the integral equations (45), if $h_a\mu_a$ is very small (less than 0.1×10^6), the solution will not converge, and shear stresses will oscillate. This can be avoided by decreasing cell size further and increasing integration points. Two computer programs, one for small crack length ($a \leq 0.4$) and the other for large crack lengths ($0.5 \leq a \leq 1.0$) are given in Appendices C and D, respectively.

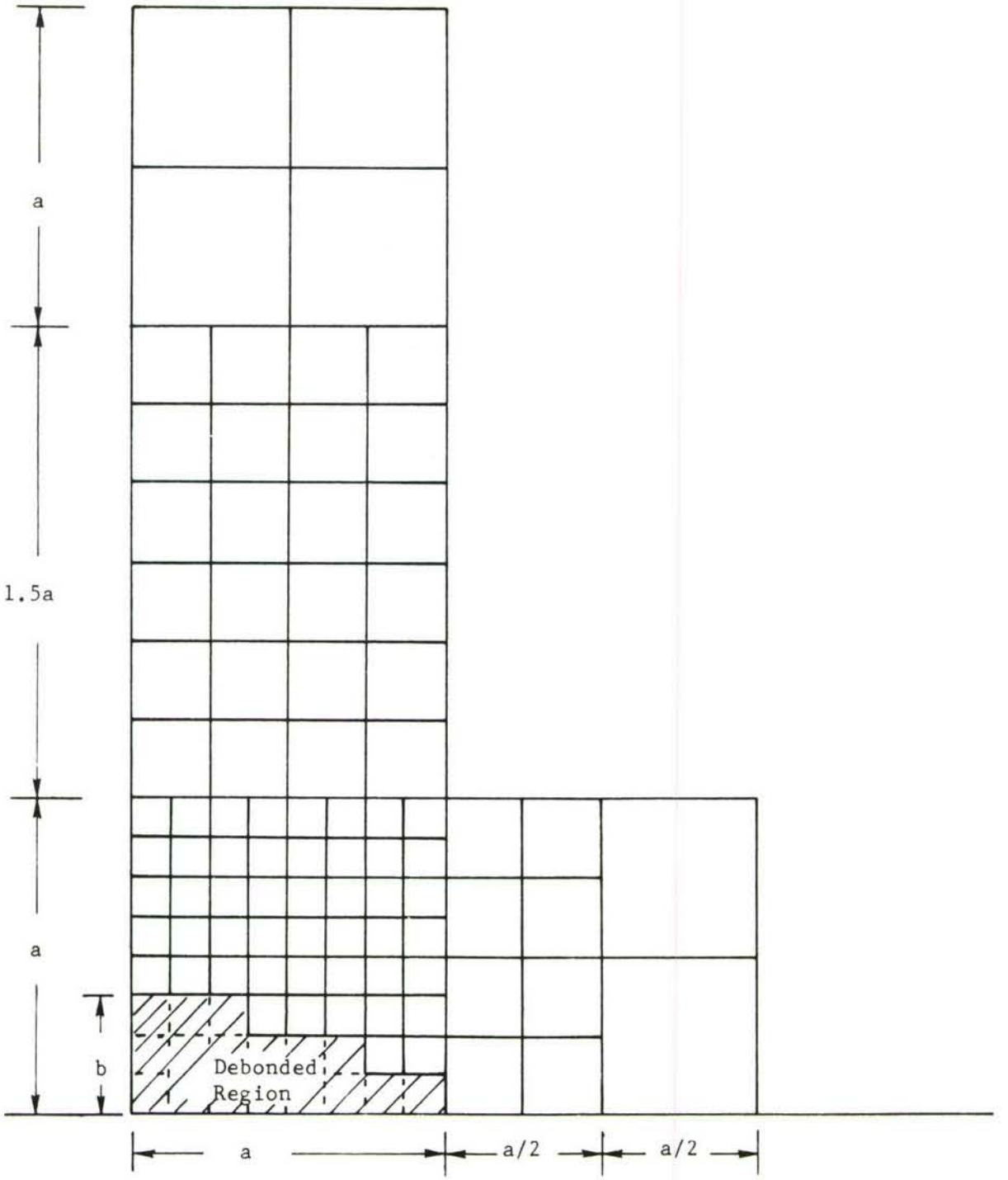

Figure 13. Subdivision of Bonding Area D for Numerical Analysis

2.3 COMPARISON OF FINITE ELEMENT AND MATEHMATICAL ANALYSES

In Paragraphs 2.1 and 2.2, the finite element and complex variable approaches to analyzing crack problems were discussed. In each of the analysis methods, certain simplified assumptions were made and the results, obtained by the two methods for the same problem, were compared. In the following paragraphs, the problems of a cracked plate with a bonded stringer, and two adhesively bonded plates with a crack in one plate, are considered for comparison purposes.

2.3.1 A Cracked Plate with a Single, Centrally Located, Adhesively Bonded Stringer

Figure 14 describes the structure (with dimensions) used for analysis comparison. Complex variable analysis assumes that plate is infinitely large. The finite element model used in the analysis is shown in Figure 5. The plot of normalized stress intensity factors $K_I/\sigma\sqrt{\pi a}$ versus the half-crack length a, obtained by two methods of analysis, is shown in Figure 15. It is seen that the results of the finite element analysis and complex variable approach are close only for small crack lengths ($a \leq 0.1$ inch). For half-crack lengths larger than 0.1 inch, the stress intensity results obtained by the complex variable technique are much larger than those obtained using the finite element analysis. In the complex variable formulation, the load transfer for the stringer is concentrated along the centerline of the stringer, hence the width of the stringer in load transfer, for short cracks (under the stringer), from the cracked plate to the stringer is not fully effective. In the finite element analysis, the entire width of the strap is modeled, allowing for load transfer over the entire width to occur, and thereby yields lower stress intensity factors compared to the complex variable approach for short cracks (under the stringer).

To obtain better solutions using the complex variable approach, it was assumed that the area of the strap is concentrated at two points that are symmetrically located about the centerline of the plate, as shown in Figure 9. These areas were assumed to be concentrated at the crack tip if $2a \leq B$ (B = width of the strap), and at the edge of the strap if $2a > B$. The problem was formulated using a complex variable approach. Due to symmetry, the problem was reduced to the solution of an integral equation for unknown shear stresses in one stringer only.

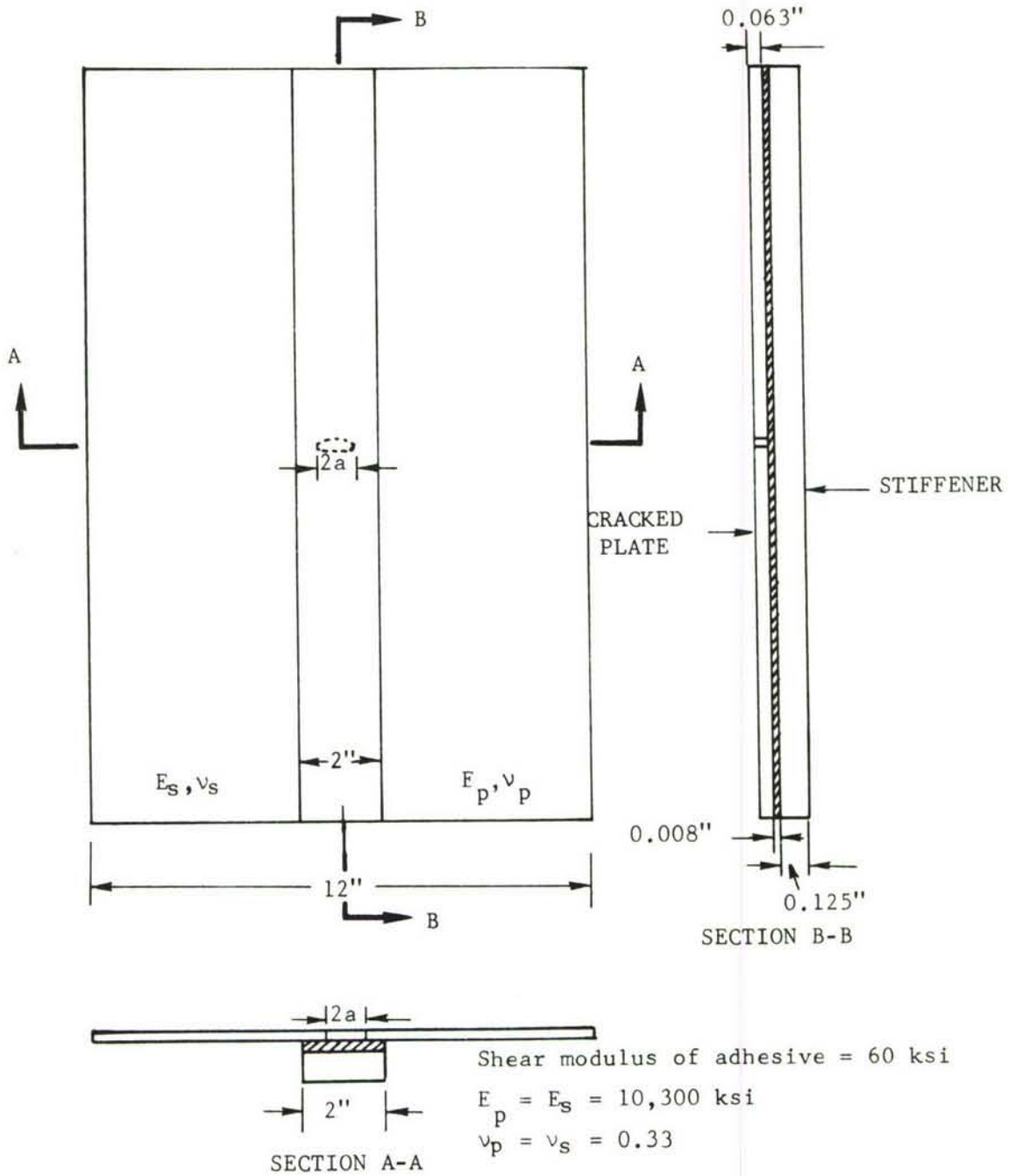

Figure 14. Geometry of a Cracked Plate with an Adhesively Bonded Stringer (no debonding) Small Crack ($2a < d_s$)

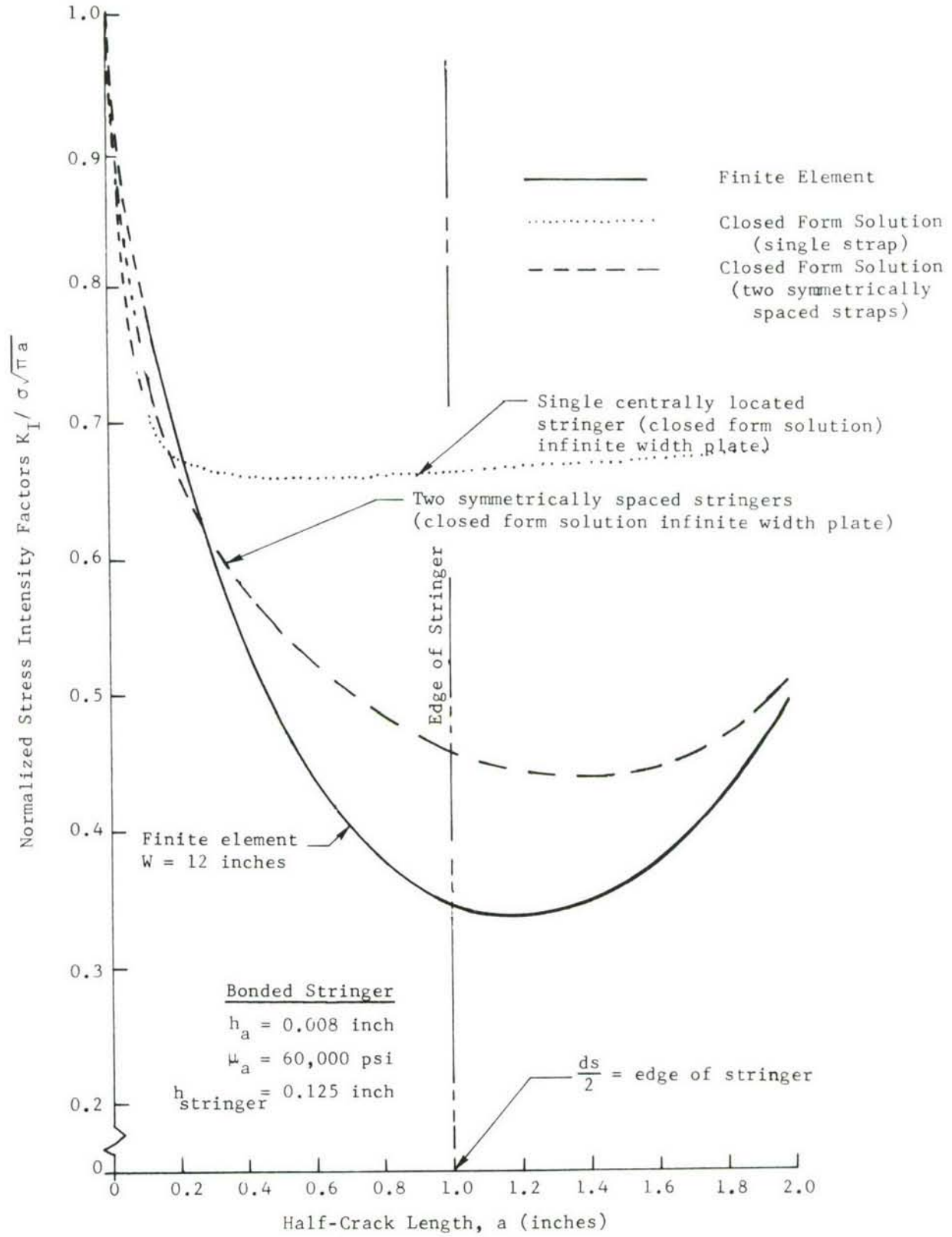

Figure 15. Comparison of Finite Element Determined Stress Intensities with Integral Equation Solutions (Cracked Plate with Bonded Stringer)

The analysis of the problem was carried out using the complex variable approach discussed in Paragraph 2.2.2. The plot of $K_I/\sigma\sqrt{\pi a}$ versus the half-crack length a for the two symmetrically placed stringers is also plotted in Figure 15. It is seen that up to a half-crack length of about 0.3 inch, the results given by the finite element analysis and the integral equation approach are very close. Beyond this point, the integral equation approach gives higher values of the stress intensity factor. The difference between the results of the finite element analysis and the integral equation approach increases as the crack length increases, up to a half-crack length of about one inch. Beyond a one-inch crack length, the difference decreases. At a half-crack length of one inch (total length equal to the strap width), the results of the integral equation approach are about 33 percent higher than those of the finite element analysis. At a half-crack length of two inches, the results of these two methods of analysis differ by only two percent. The results of Figure 15 indicate that the complex variable approach, assuming a concentrated stringer area at one point, may be used for very small or very large crack lengths only. For larger crack lengths, either the finite element method or the two-stringer formulations may be used. The computer run time for the finite element analysis is about 120 seconds (CPU time), whereas the integral equation approach computer run time is approximately 8 seconds (CPU time). Thus, it can be seen that a considerable saving in computer run time is obtained by using a complex variable approach. It should be noted however, that more accurate solutions can be obtained using the complex variable method if the stringer area is subdivided in two or more concentrated strips.

2.3.2 Two Adhesively Bonded Plates with a Crack in One Plate

The dimensions of the structure are shown in Figure 16 for the problem of a cracked plate adhesively bonded to an uncracked plate. The adhesive is assumed to have an elliptically shaped debond with a ratio of minor axis to major axis equal to 0.1. The leading edge of the debond is assumed to coincide with the leading edge of the crack. This shape of debond was predicted from analysis as discussed in Section 6 of this volume and has also been observed in experiments (Section 4, Volume I).

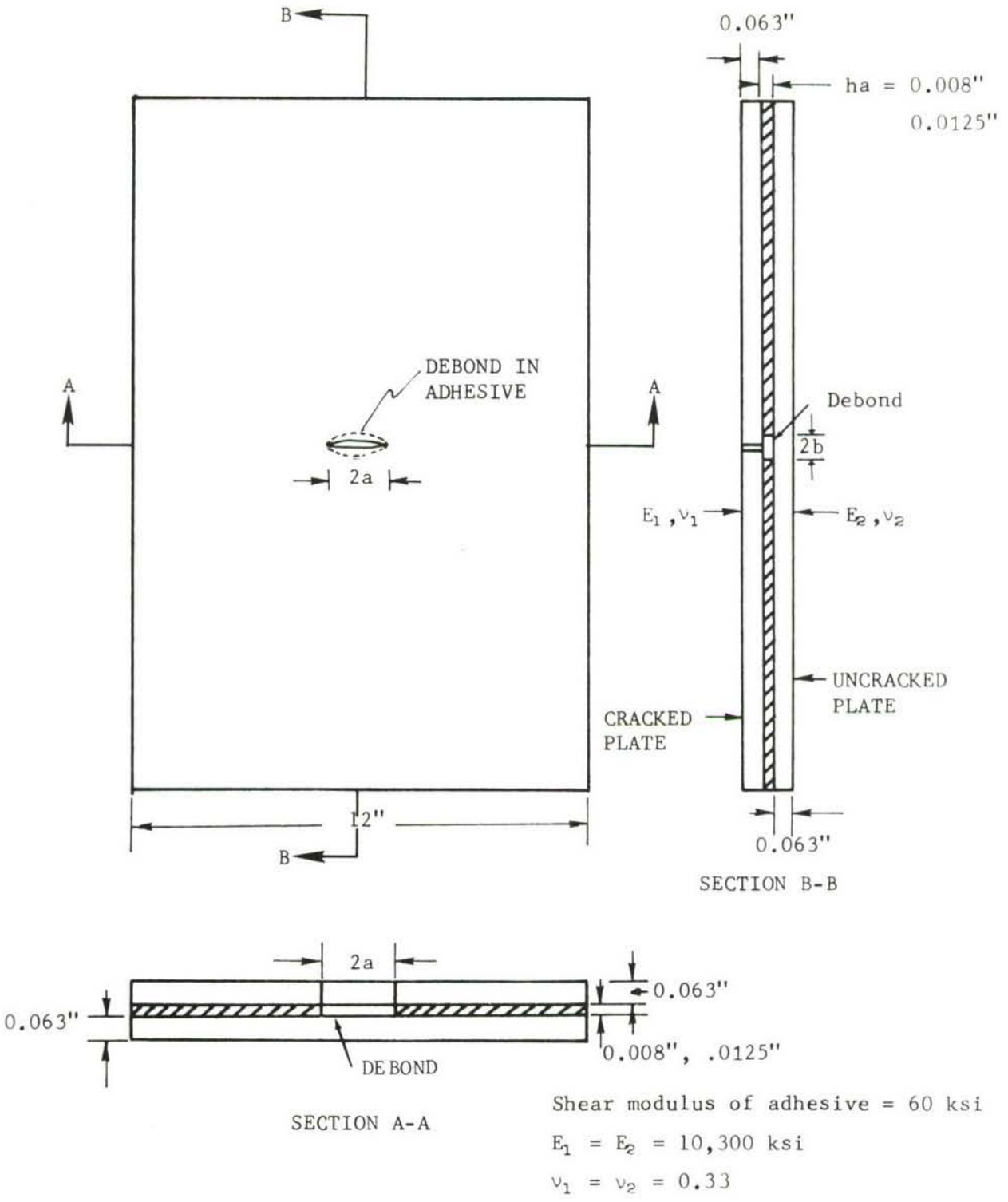

Figure 16. Geometry of Cracked Plate Adhesively Bonded to an Uncracked Plate

The finite element model used in the analysis of the cracked structure is shown in Figure 4. In the finite element analysis, the plate width is assumed to be 12 inches, and in the complex variable approach, the plate width is assumed to be infinite. Up to a half-crack length of one inch $\frac{a}{w} = 0.0833$, the finite width effect is negligable. It can be noted from Figure 17 that the normalized stress intensity factors obtained by the two methods of analysis agree very well.

The computer run times for finite element analysis are about 240 seconds (CPU time), and for mathematical methods, the computer run times are 48 seconds (CPU time), for small crack length programs, and between 60 and 90 seconds (CPU time) for long crack length programs, depending on the debond size. Thus, with the mathematical solutions, a considerable saving in computer run times is achieved when a study of various material/geometrical sensitivities are required.

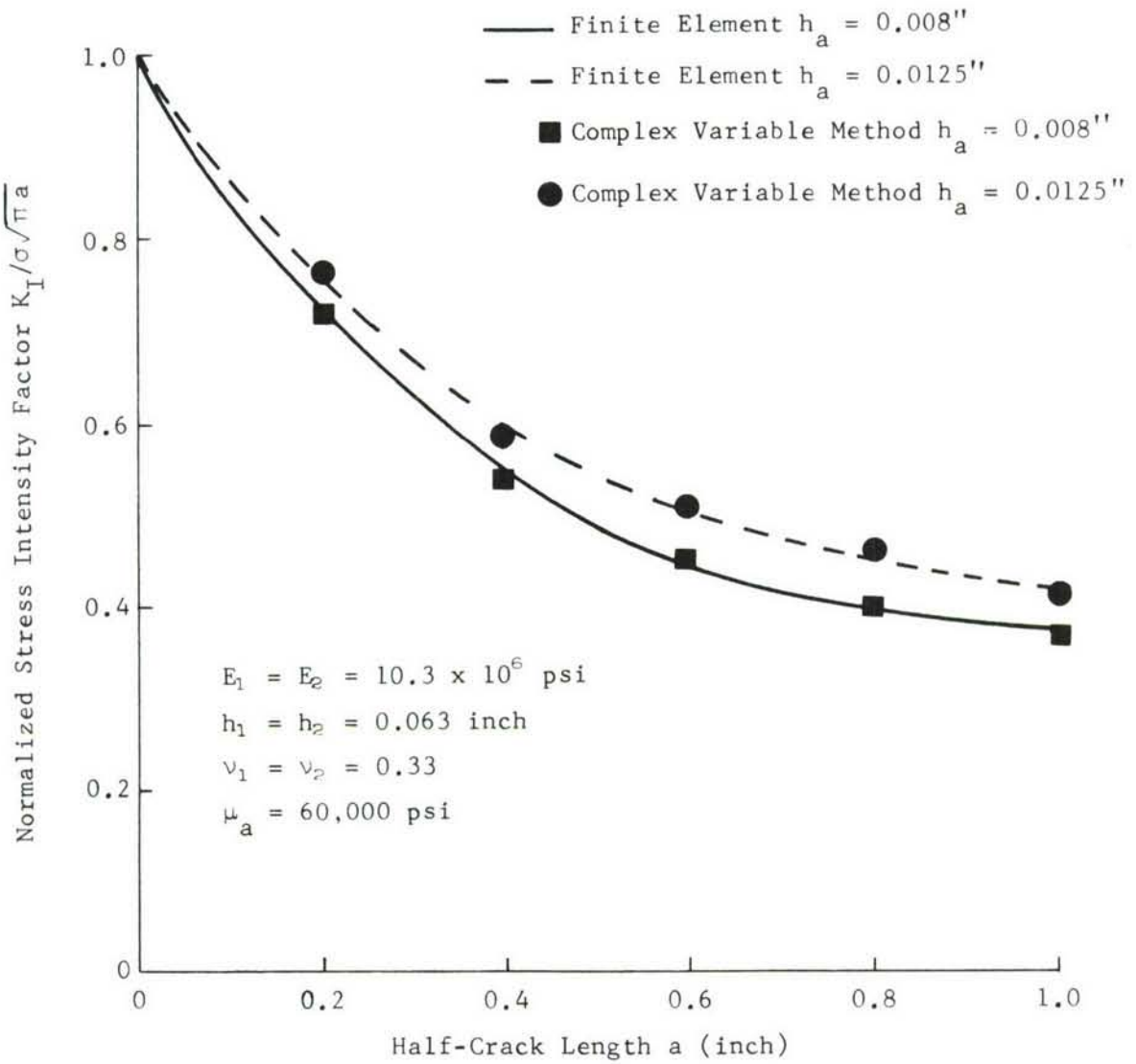

Figure 17. Comparison of Finite Element Determined Stress Intensities with Integral Equation Solutions (two plates bonded)

SECTION 3

APPLICATION OF ANALYSIS TO MULTILAYERED AND OTHER BONDED STRUCTURES

Finite element and mathematical methods of analysis were discussed in Section 2, primarily in relation to two-ply, adhesively bonded structures. However, these methods are also applicable to cracked, multilayered, bonded structures, as well as to rivet bonded, weldbonded, and brazed structures. The application of the methods to these structures is discussed in the following paragraphs.

3.1 APPLICATION OF ANALYSES TO CRACKED STRUCTURES CONSISTING OF MORE THAN TWO LAYERS

The finite element and mathematical analysis methods discussed in Section 2 can be extended to multilayered, adhesively bonded structures with cracks in more than one layer. The application of two analysis methods to cracked multilayered structures is discussed in the following paragraphs.

3.1.1 Application of Finite Element Analysis to Cracked Multilayered Structures

The modified two-dimensional finite element method described in Paragraph 2.1 can easily be applied to cases of more than two bonded plates. Consider the structure of Figure 18, which has through-the-thickness cracks in Plates 1 and 2, and debonding in adhesive Layers 1 and 2. The plate is subjected to Force T_y, in y direction, per unit length of the plate. In the finite element modeling of this structure, a cracked element is provided ahead of each crack tip in Plates 1 and 2. If only one of the plates has a crack, then cracked elements are only provided for the crack tips in the cracked plate. Plates 1 and 2, as well as Plates 2 and 3, are connected by shear elements. The shear elements are assumed to run continuously throughout the length of the plates in the bonded regions. In these regions, the finite elements are closely spaced around the periphery of the debond as discussed in Paragraph 2.1, and shown in Figure 19. The case of three adhesively bonded plates is shown

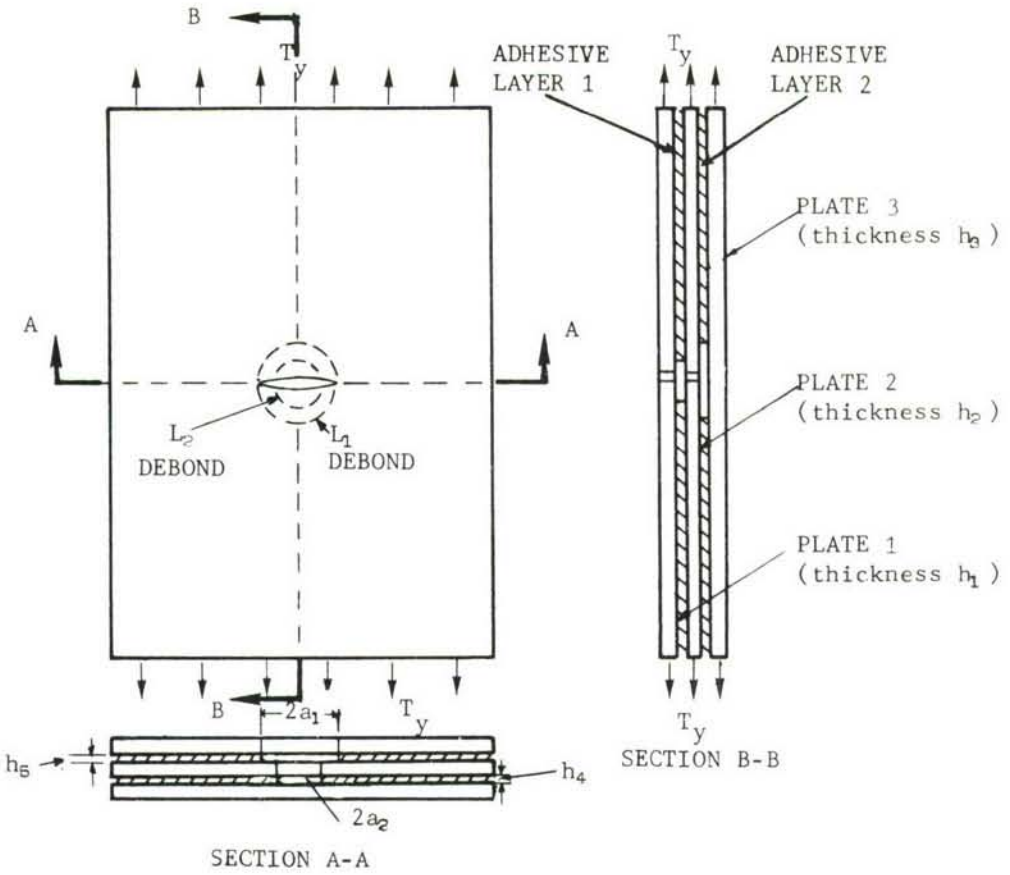

Figure 18. Adhesively Bonded Plates Consisting of Three Layers

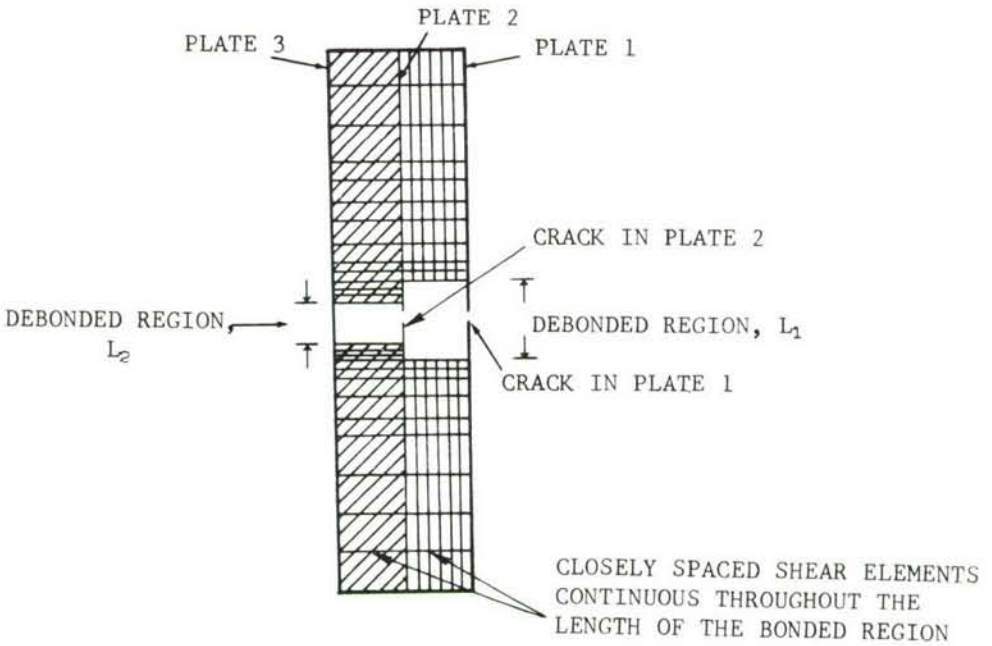

Figure 19. Modeling of Shear Elements for a Bonded Structure

in Figure 18, however, if there are more than three plates in the structure, this method of modeling can be extended in a manner similar to that described above.

3.1.2 Application of Mathematical Method of Analysis to Cracked Multilayered Structures

The mathematical technique described in Paragraph 2.2 can be extended to the case of a bonded structure consisting of more than two layers, like the structure shown in Figure 18. Each layer is assumed to be infinite. The solution to the loading condition shown in this figure can be obtained by solving the perturbation problem with crack surface loading as discussed in Paragraph 2.2 The body forces and crack surface loading on each plate in the perturbation problem is shown in Figure 20. Let τ_{x1} and τ_{y1} be the shear stresses in adhesive layer 1, and τ_{x2} and τ_{y2} be the shear stresses in adhesive layer 2. If u_1, v_1, and u_2, v_2 are the x-y components of the in-plane displacement vectors in Materials 1 and 2 respectively, then the continuity conditions for Adhesive Layer 1 are given by:

$$u_1 - u_2 = \frac{h_4}{\mu_a} \tau_{x_1}$$

$$v_1 - v_2 = \frac{h_4}{\mu_a} \tau_{y_1} \qquad (50)$$

Similar conditions for adhesive layer 2 are given by:

$$u_2 - u_3 = \frac{h_5}{\mu_a} \tau_{x_2}$$

$$v_2 - v_3 = \frac{h_5}{\mu_a} \tau_{y_2} \qquad (51)$$

where u_3, v_3, are x-y are components of displacements in Plate 3. As shown in Figure 20, the formulation for displacements in Plates 1 and 3 will be similar to the case of two bonded plates discussed in Paragraph 2.2. The displacements u_2 and v_2 in Plate 2 will consist of 3 parts: 1) due to crack surface loading; 2) due to body forces X_2 and Y_2; and 3) due to body forces X_3 and Y_3. In Green's function formulation of displacements, the body forces

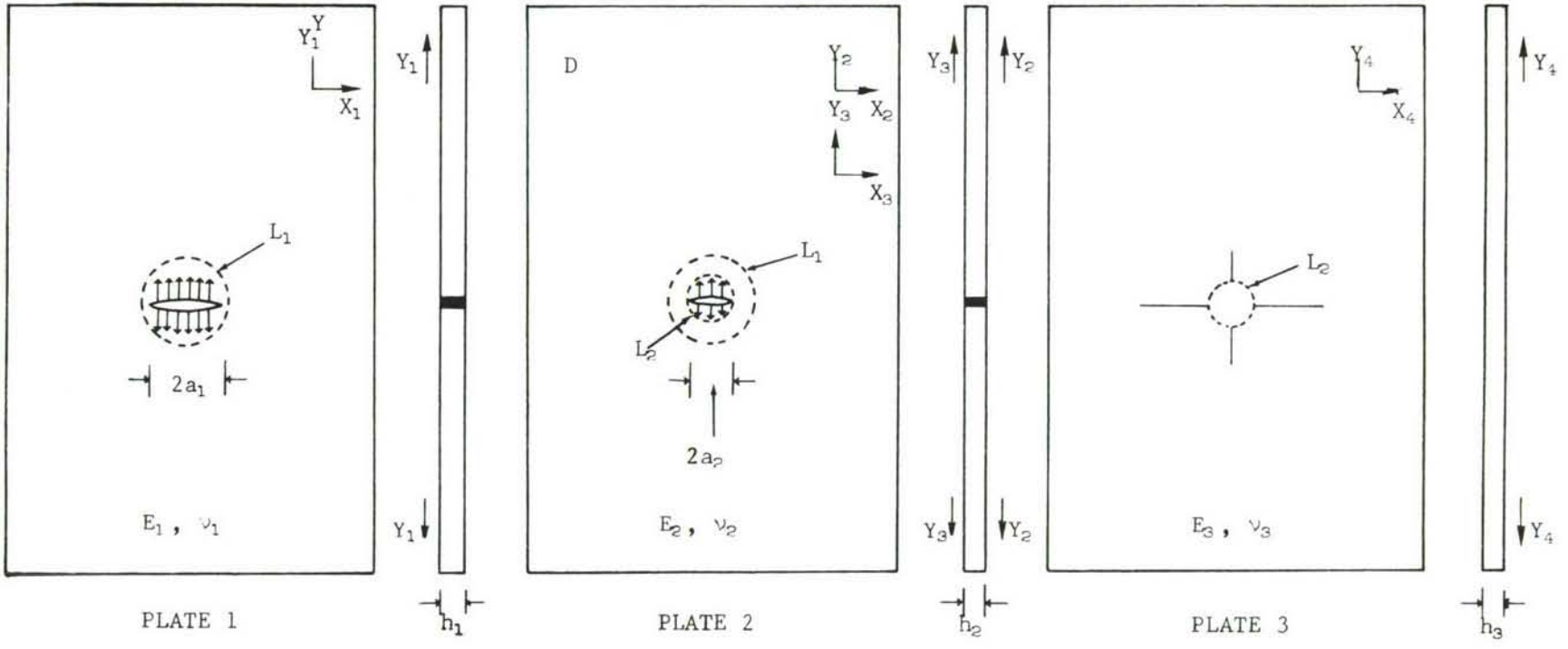

Figure 20. Plates with Body Forces and Crack Surfaces Loaded

X_2 and Y_2 are integrable in domain D-L_1 and body forces X_3 and Y_3 are integrable in domain D-L_2. The relation between body forces and shear stress is given by

$$X_1 = -\frac{\tau_{x_1}}{h_1}, \quad Y_1 = -\frac{\tau_{y_1}}{h_1}$$

$$X_2 = \frac{\tau_{x_1}}{h_2}, \quad Y_2 = \frac{\tau_{y_1}}{h_2}$$

$$X_3 = \frac{\tau_{x_2}}{h_2}, \quad Y_3 = \frac{\tau_{y_2}}{h_2}$$

$$X_4 = -\frac{\tau_{x_2}}{h_2}, \quad Y_4 = -\frac{\tau_{y_3}}{h_2} \qquad (52)$$

Using the displacement continuity conditions (Equations (26) and (27)), a system of integral equations for τ_{x1}, τ_{y1} and τ_{x2}, τ_{y2} can be obtained. The integral equations are of the Fredholm type, with kernels having logarithmic singularities. These equations can be solved numerically, and shear stresses and stress intensity factors computed as discussed in Paragraph 2.2.

3.2 APPLICATION OF ANALYSIS TO RIVET BONDED, WELDBONDED, AND BRAZED STRUCTURES

The modified two-dimensional finite element analysis discussed in Paragraph 2.1 is applicable to rivet bonded, weldbonded, and brazed structures. In rivet bonded, weldbonded, or brazed structures, the method of stringer attachment is modeled as a shear element, continuous throughout the length of the attached portion. In this type of modeling, the attached stringer may be of any shape.

Consider the structure of Figure 21, where a strap is spotwelded and bonded to the sheet, using the weldbonding process. There is a debond in the adhesive around the spotweld caused by lack of adhesive flow, as noted in this figure. The flaw in the weld may be caused by the entrapped air. This is typical of situations that might possibly occur in weldbonded structures. The through-crack in the sheet may have originated as a part-through flaw that had

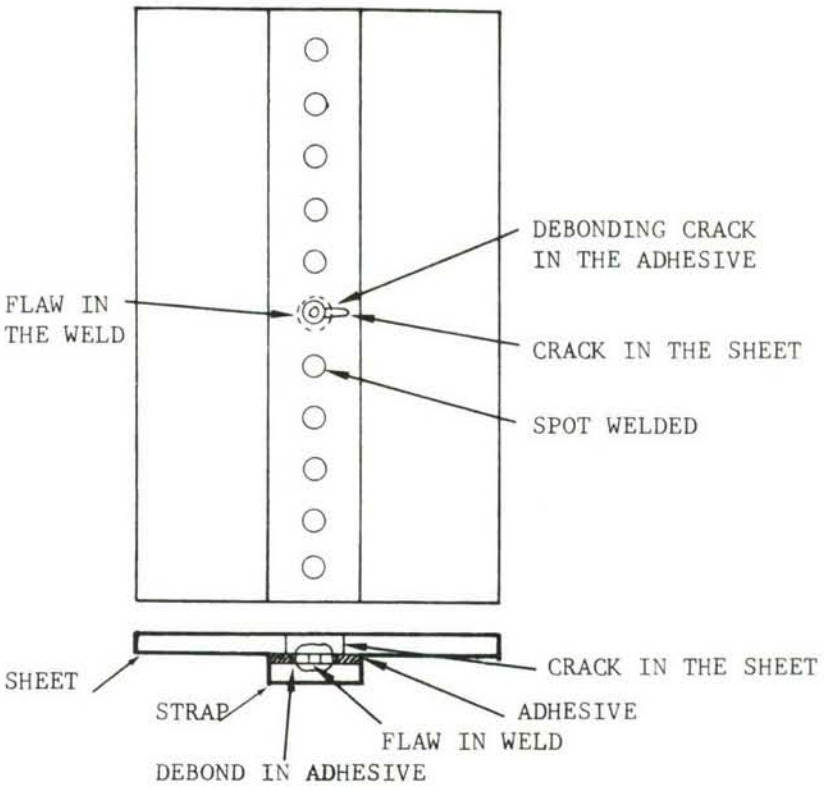

Figure 21. Weldbonded Structure

grown to a through-the-thickness flaw during fatigue cycling. The precise finite element analysis of this type of structure would require several orders of magnitude of complication over that previously discussed, therefore certain simplifying assumptions have to be made. This structure can be easily modeled using a two-dimensional finite element model based on the principles discussed in Paragraph 2.1. Both the spotweld and the adhesive are represented as shear elements. No shear elements are provided in the portion of the adhesive where there is debonding, nor in the portion of the weld where there is a void, as shown in Figure 22. In this model, the properties of the shear elements representing the spotweld and adhesive will be different, since the stiffnesses of the adhesive and spotweld are different. The shear elements are closely spaced in the vicinity of the crack and debond. The grid point interval for shear elements, and consequently, the size of the plate elements in both skin and strap, are gradually increased away from the crack and debond. The strap is assumed to be bonded throughout its length by having shear elements along the length. In a cracked structure, the first six rivets or welds adjacent to the crack surface will be effective in load transfer for crack lengths up to about 2.0 inches, hence in the structure of Figure 21, the first six spotwelds

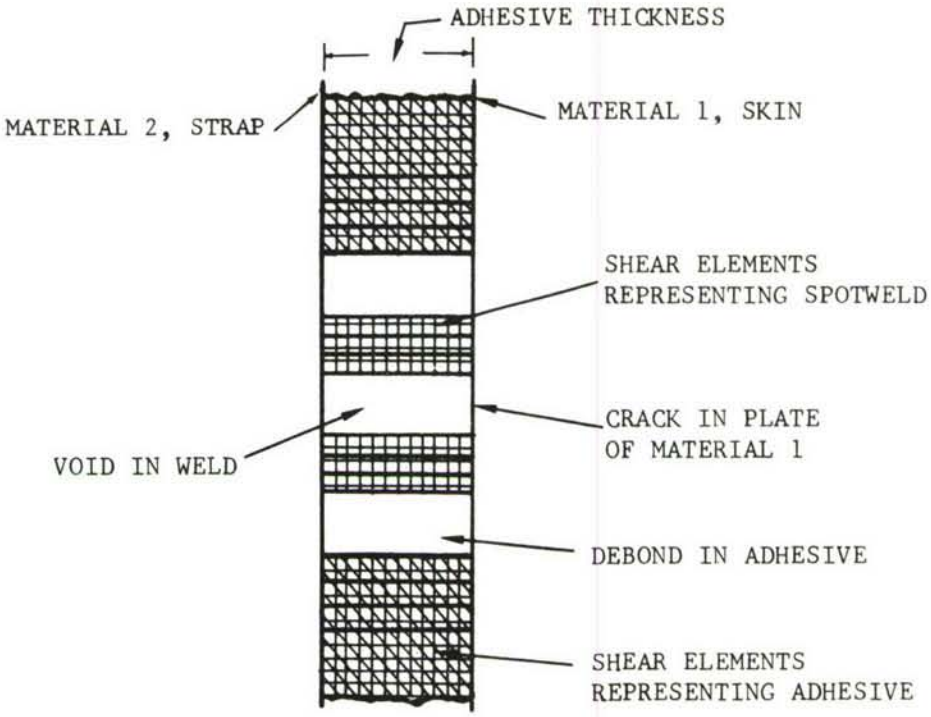

Figure 22. Modeling of Weldbonded Structure Showing Shear Elements Representing Spotwelds and Adhesive

would require special modeling. The shear elements representing the adhesive have the same elastic properties as the adhesive. The shear elements representing the rivet or weld are proportioned to have the same deflection as that of the riveted or welded joint (Reference 1). Let Δ be the deflection of a welded lap joint under unit load. In the idealized shear element in the finite element model, the deflection under unit load is given by

$$\delta = \frac{h}{A_s \mu_a} \tag{53}$$

where

A_s = the area of the shear element
μ_a = shear modulus of the weld material
h = distance between the points connected by the shear element

This deflection of the shear element should be equal to the deflection of a spotwelded lap joint, or

$$\Delta = \delta = \frac{h}{A_s \mu_a}$$

$$A_s = \frac{\Delta \mu_a}{h} \tag{54}$$

This method of modeling was used for riveted and bolted panels in Reference 1 with excellent correlation obtained between analytical and experimental data for crack openings and load transfer from cracked member to uncracked member. It should be noted that this method of modeling will require deflection data from lap joint tests.

Next, consider the rivet bonded structure of Figure 23. The shear elements representing rivets will be specially modeled so that the deflection of the shear element is the same as the deflection of the riveted joint. As discussed in Reference 1, the deflection in riveted aluminum alloy sheets is given by

$$\delta = \frac{Pf}{E_a d} \tag{55}$$

where

δ = deflection
P = applied load
E_a = modulus of aluminum
d = rivet diameter
f = constant

For aluminum alloy rivets,

$$f = 5.0 + 0.8 \frac{d}{h_2} + \frac{d}{h_1} \tag{56}$$

where h_1 and h_2 are the thicknesses of the joined sheets.

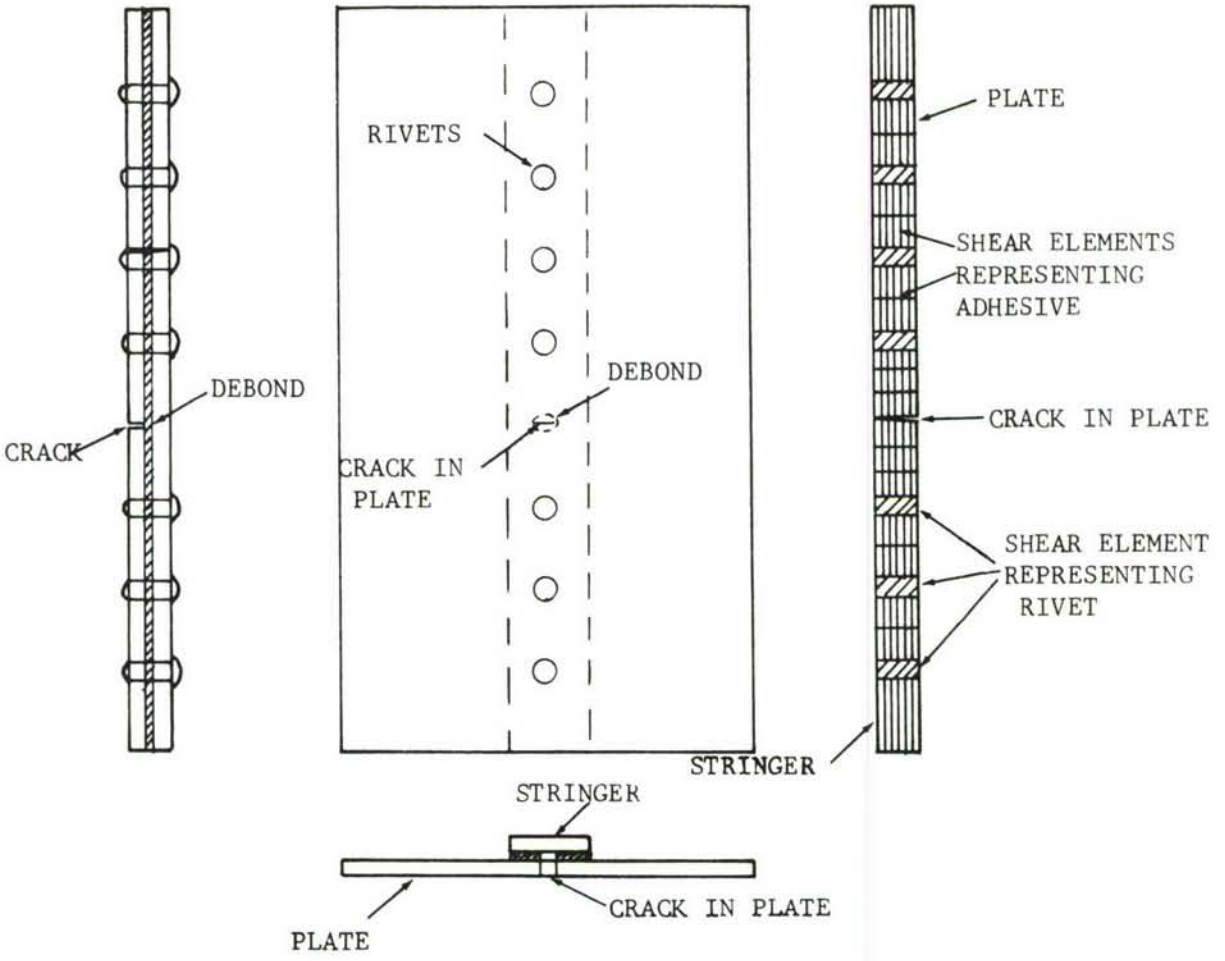

Figure 23. Rivet Bonded Structure

In the idealized shear element, the deflection is given by

$$\delta = \frac{Ph}{A_s \mu_a}$$

where

A_s = the area of the shear element

μ_a = shear modulus of aluminum

h = distance between the grid points connected by the shear element

Equating the two deflections

$$\frac{Pf}{E_a d} = \frac{Ph}{A_s \mu_a}$$

and solving for area of the shear element, A_s

$$A_s = \frac{h}{\mu_a} \frac{E_a d}{f} \tag{57}$$

If the materials connected by the attachments have different moduli, the empirical constant in the fastener deflection Equation (55) is given by

$$f = 5.0 + 0.8 \frac{d}{h_1} \frac{d}{h_2} \frac{E_1}{E_2} \tag{58}$$

where E_1 and E_2 are Young's moduli of the two connected sheets.

This type of finite element modeling can also be used for brazed structures. In order to proportion shear elements for brazed structures, it will be necessary to establish a deflection equation of the type represented by Equation (53). This will have the form

$$\delta = KP \tag{59}$$

where

δ = deflection per unit length

P = applied load

K = constant.

The constant K can be obtained from load displacement data obtained from simple tests on double lap joints.

SECTION 4

EFFECT OF BENDING

4.1 INTRODUCTION AND GENERAL COMMENTS

The finite element and mathematical analyses of adhesively bonded structures discussed in Section 2 were described for extensional type loading where it was assumed that neither the cracked layer nor the sound layer have bending stiffness. In reality, however, the presence of a crack in one layer of a two-ply, adhesively bonded structure or a plate with a bonded stiffener gives rise to out-of-plane deformation due to unsymmetry. This causes bending in the structure. The influence of this out-of-plane bending will be to increase the tensile stresses in the cracked layer and thus increase the stress intensity factor. Thus, the stress intensity factors obtained by two-dimensional analysis need to be corrected for the influence of bending. In this section, a method to do this, based on load transferred to the sound layer of a two-ply structure is described.

4.2 DEVELOPMENT OF CORRECTION FOR CENTER CRACKED STRUCTURE.

Consider a single cracked layer shown in Figure 24a. The solution to this problem is obtained by superposing the cases shown in Figures 24b and 24c. From Figure 24c, the crack has a uniform stress σ^{∞}. The total force at the crack plane is area x stress = $(2ah_1)\sigma^{\infty}$. This force is taken entirely by the stress singularities ahead of the crack tips. Next, consider a two-ply adhesively bonded panel with a crack in one layer as shown in Figure 25a. In this structure, the same force release ($2a\sigma^{\infty} h_1$) at the crack plane is taken partly by the cracked layer in the form of stress singularities similar to a single layer, and the remainder of the force is transmitted to the adjacent sound layer through the adhesive. Let the force transmitted to the sound layer be $2ah_1\sigma_t$ (area x stress) where σ_t is the stress transferred to the sound layer. The total force acting on the end of each layer is shown in Figure 25b. Due to the force transferred to the sound layer, the force in

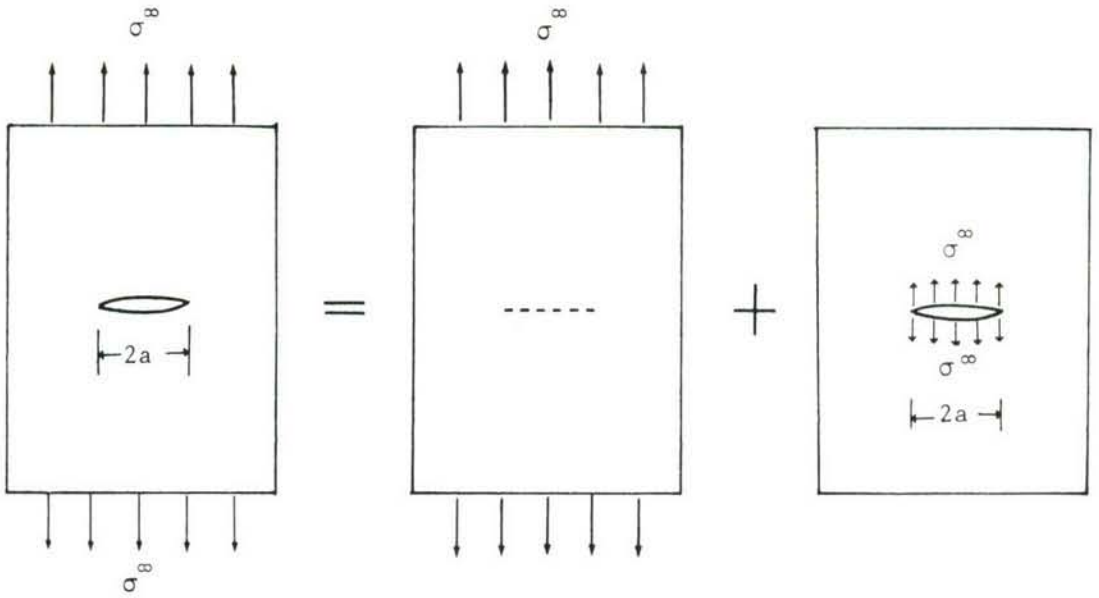

(a) Cracked plate with remote stress (b) No crack (c) Crack with uniform stress field

Figure 24. Superposition Technique for a Single-Layer Crack

each plate at the plane of the crack will be different from that at the ends as shown in Figure 25c. The net internal unbalanced force between the two layers at the crack plane is equal to that which is transferred from the cracked to the sound layer, i.e., $2ah_1\sigma_t$. This unbalanced force causes the bending (Figure 25d).

Assuming the thickness of adhesive to be small compared to plate thickness, the couple generated by the load transfer between the two plies is given by

$$C = 2ah_1\sigma_t \left(\frac{h_1+h_2}{2}\right)$$

where $\left(\frac{h_1+h_2}{2}\right)$ is the distance between the centerlines of the plates.

or
$$C = ah_1 \left(h_1+h_2\right)\sigma_t \tag{60}$$

Assuming that the bending is resisted by the entire plate width W, the maximum bending stress in the layer is given by

$$\sigma_b = \frac{C\, y_{max}}{I} \tag{61}$$

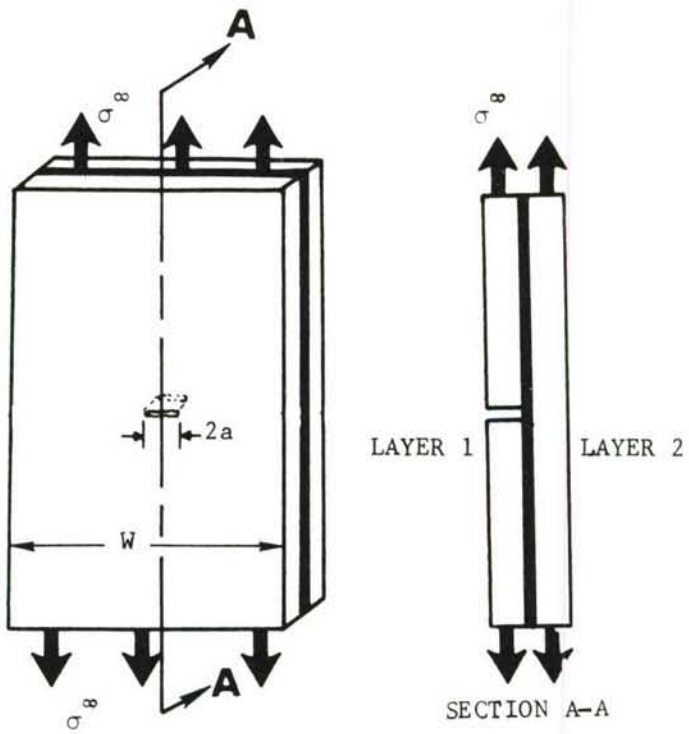

(a) Two-ply, adhesively bonded panel with a crack in one ply

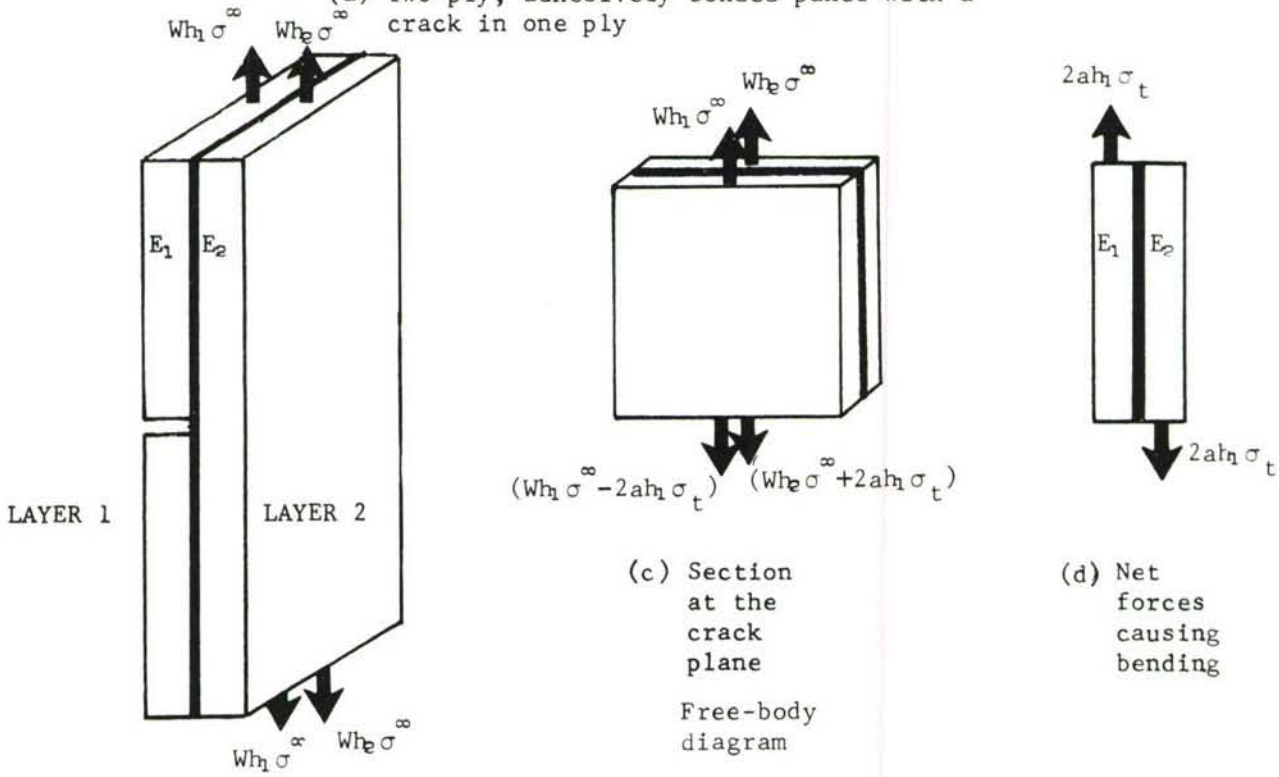

(b) Side view showing the total force at the ends

(c) Section at the crack plane

Free-body diagram

(d) Net forces causing bending

Figure 25. Bending Correction for Adhesively Bonded Panel with a Crack in One Ply

where y_{max} is the distance of extreme fibers of the cracked plate from the neutral axis and I is the moment of inertia of the section. For computing the values of y_{max} and the moment of inertia I of the section, the thickness of the adhesive may be neglected and the calculations based on the initially uncracked cross-section of both plies. Thus, the cross-section of Figure 26a may be represented by the one shown in Figure 26b. For computing the neutral axis and moment of inertia of the section based on the uncracked section, the equivalent section (Reference 10) is shown in Figure 27, where it is assumed that E_2 is greater than E_1.

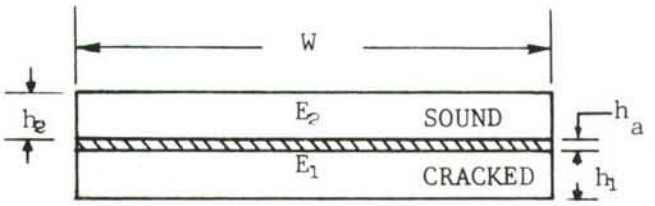

(a) Section of an adhesively bonded panel

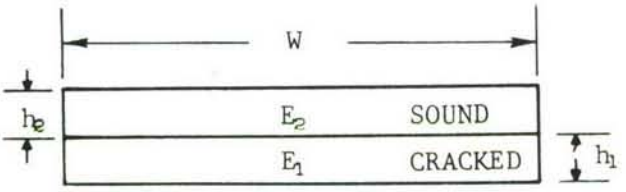

(b) Idealized section for bending analysis

Figure 26. Section for Applying Bending Correction

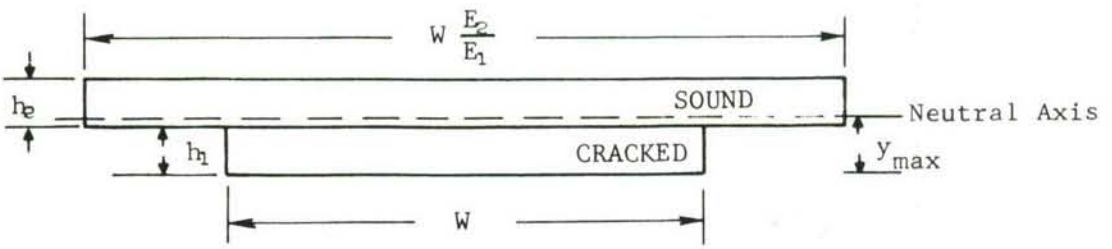

Figure 27. Equivalent Section for Bending Stress Analysis (neither layer assumed cracked for calculation)

Substituting Equation (61) in (60), gives

$$\sigma_b = \frac{ah_1(h_1 + h_2)\sigma_t}{I} y_{max} \tag{62}$$

4.2.1 Load Transfer Factor

Define the term load transfer factor with symbol M as the ratio of the load transferred (to the sound layer) to the load released due to a crack.

$$M = \frac{2ah_1\sigma_t}{2ah_1\sigma^\infty} = \frac{\sigma_t}{\sigma^\infty} \tag{63}$$

Equation (62) reduces to

$$\sigma_b = \frac{ah_1(h_1 + h_2)}{I} M\sigma^\infty y_{max}$$

$$\frac{\sigma_b}{\sigma^\infty} = \frac{ah_1(h_1 + h_2)}{I} My_{max}$$

$$= Bc, \text{ Bending correction factor} \tag{64}$$

The effective stress in computing the stress intensity factors is increased by an amount σ_b. For the case $h_1 = h_2 = h$ and $E_1 = E_2$, $y_{max} = h$ and $I = 1/12\ W(2h)^3$

$$\frac{\sigma_b}{\sigma^\infty} = \frac{3a}{W} M \tag{65}$$

4.2.2 The Concept of Effective Stress

In a cracked, finite width, single-layer structure (Figure 24a), the stress intensity factor varies as a function of crack length according to

the equation

$$K_s = \sigma^{\infty} \sqrt{\pi a}\, f(a/W) \tag{66a}$$

where f(a/W) is the finite width correction

or

$$f(a/W) = \frac{K_s}{\sigma^{\infty} \sqrt{\pi a}} \tag{66b}$$

Let K_A be the stress intensity factor in a crack, adhesively bonded structure with half-crack length a and subjected to an applied stress of σ^{∞} (Figure 25a). The equivalent stress σ_e, acting remotely on a single-layer structure such as shown in Figure 24a, and giving the stress intensity factor K_A at half-crack length a, is given by

$$K_A = \sigma_e \sqrt{\pi a}\, f(a/W) \tag{67}$$

using Equation (66b), K_A can be expressed as

$$K_A = \sigma_e \frac{K_s}{\sigma^{\infty}}$$

or

$$\sigma_e = \frac{K_A}{K_s} \sigma^{\infty} \tag{68}$$

4.2.3 Interrelation Between Load Transfer Factor and Stress Intensity Factors

The stress transferred to the sound layer is the difference between the remotely applied stress and the uniform inplane stress that matches the required singularity effect in the cracked layer, i.e.,

$$\sigma_t = \sigma^{\infty} - \sigma_e$$

Using Equation (68)

$$\sigma_t = \sigma^\infty - \frac{K_A}{K_s}\sigma^\infty \tag{69}$$

The load transfer factor is

$$M = \frac{\sigma_t}{\sigma^\infty} = 1 - \frac{K_A}{K_s} \tag{70}$$

K_A is the stress intensity factor obtained from the finite element or mathematical analysis of an adhesively bonded structure with a crack in one layer, and K_s is the stress intensity factor for a single layer with a crack the same size as the adhesively bonded structure. K_s is available in the form of Equation (66a) (References 11 and 12). The value of M obtained here, is used in computing bending correction in Equation (64).

4.3 EXAMPLE OF BENDING CORRECTION

As a bending correction example, consider a two-ply, adhesively bonded panel with a center crack. The panel width is taken as six inches, and each layer has the same modulus with a thickness of 0.063 inch. The stress intensity factors for this structure, assuming an elliptical debond with b/a = 0.1 (semiminor to semimajor axis ratio equal to 0.1), are determined by finite element analysis and are shown in Figure 28, and Column 2 of Table 1. For the structure under consideration, Equation (65) reduces to

$$\frac{\sigma_b}{\sigma^\infty} = \frac{3a}{W} M$$

for W = 6 inches,

$$\frac{\sigma_b}{\sigma^\infty} = 0.5aM$$

Various steps involved in the application of the bending correction are shown in Table 1. The value of a/W is computed for each crack length

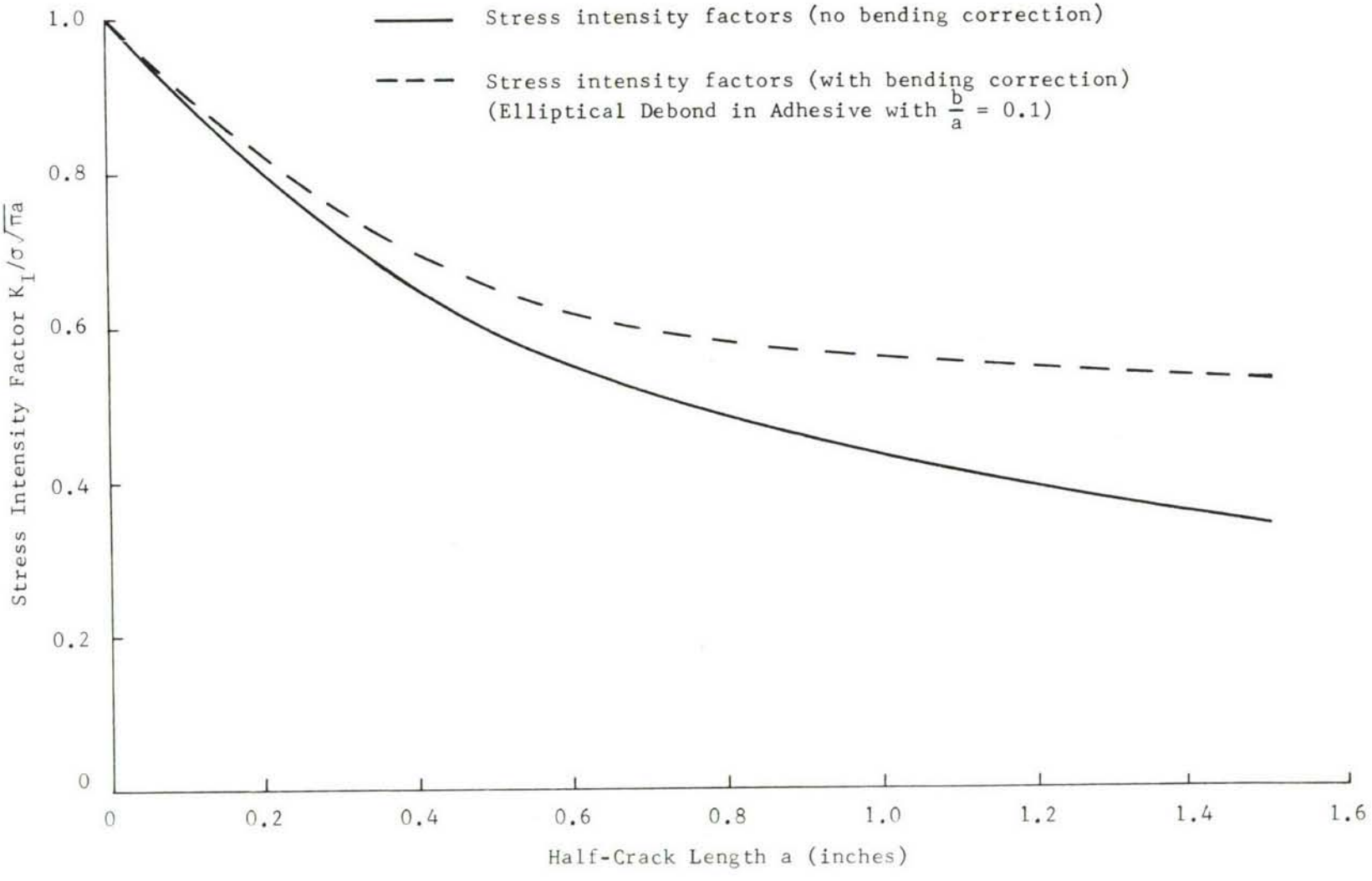

Figure 28. Influence of Bending on Stress Intensity Factors

TABLE 1. BENDING CORRECTION FOR A SIX-INCH (6") WIDE, CRACKED, ADHESIVELY BONDED PANEL

Half Crack Length a ①	$\frac{K_A}{\sigma\sqrt{\pi a}}$ ②	a/W ③	Single Panel Finite Width Correction $\frac{K_s}{\sigma\sqrt{\pi a}}$ ④	Load Transfer factor M = $1 - K_A/K_s$ ⑤	Bending Correction Bc = 0.5 aM (% increase in K_A) ⑥	Corrected Stress Intensity factor = $(1+Bc)K_A$ ⑦
0.25	0.7544	0.0416	1.0041	0.2486	0.0311	0.7778
0.50	0.5897	0.0833	1.0167	0.4200	0.1050	0.6516
1.00	0.4299	0.1667	1.0720	0.5990	0.2995	0.5589
1.25	0.3894	0.2080	1.1196	0.6520	0.4075	0.5480
1.50	0.3422	0.2500	1.1862	0.7115	0.5336	0.5248

and is shown in Column 3. For these values of a/W, finite width correction factors can be obtained from any fracture mechanics handbook (References 11 and 12), and are shown in Column 4. Load transfer factor M, given by $1 - \frac{K_A}{K_s}$, is computed and is shown in Column 5. Bending correction factor Bc is given by 0.5aM and is shown in Column 6. The stress intensity factors corrected for bending are given by (1 + Bc) times those obtained from the two-dimensional analysis, and are shown in Column 7. The plot of bending corrected stress intensity factors is shown in Figure 28. It is seen that for a half-crack length of 1.5 inches in a six-inch wide panel, the stress intensity factors may increase by as much as 53 percent due to bending. These stress intensity factors corrected for bending have shown excellent agreement with those obtained from experiments. Also, using these bending corrected stress intensity factors, it was possible to predict crack growth life within ten percent of actual life.

It may be noted that the bending correction discussed above is applicable to thin plates. Also, it is assumed that entire width of the plate is effective in resisting bending. If the panel width is large in adhesively bonded structure, the influence of bending will be localized in some width on either side of the crack tips. Hence, the effective width resisting bending will be smaller than the width of the plate.

4.4 BENDING CORRECTION FOR CRACKS AT STRESS CONCENTRATIONS

In Section 4.2 bending correction for center crack panels was discussed. In following subsections the application of the method to cracks at stress concentrations is discussed.

4.4.1 Application of Analysis to Cracks at Holes

The method of bending correction, based on a load transfer factor M, has a general application even to cases where cracks are emanating from holes, etc. For the case of a center-cracked panel, the force release was taken as $2a\sigma^{\infty}h_1$, but for cases where cracks are emanating from holes, this stress release will be different. For example, the adhesively bonded structure with a crack emanating from a hole as shown in Figure 29, will have a stress concentration around the hole, hence the stress release will be larger than the center cracked panel. The stress distribution around a hole in an uncracked plate is shown in

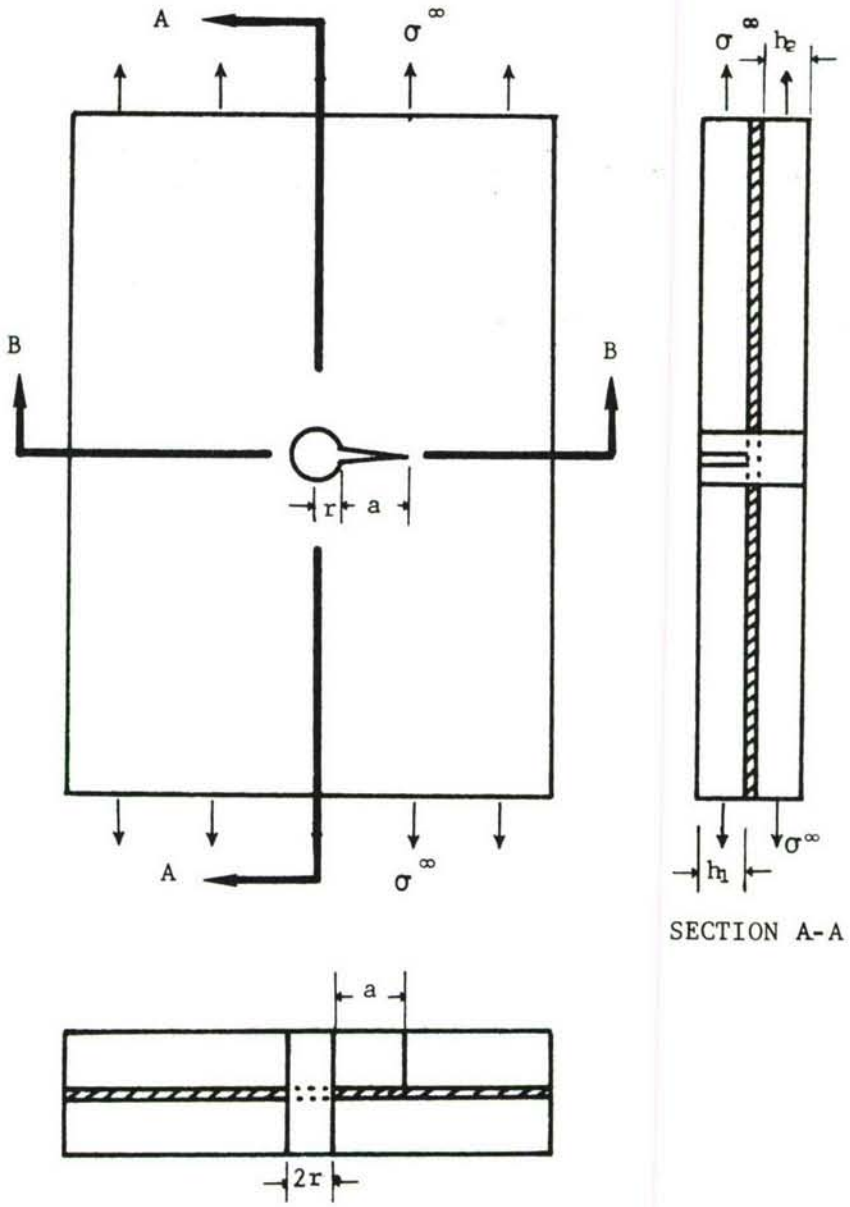

Figure 29. Adhesively Bonded Structure with a Crack at Hole

Figure 30, the stress being σ_1 ($\sigma_1 > \sigma^\infty$) at distance a from the edge of the hole. In the elastic range, the stresses σ_{max} and σ_1 will be directly proportional to the remote applied stress. The shaded area A shown in the figure, multiplied by the thickness of the plate will be the force re release due to the presence of a crack (Figure 30b). Let G be the average stress concentration factor over the entire crack length. The area of the stress diagram in Figure 30a will be $Ga\sigma^\infty$. The load transferred to the sound layer = $ah_1 G\sigma_t = ah_1 GM\sigma^\infty$. The bending moment (couple) caused by load transfer is

$$C = aGM\sigma^\infty h_1 \frac{(h_1 + h_2)}{2} \tag{72}$$

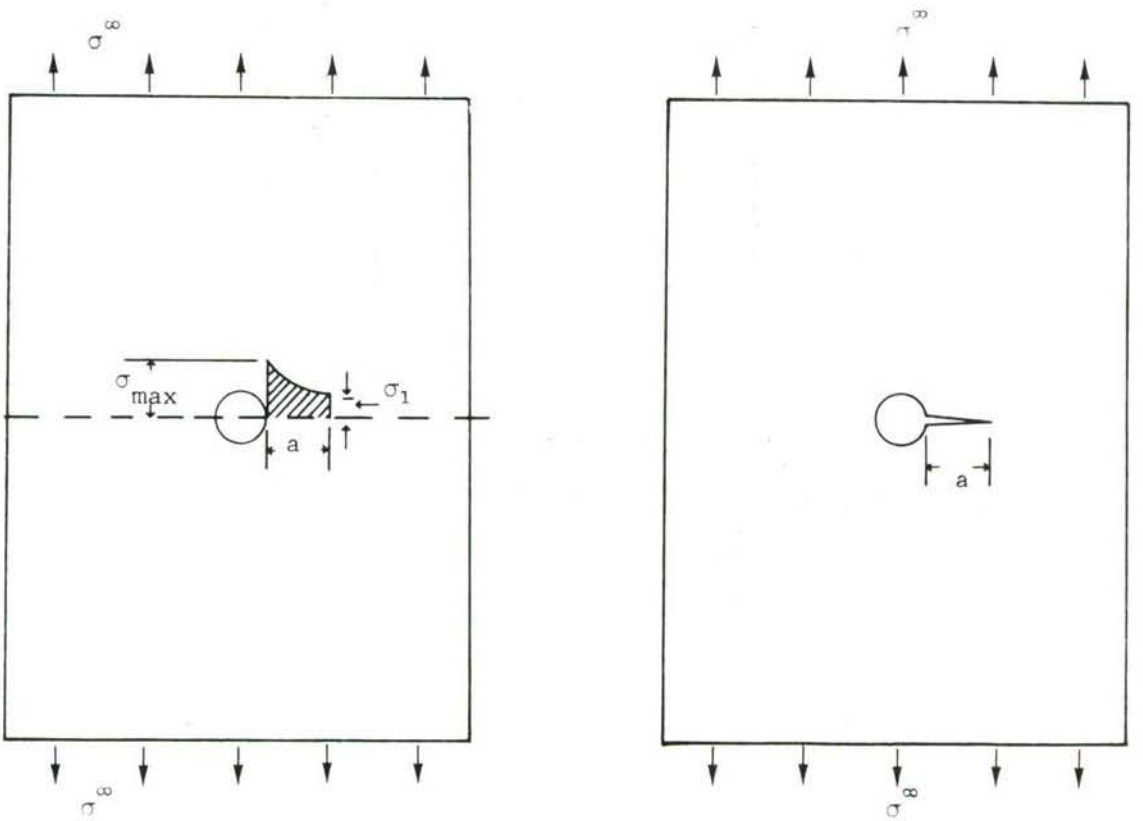

(a) Stress concentration at a hole

(b) Single layer with a crack at a hole

Figure 30. Crack at Stress Concentration

The stress due to bending is

$$\sigma_b = \frac{Cy_{max}}{I} \tag{73}$$

The value of M is given by Equation (70)

$$M = 1 - \frac{K_A}{K_s}$$

where K_A is the stress intensity factor in the adhesively bonded structure (Figure 29), and K_s is now the stress intensity factor for a single layer with a radial crack at a hole (Figure 30b)

4.4.2 Example of Bending Correction for a Crack at Stress Concentrations

Consider the two-ply bonded structure with a crack emanating from a hole, as shown in Figure 29. The panel has a width of 12 inches and a hole diameter of 3/16-inch. Each layer is 7075-T73 aluminum with a thickness of 0.063-inch. The bending moment is given by Equation (72) as

$$C = aGM\sigma^{\infty}h_1 \frac{(h_1 + h_2)}{2}$$

and

$$\sigma_b = \frac{Cy_{max}}{I}$$

For the structure under consideration

$$h_1 = h_2 = h$$

$$y_{max} = h$$

and

$$I = \frac{1}{2} W(2h)^3$$

using these values

$$\sigma_b = \frac{3a\sigma GM}{2W}$$

for $W = 12''$

$$\sigma_b = 0.125\ aGM \tag{74}$$

Various steps in applying bending correction are shown in Table 2. The stress intensity factor for crack at a hole in a single layer (K_s) is obtained by multiplying K_H (stress intensity factor for crack at a hole in a single layer infinite width) by the finite width effects for center crack panels. This finite width correction does not account for the presence of a hole.

The values of K_A are obtained by finite element analysis. The values of G are computed from unknown solutions of stress distributions around holes (e.g. Reference 13).

Table 1 shows that the influence of bending correction on stress intensity factors is significant for large crack lengths. The influence of stress concentration (G) on bending correction is significant for small crack lengths only. The total bending correction at the small crack lengths may be negligible.

TABLE 2. BENDING CORRECTION FOR A PANEL WITH A CRACK AT A HOLE

$a^* = a + r$	a	$\frac{a}{r}$	K_H (CRACK AT A HOLE INFINITE WIDTH)	$\frac{2a}{W}$	FINITE WIDTH CORRECTION (Y)	$K_s = K_H Y$	K_A ADHESIVELY BONDED	G	$M = 1 - \frac{K_A}{K_s}$	Bc = 0.125aGM	CORRECTED STRESS INTENSITY FACTORS
0.2	0.1062	1.13	1.319	0.018	1.001	1.3200	0.9800	1.6487	0.2575	0.0056	0.9855
0.5	0.4062	4.33	0.853	0.068	1.002	0.8547	0.5422	1.2100	0.3656	0.0224	0.5544
1.0	0.9062	9.66	0.750	0.151	1.016	0.7620	0.3654	1.0967	0.5204	0.0646	0.3890
1.5	1.4062	14.99	0.730	0.234	1.031	0.7540	0.2874	1.0720	0.6188	0.1166	0.3210
2.0	1.9062	20.30	0.720	0.318	1.07	0.7704	0.2492	1.0520	0.6765	0.1696	0.2915
3.0	2.9062	31.00	0.707	0.484	1.175	0.8307	0.2150	1.0410	0.7412	0.2803	0.2753

* 3/16-inch hole

SECTION 5

CRITERION FOR THE CRACKING OF A SOUND LAYER

Under cyclic loading a crack may initiate in a sound layer that is directly attached to a cracked layer because there is a large amount of load transfer between cracked and initially sound layers. The load transferred to the sound layer causes high stress concentrations in the load transfer regions, and subsequent cycling initiates a crack. The cracking of an initially sound layer will depend on the level of the load transferred and the number of fatigue cycles applied. As shown in Section 4, the load transferred to the sound layer will depend on the crack length.

A general criterion for the cracking of a sound layer, based on load transfer to the sound layer, is developed here. It is assumed that the initially cracked layer has a small flaw that propagates under fatigue loads. During the crack propagation, the sound layer is subjected to increasing fatigue loads in the load transfer region as the load transfer increases with crack length. When the load transferred to the sound layer reaches a critical value, the crack will initiate in the sound layer. The application of this criterion to various structures is discussed in the following paragraphs.

5.1 CRACKING OF A SOUND LAYER IN CENTER-CRACKED BONDED STRUCTURES

The concept of load transfer factor M was introduced in Section 4 and was defined as the ratio of the load transferred to the cracked layer, to the load released due to the presence of a crack (Equation 63). It is assumed that a crack will initiate in the sound layer when the load transfer factor reaches the critical value M_c, defined as the ratio of the load transferred to the sound layer, to the remote load in this critical portion under consideration. Consider the center-cracked, two-ply, adhesively bonded structure shown in Figure 25a. In this structure, force release

due to the presence of a crack is $2a\sigma^{\infty}h_1$ and the load transfer factor associated with bending for this structure was defined in Section 4 as

$$M = \frac{2ah_1\sigma_t}{2ah_1\sigma^{\infty}} = \frac{\sigma_t}{\sigma^{\infty}}$$

In Section 4, the discussion on interaction between cracked and sound layers was restricted to load transfer without any special consideration to the local distribution of stresses. The sound layer will be subjected to stresses higher than σ^{∞} (remote applied stress), on the crack plane, over a width approximately equal to 2a, with maximum stress expected to occur in the center of the plate. Thus, a crack will initiate at the center of the crack. The method of computing the value of load transfer factor was discussed in Section 4 and calculations for a 6-inch wide panel were shown in Table 1. A plot of load transfer factor M versus half-crack length a for this panel is shown in Figure 31. A similar plot for a 12-inch wide center cracked bonded panel is also shown in the figure.

The experimental data on various center crack two-ply bonded panels showed crack initiation in the sound layer. The experimental values of the crack lengths at which the sound layer cracked for various panels are shown in Table 3. The load transfer factor at these crack lengths is obtained from Figure 31 and is shown in Table 3. It is seen that the value of the critical load transfer factors are fairly constant.

Assuming that the crack initiated in the sound layer when the half-crack length a in the cracked layer was about 0.8 inch, the number of cycles required to propagate a crack from a half-crack length of 0.8 inch to 1.4 inch are shown in Table 3. These cycles may be considered as the cycles for crack transfer to the sound layer.

Also shown in Table 3, are the stress intensity factors in the cracked plate at which the sound layer cracked. It is seen that except for Panel II-16, the values of K_{max} are fairly constant. Hence, it would appear that a crack will initiate in a sound layer when the crack length in an initially cracked layer reaches a critical value, or at a critical stress intensity factor. This criterion for the cracking of a sound layer, based on the critical stress intensity factor in the crack layer, may be valid for a

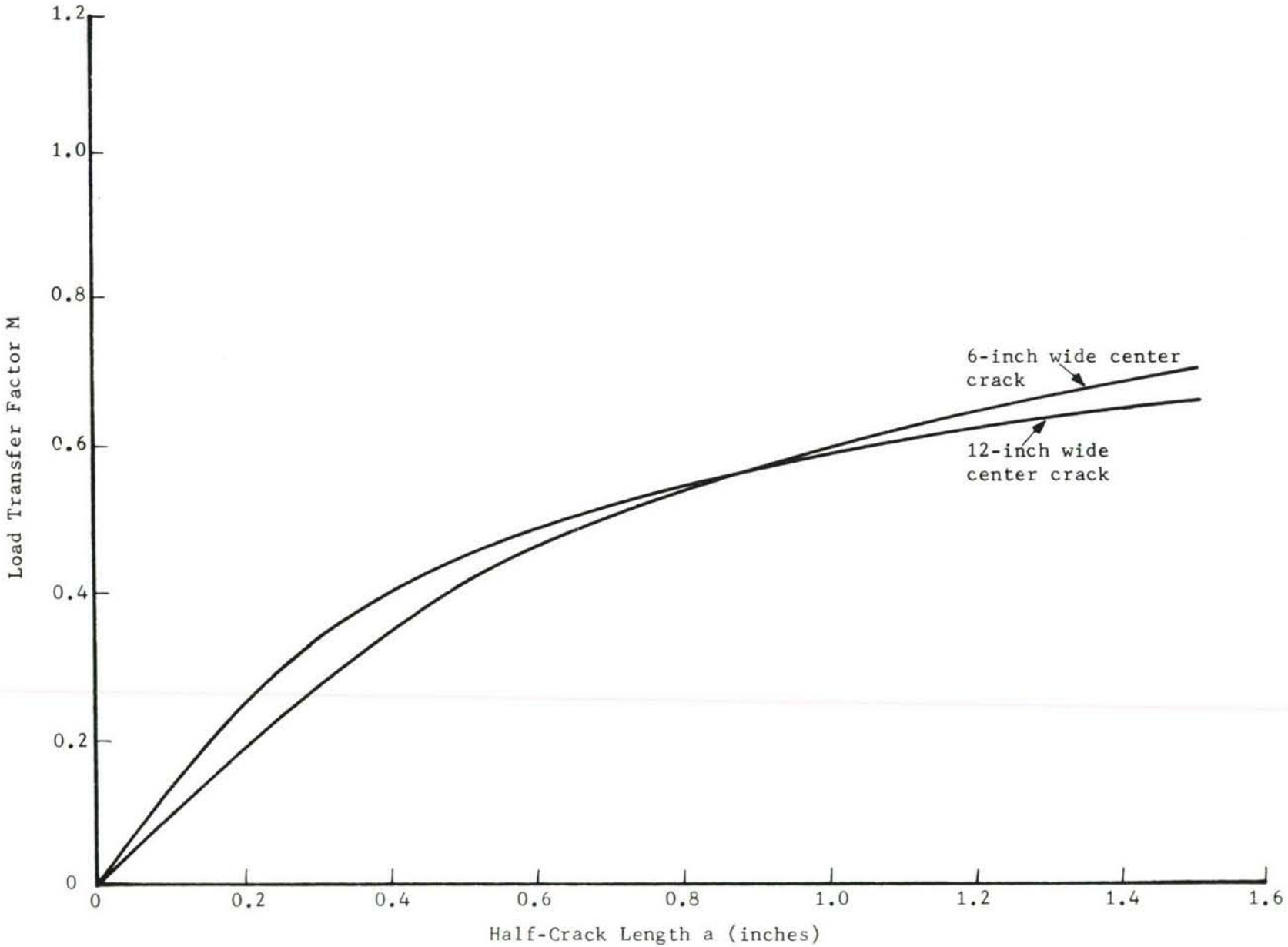

Figure 31. Load Transfer Factor M versus Half-Crack Length a

TABLE 3. CRITICAL LOAD TRANSFER FACTORS FOR THE CRACKING OF A SOUND LAYER

SPECIMEN AND TYPE OF FLAW	SECOND PLY CRACKING AT a = AND LOCATION ( ) (inches)	CRITICAL LOAD TRANSFER FACTOR M_C (inches)	N CYCLES FOR CRACK TRANSFER	K_{max}** Ksi $\sqrt{in}$
Center Crack				
I-1				
12" Wide	1.363 (A)	0.640	33,400	15.870
h_a = 0.0125"	1.433 (B)	0.645	37,400	16.220
	1.339 (C)	0.635	34,000	15.730
II-2				
12" Wide	1.357 (A)	0.645	33,800	15.620
h_a = 0.0125"	1.295 (B)	0.631	37,500	15.230
II-16				
12" Wide	1.114 (A)	0.605	12,400	19.480
h_a = 0.008"	1.270 (C)	0.630	14,100	20.560
II-10				
6" Wide	1.353 (B)	0.657	36,500	15.480
I-11				
6" Wide	1.382 (A)	0.680	35,000	15.890
h_a = 0.015"	1.460 (C)	0.685	34,500	16.180
	Average M_C =	0.645		

**Stress intensity in the cracked layer when the sound layer cracked

particular geometry, however, it will not be generally applicable due to the fact that for cracks emanating from holes, there is a large load transfer to the sound layer near the holes even though the corresponding stress intensity factors may not be high.

5.2 CRACKING OF A SOUND LAYER IN AN ADHESIVELY BONDED STRUCTURE WITH A CRACK AT A HOLE

Consider the case of a crack emanating from a hole in a two-ply bonded structure as shown in Figure 29. In such a structure, the presence of a hole

causes stress concentration with a maximum value at the edge of the hole, as shown in the single layer of Figure 30a. Hence, in a bonded structure with a crack at a hole, maximum load transfer to the sound layer will be at the edge of the hole. Thus, a crack in the sound layer will initiate at the edge of the hole when the load transfer factor there reaches a critical value. In computing the critical load transfer factor, some arbitrary width of plate ϵ around the hole has to be defined.

For computing the critical load transfer factor, it is assumed that a plate width of ϵ = 0.1 inch near the hole is effective, as shown in Figure 32. For an uncracked plate with a crack at a hole, let the shaded area (over 0.1 inch width, Figure 32, of the plate) be given by $0.1\,H\sigma^{\infty}$, H being the average

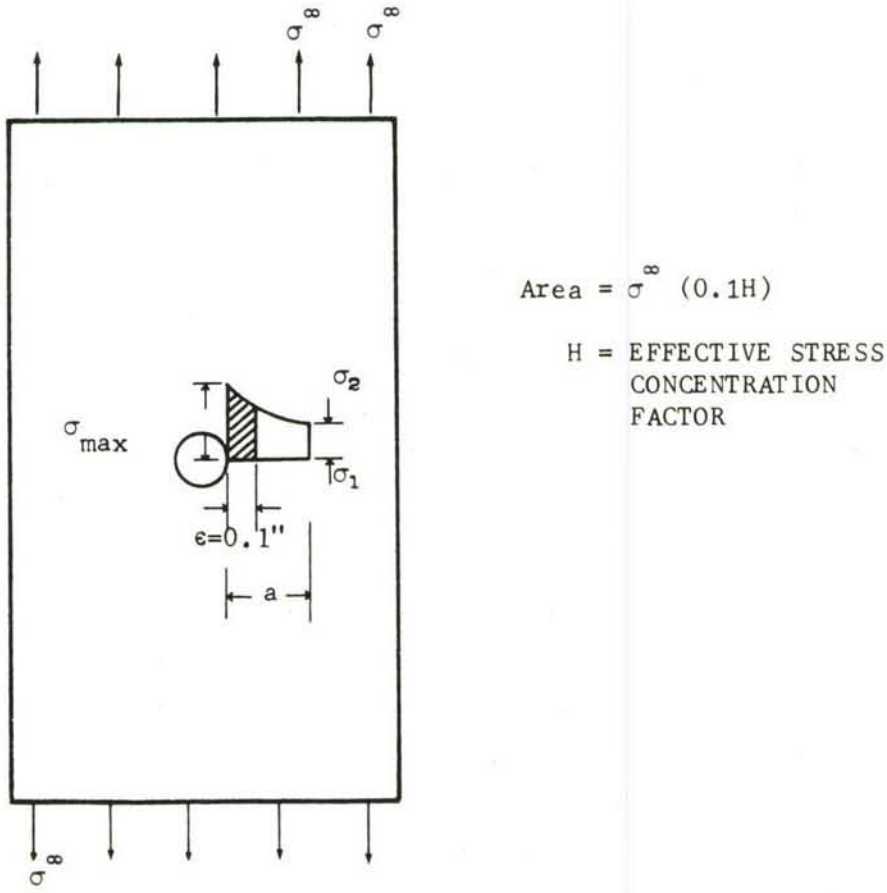

Figure 32. Effective Width for the Critical Load Transfer Factor

stress concentration factor over 0.1 inch width. The load released is equal to $0.1h_1 H\sigma^{\infty}$ and the load transferred to the sound layer equals $h\sigma_t(0.1)h_1 = 0.1h_1 HM\sigma^{\infty}$. The local load transfer factor associated with crack transfer is M^*

$$M^* = \frac{0.1HM\sigma^{\infty}h_1}{0.1\sigma^{\infty}h_1}$$

$$= HM$$

= Average stress concentration factor x load transfer factor

The average stress concentration factor H for a plate with a 3/16-inch diameter hole over 0.1-inch wide, is 1.693

5.3 EXAMPLE OF THE CRACKING OF A SOUND LAYER IN A PANEL WITH A CRACK AT A HOLE

The load transfer factor M for a two-ply, 12-inch bonded structure with a crack at a central hole, was computed in Section 3 and shown in Table 2. Using these values, local load transfer factor M^*, corresponding to $\epsilon = 0.1$ (H = 1.693), was computed. The plot of the local load transfer factor M^* as a function of crack length a, is shown in Figure 33. The figure also shows the plot of local load transfer factor M^* for a 12-inch wide panel with a crack at an eccentric hole.

The value of critical load transfer factor M_C at the cracking of the sound layer was observed to be 0.645, from Table 3 for center-cracked panels. Using this value of M_C, the crack length at which a crack will initiate in the sound layer for the panel with a crack at a hole, is obtained from Figure 33. These crack lengths are 0.415 inch for the crack-at-a-central-hole panel and 0.385 inch for the crack-at-an-eccentric-hole panel. Table 4 shows the comparison of experimental and predicted crack lengths at which the cracking of the sound layer takes place in various crack-at-a-hole panels. It is seen that the correlation between predicted and experimental

TABLE 4. PREDICTED CRACK LENGTHS FOR CRACKING OF A SOUND LAYER

SPECIMEN AND TYPE OF FLAW	SECOND PLY CRACKING AT a = AND LOCATION ( ) (inches)	PREDICTED 'a' FOR SECOND PLY CRACKING (inches)	K_{max}** Ksi $\sqrt{in}$
Crack at a central hole			
I-5			
12" wide	0.370 (A)	0.415	9.924
h_a = 0.007"	0.395 (B)	0.415	9.900
	0.360 (C)	0.415	9.957
II-22			
12" wide	0.528 (A)	0.415	9.198
h_a = 0.007"	0.420 (B)	0.415	9.935
	0.403 (C)	0.415	9.910
I-24			
6" wide	0.495 (A)	0.415	10.488
h_a = 0.01"	0.395 (B)	0.415	10.070
	0.423 (C)	0.415	10.280
Average	0.421	0.415	9.962
Crack at an eccentric hole			
II-12			
12" wide	0.364 (A)	0.385	9.843
h_a = 0.009"	0.328 (B)	0.385	9.827
	0.384 (C)	0.385	9.935
Average	0.359	0.385	9.868

**Stress intensity in cracked layer at sound layer cracking.

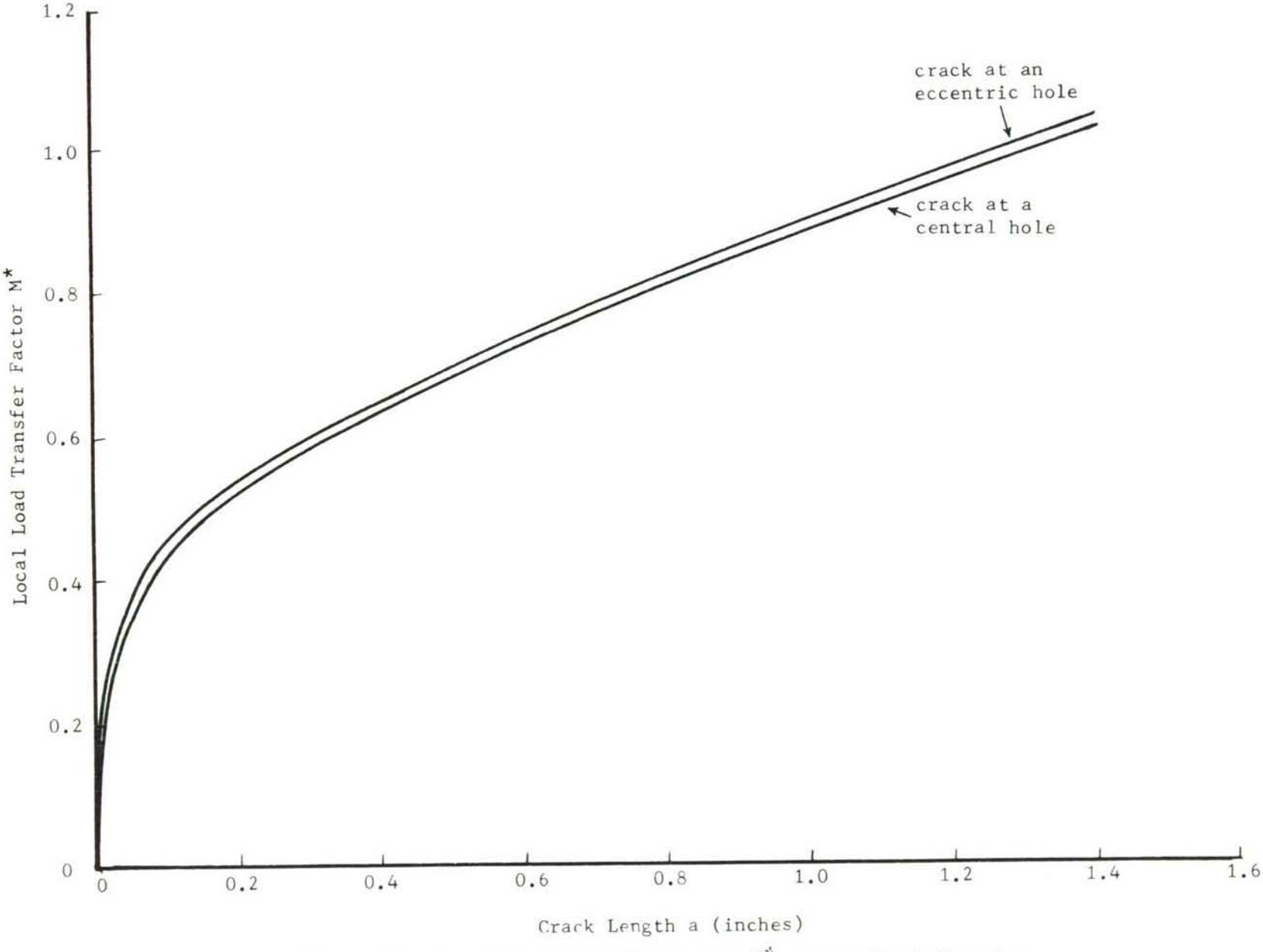

Figure 33. Local Load Transfer Factor M^* versus Crack Length a

values is good. The table also shows that the stress intensity factors in the cracked layer at the cracking of the sound layer are fairly constant. However, these values differ significantly from those for the case of the center-cracked panel. Hence, the cracking of a sound layer could not be based on the critical load transfer factor in a cracked layer.

The predicted values of crack lengths at the cracking of a sound layer will be affected by the assumed plate width ϵ for the local load transfer factor. The value of average stress concentration factor H will depend on the value of ϵ. For ϵ = 0.05 and 0.15, the values of H are 2.047 and 1.533, respectively. The values of local load transfer factor M^* for ϵ = 0.05, 0.1, and 0.15 are shown in Table 5 for a 12-inch wide panel with a crack at a central hole. The plot of local load transfer factor M^* as a function of crack length a for the three values of ϵ is shown in Figure 34. Using the value of critical local transfer factor M_c as 0.645, the predicted crack lengths for the cracking of a sound layer are shown in the Figure 33. The predicted crack lengths may vary between 0.255 inch and 0.485 inch for ϵ between 0.05 inch and 0.15 inch.

TABLE 5. LOCAL LOAD TRANSFER FACTOR FOR A 12-INCH WIDE PANEL WITH A CRACK AT A CENTRAL HOLE

a+r* (inch)	a (inch)	$\frac{a}{r}$	$M=1-\frac{K_A}{K_s}$	$M^* = MH$ = 2.047M (ϵ = 0.05")	$M^* = MH$ = 1.693M (ϵ = 0.1")	$M^* = MH$ = 1.533M (ϵ = 0.15")
0.2	0.1062	1.13	0.2575	0.5271	0.4360	0.3947
0.5	0.4062	4.33	0.3656	0.7484	0.6190	0.5605
1.0	0.9062	9.66	0.5204	1.0653	0.8810	0.7978
1.5	1.4062	14.99	0.6188	1.2667	1.0476	0.9486
2.0	1.9062	20.30	0.6765	1.3848	1.1454	1.0371
3.0	2.9062	31.00	0.7412	1.5172	1.2550	1.1363

*3/16-inch hole

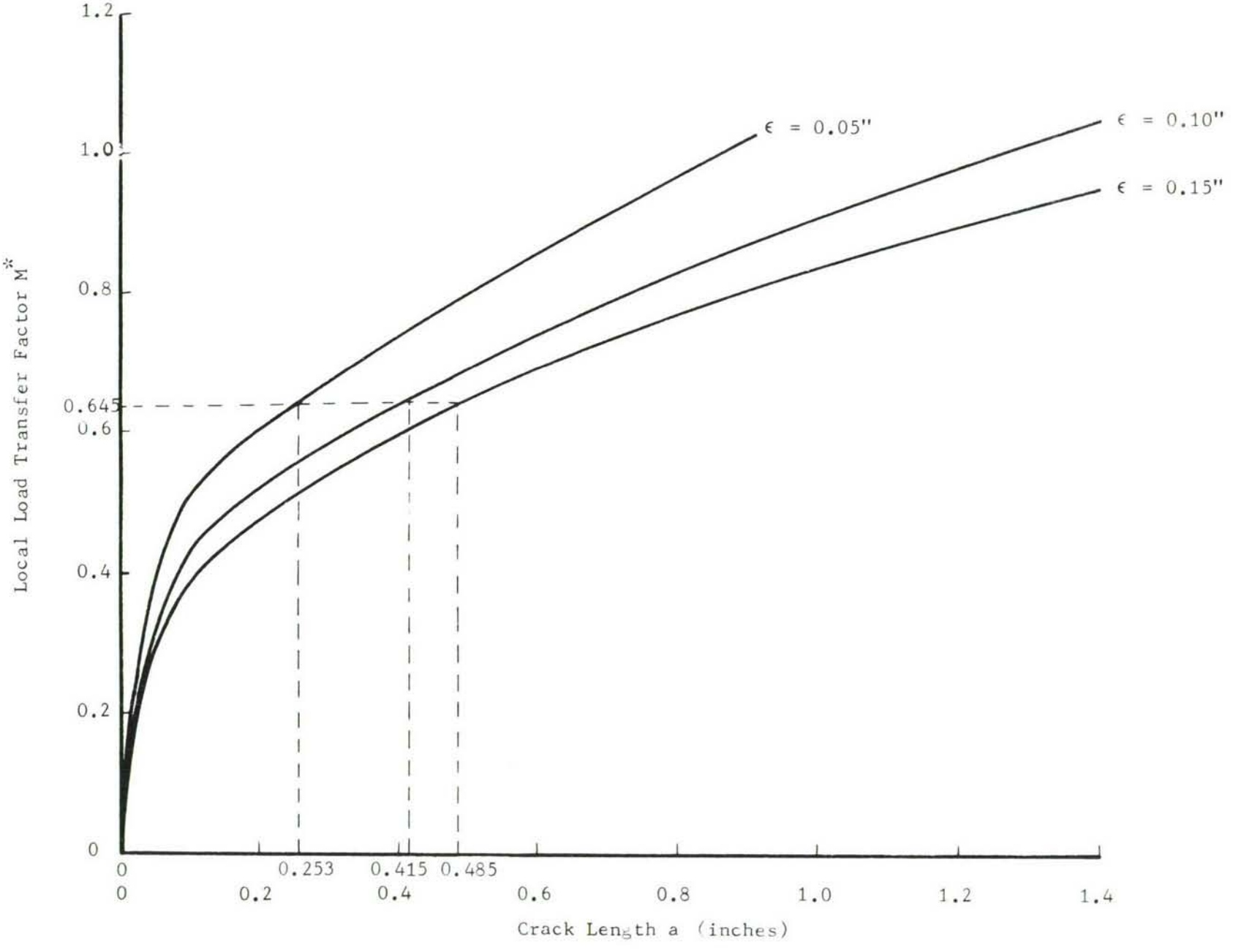

Figure 34. Local Load Transfer Factor M^* versus Crack Length a for Various Values of ϵ

5.4 LIMITATIONS OF CRACK TRANSFER CRITERIA

The crack transfer criteria based on critical load transfer factor M_c are applicable to cases where the cracked layer and sound layer are approximately the same thickness. The value of M_c may depend on the material and thickness of the sound layer. The thickness and the modulus of the sound layer material are taken into consideration in the analysis. However, the metallurgical factors will influence the initiation of a crack in the sound layer, hence the value of M_c may be different for different materials and thicknesses.

All but one test was conducted at same maximum stress. In Table 3, panel II-16 had a maximum stress about 30 percent higher than that for the other panels. The value of M_c for this panel is still within the experimental data scatter. The value of maximum stress may have some effect on the value of critical load transfer factor M_c.

SECTION 6

ANALYSIS OF DEBOND PROPAGATION

Cracked, adhesively bonded structures subjected to cyclic loading exhibit debonding in the adhesive layer around the crack. The debond propagates as the crack in the metallic layer propagates. The rate of debond propagation will depend on the type of adhesive and load transferred to the sound layer through the adhesive. The load transferred through the adhesive will depend on the properties and thicknesses of the adhesive and adherend materials and the applied loads. The propagation of the debond will be governed by the criterion connected with the failure of the adhesive. For materials exhibiting plastic deformation, a simple criterion for failure of the adhesive could be the critical strain. It may be assumed that the adhesive has failed if the strain in the adhesive reaches a critical value. This critical value of strain may be taken as the strain at failure in a static test on the adhesive. Based on these assumptions, a criterion for the propagation of a debond was developed in this research program. The details of this criterion for debond propagation and its application to various crack geometries is discussed in the following paragraphs.

6.1 CRITERION FOR THE PROPAGATION OF A DEBOND

Consider a single-layer plate with a crack, as shown in Figure 35a. Under applied loading the crack will open, as shown in Figure 35b. Next, consider a case where this plate is the cracked layer in a two-layer, adhesively bonded structure (Figure 1). In such a structure, the crack opening will be smaller than the single-layer opening, as shown in Figure 35c. The reduction in the crack opening will depend on the load transferred to the uncracked layer, which is a function of the thickness and material properties of the adhesive and adherends. Also, the presence of a crack in one layer of a bonded structure gives rise to out-of-plane bending. This load transfer to the sound layer and the out-of-plane bending will

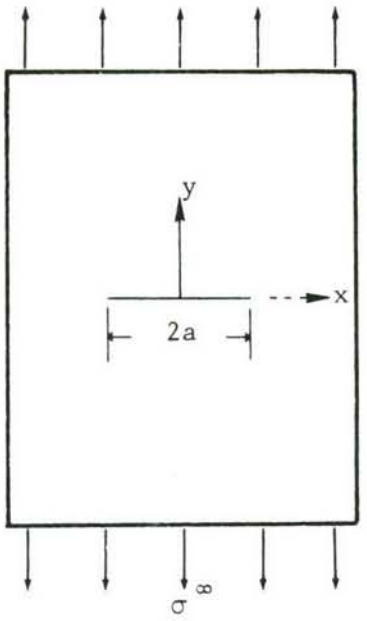

(a) Single-layer Plate with a Crack

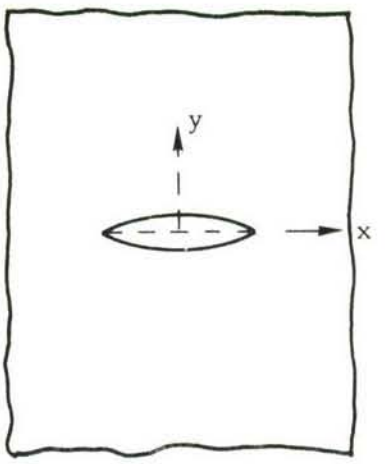

(b) Crack Opening in a Single-layer Plate

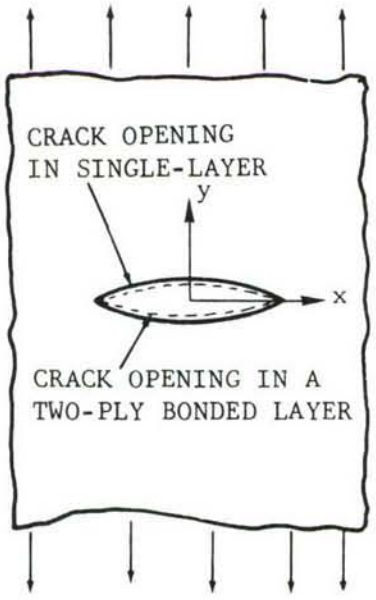

(c) Crack Opening in a Two-ply, Adhesively Bonded Structure

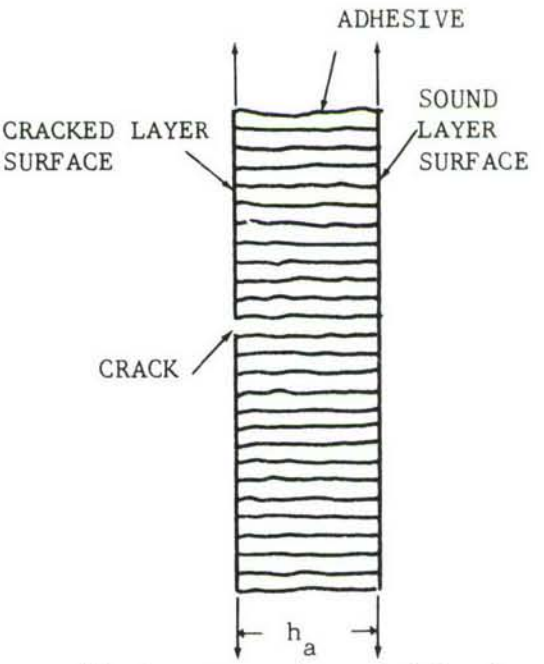

(d) Cross-section of Adhesive in a Two-ply, Cracked, Bonded Structure

Figure 35. Crack Openings in Cracked Structures

create normal and shear stresses in the adhesive. If both layers had cracks of the same size, the crack openings in both layers would be the same, and there would be no shear or normal stresses in the adhesive.

Consider the cross-section of the two-ply, bonded structure shown in Figure 35d. The displacements in the cracked and sound layer far from the crack plane will be the same, hence no load transfer through the adhesive. In the vicinity of the crack plane, the cracked sheet will undergo large deformation compared to the sound layer, with the result that the adhesive on the surface of the cracked plate will deform more in the y direction than the adhesive on the surface of the sound layer. The difference in the deformation of the two plates will depend on the distance from the crack plane. The adhesive in the bonded structure may be looked on as a discrete element (both in the x and y directions) connecting two plates, as shown in Figure 36a. These elements are denoted by $A_1 B_1$, $A_2 B_2$, $A_3 B_3$, etc. (at $x = 0$), and $D_1 E_1$, $D_2 E_2 \ldots$, $F_1 G_1 \ldots$ at other x locations, as shown in Figure 36c. Under applied loads, the elements will undergo deformation (Figure 36b). The points A_1, B_1, $A_2, B_2 \ldots$ will displace to A'_1, B'_1, A'_2, $B'_2 \ldots$, respectively, as shown in Figure 36b, which also shows that the displacements are larger in a cracked plate. Point A_1 displaces V_{C1} and B_1 is displaced by V_{S1}. The relative displacement of the two points will be $V_{C1} - V_{S1}$.

The strain ϵ_1 in the adhesive (element $A_1 B_1$ at $x = 0$), is given by

$$\epsilon_1 = \frac{V_{C1} - V_{S1}}{h_a} \qquad (\text{at } y = 0) \tag{76}$$

Similarly, strain ϵ_2, ϵ_3, ϵ_4, in elements $A_2 B_2$, $A_3 B_3$, and $A_4 B_4$ (at $x = 0$) is given by

$$\epsilon_2 = \frac{V_{C2} - V_{S2}}{h_a} \qquad (y = y_1)$$

$$\epsilon_3 = \frac{V_{C3} - V_{S3}}{h_a} \qquad (y = y_2)$$

$$\epsilon_4 = \frac{V_{C4} - V_{S4}}{h_a} \qquad (y = y_3) \tag{77}$$

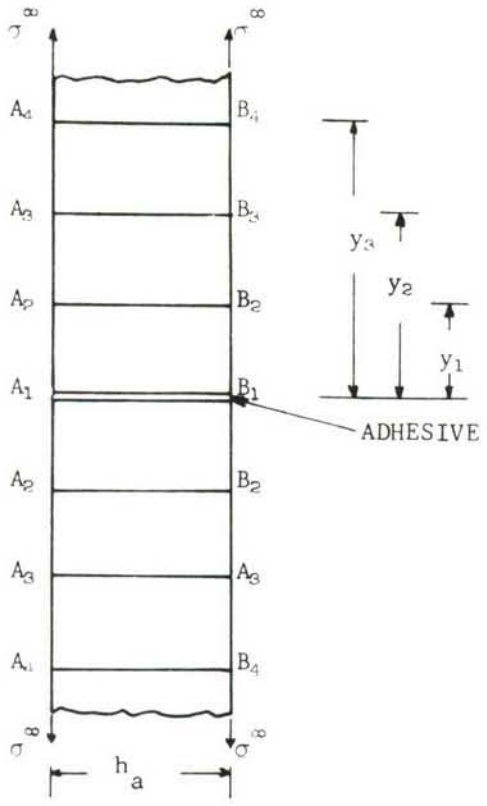

(a) Cross-section showing representation of adhesive at x = 0

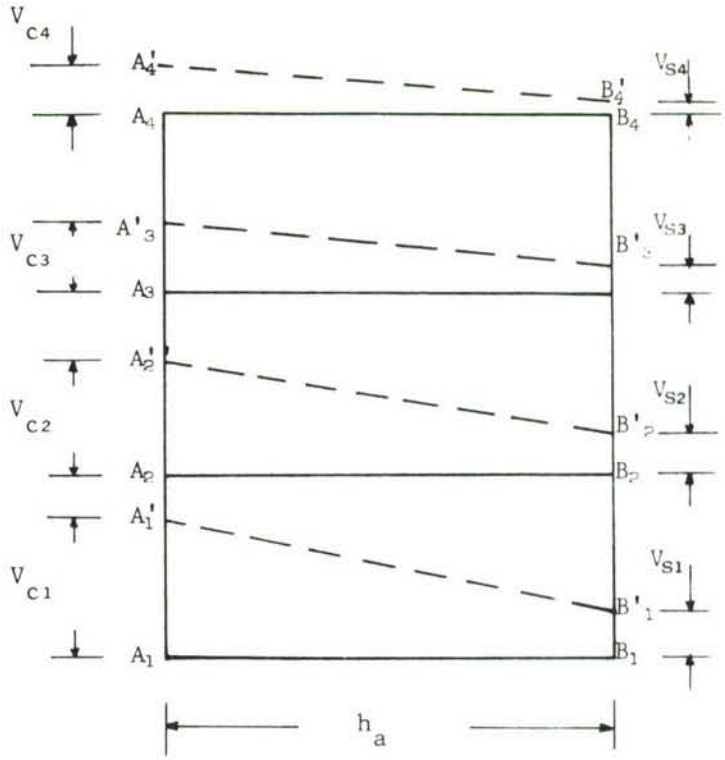

(b) Displacements in plates (upper half only)

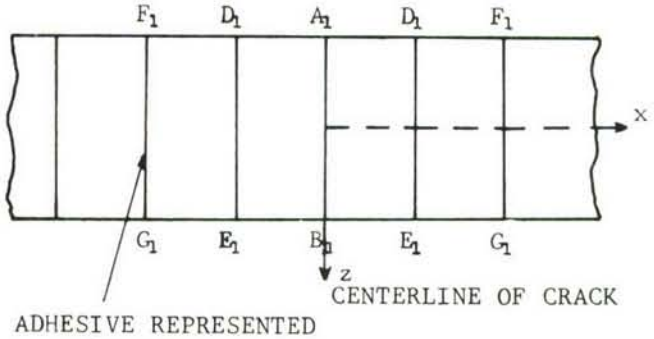

h_a = Adhesive thickness

(c) Sectional plan at y = 0 showing representation of adhesive

Figure 36. Discrete Element Representation of Adhesive

In general, the strain ϵ, at any location is given by

$$\epsilon = \frac{V_c - V_s}{h_a} \tag{78}$$

The value of the strain will decrease as the distance from the crack plane increases. The strains at other x locations (elements $D_1 E_1$ ....Figure 36c) can be obtained in a similar manner. The adhesive will fail if the strain in the adhesive reaches a critical value ϵ_R, which is defined as the resistance of the adhesive to fracture. ϵ_R is taken as the failure strain of the adhesive from the tensile test on the adhesive.

The displacements V_c and V_s in cracked and sound layers are obtained from the mathematical or finite element analysis of the cracked, adhesively bonded structures at a particular crack length a_o. The strain in the adhesive is obtained from these displacements using Equation 78. The strain in the adhesive is obtained from the displacements at various (x, y) locations and from this, lines of constant strain ϵ in the adhesive can be plotted. These lines are schematically shown in Figure 37. The debond shape and size will be given by the curve corresponding to critical strain ϵ_R. The predicted shape of the debond in an adhesively bonded structure corresponds to a particular crack length a_o in the cracked layer.

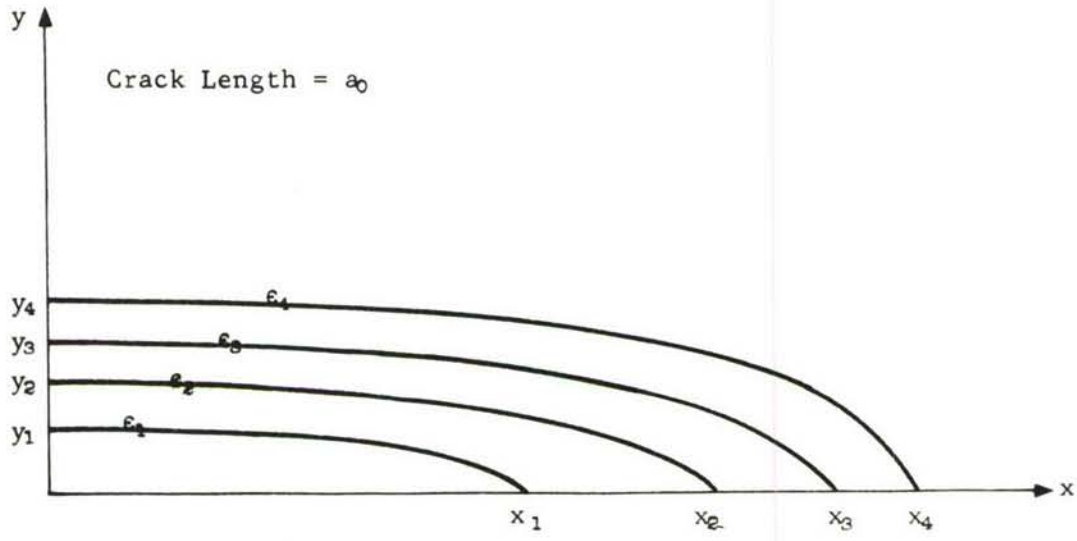

Figure 37. Lines of Constant Strain in Adhesive for a Fixed Applied Stress in a Bonded Structure (one-quarter of contours shown)

As the crack propagates under fatigue loads, the crack opening and load transfer to the sound layer will increase, hence the relative displacements between the two layers will increase, or the strain in the adhesive at various x, y locations will continue to increase. As soon as the strain at any (x, y) location in the bonded region reaches the critical strain ε_R, the adhesive will fail, hence the size of the debond will increase. Thus, the size of debond can be determined for every crack length as the crack in the cracked layer propagates. From the above criterion of debond propagation, the following points are observed.

1. The size of the debond is dependent on the adhesive thickness and properties. From Equation (78), it is seen that if the thickness of the adhesive is large, the strain in the adhesive will be small, hence the size of the debond will be small. If the adhesive thickness is very large, the size of the debond may be zero.

2. The size of the debond will depend on the applied loads (σ_{max} for fatigue loads). The large applied loads will cause large crack openings, hence large shear strain in the adhesive.

3. The size of the debond will depend on the relative elastic properties of the sound and cracked layer, as these will influence the relative displacement between the two layers.

6.2 PROCEDURE FOR OBTAINING CONSTANT STRAIN LINES

The size of debond is determined by constant strain lines. The following analytical steps are observed to obtain constant strain lines.

1. The finite element or mathematical analysis of the cracked bonded structure under consideration is carried out assuming no debond (if debond size not known), or assuming known debond.

2. The displacements in the y direction, at various locations around the crack, in the cracked and sound layer are obtained at the known applied load. Using these displacements and Equation (78), the strain in the adhesive at various locations is obtained.

3. The strain in the adhesive can be plotted (corresponding to any applied load) as a function of distance x from the centerline of the crack for various distances from the y plane. These plots are schematically shown in Figure 38. The figure also shows the line corresponding to strain ϵ_1. It is seen that line y = 0 cuts line ϵ_1 at $x = x_0$, hence on the y = 0 plane, the strain in the adhesive is larger than ϵ_1, up to $x = x_0$. For x greater than x_0, the strain in the adhesive at y = 0 is smaller than ϵ_1. Thus, one end of the constant strain line will be at y = 0 and $x = x_0$. At x = 0, the line ϵ_1, cuts the $y = y_3$ line, hence for y greater than y_3, the strain in the adhesive is less than a ϵ_1, thus the other end of the constant strain line is at x = 0 and $y = y_3$. The other boundaries of the constant strain line (Figure 38) are, at $x = x_1$, $y = y_1$, and at $x = x_2$, $y = y_2$. Thus the shape of the constant strain line corresponding to ϵ_1, is obtained. Similar lines can be obtained for other ϵ values. The lines of constant strain are shown in Figure 37.

4. The size of debond is given by constant strain line having a strain equal to critical strain ϵ_R.

5. If the analysis was carried out assuming no debond in the adhesive and the predicted debond size is large, the finite element or mathematical analysis is carried out again assuming the predicted debond size of Step 4 in the adhesive. Using this new analysis, the size of the debond is predicted again. Thus, an iteration process will be necessary to compute the debond size. However, if the predicted debond size in Step 4 is small, the iteration process need not be done and the predicted debond size (based on assuming no debond in the adhesive) will be close to actual debond size.

6.3 DEBOND PREDICTION IN A TWO-LAYER, ADHESIVELY BONDED STRUCTURE WITH A CENTER CRACK

A two-ply, adhesively bonded structure 12 inches wide, with a center crack (Figure 1) is considered. The structure has a half-crack length of

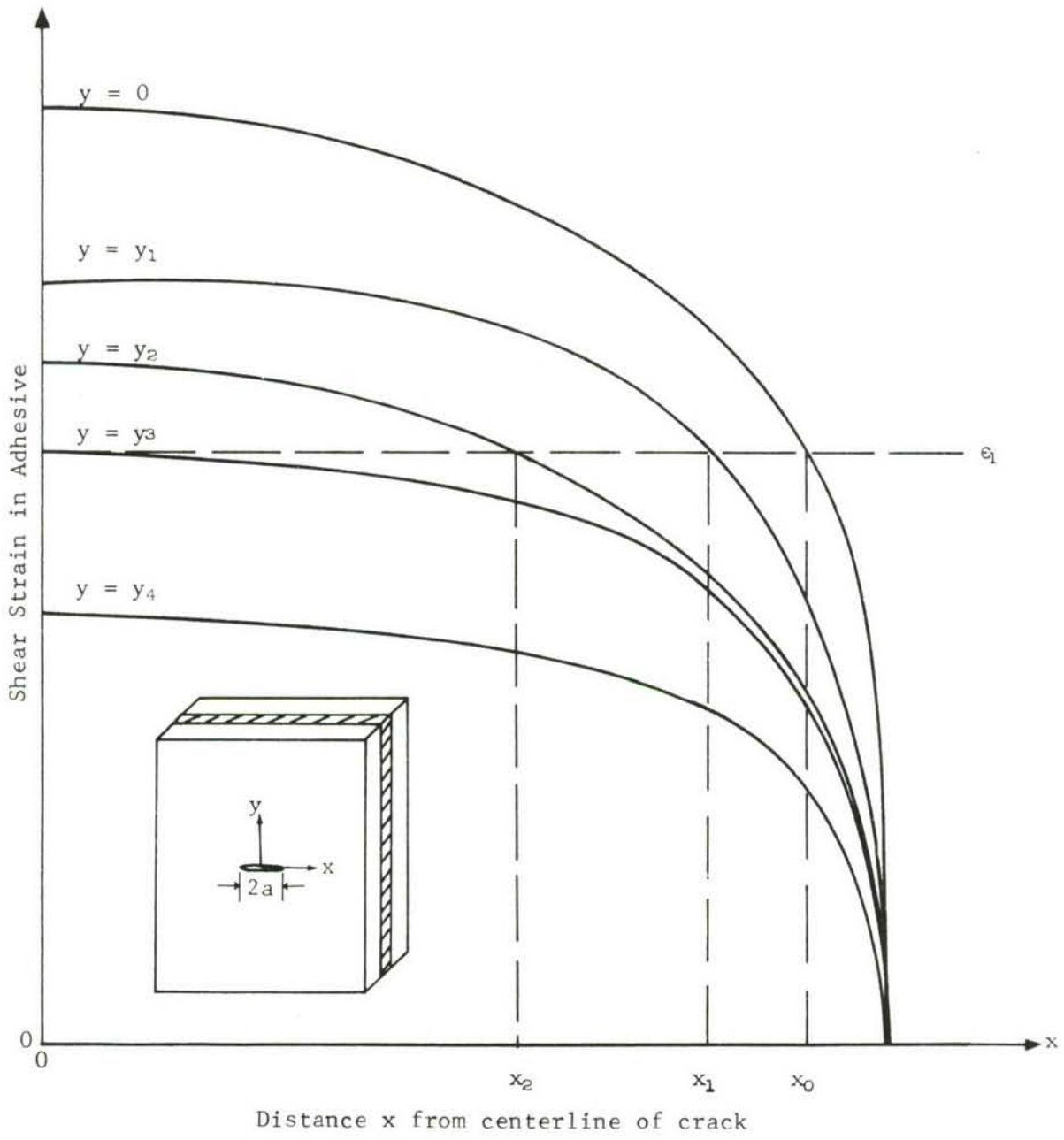

Figure 38. Schematic Variation of Adhesive Strain with Distance from Centerline of Crack for Various Values of y (one-quarter of the panel considered)

one inch and the maximum applied stress is 15,500 psi. From the finite element analysis (assuming no initial debond in the adhesive), the displacements in the y direction at various grid points (x, y locations) are known. The shear strain in the adhesive will be given by Equation (78). The thickness of the adhesive layer for the panel is taken as 0.008 inch. The values of strain are computed at various (x, y) locations around the crack and plotted as a function of x for various values of y, as shown in Figure 39. The value of critical strain for adhesive FM-73 is approximately 0.04 (Reference 14) and is also shown in Figure 39. From the figure, at x = 0, all points greater than y = 0.11 (by interpolation) will have a strain less than a critical strain, thus the boundary of debond at x = 0 is y = 0.11. Similarly, other points on the boundary of the debond are given by

$$y = 0.10 \text{ at } x = 0.60$$
$$y = 0.05 \text{ at } x = 0.82$$
$$y = 0 \quad \text{at } x = 0.95$$

The predicted shape of the debond (one-quarter) is shown in Figure 40a by the area between Curve A and the x and y axes. It may be noted that the shape of the debond is approximately elliptical and similar to the shape of the crack openings.

6.4 DEBOND PREDICTION IN A CRACKED PLATE WITH AN ADHESIVELY BONDED STRINGER

Consider the cracked plate with an adhesively bonded stringer (Figure 14). For this structure, the crack surface openings, as a function of the distance from the centerline of the crack obtained from finite element analysis assuming no debond, are plotted in Figure 41 for various crack lengths. For crack lengths smaller than the width of the stiffener, the shape of the crack surface displacement curve is elliptical, hence the debond shape will be similar to the case of the center crack in a two-ply, adhesively bonded panel. The predicted shape for a = 0.75 is shown in Figure 40b. For crack lengths larger than the width of the stiffener, the crack surface openings show an increasing trend toward the edge of the stiffener, as shown in Figure 41. The shape of the debond will be different in this case. The relative displacement at various (x, y) locations are

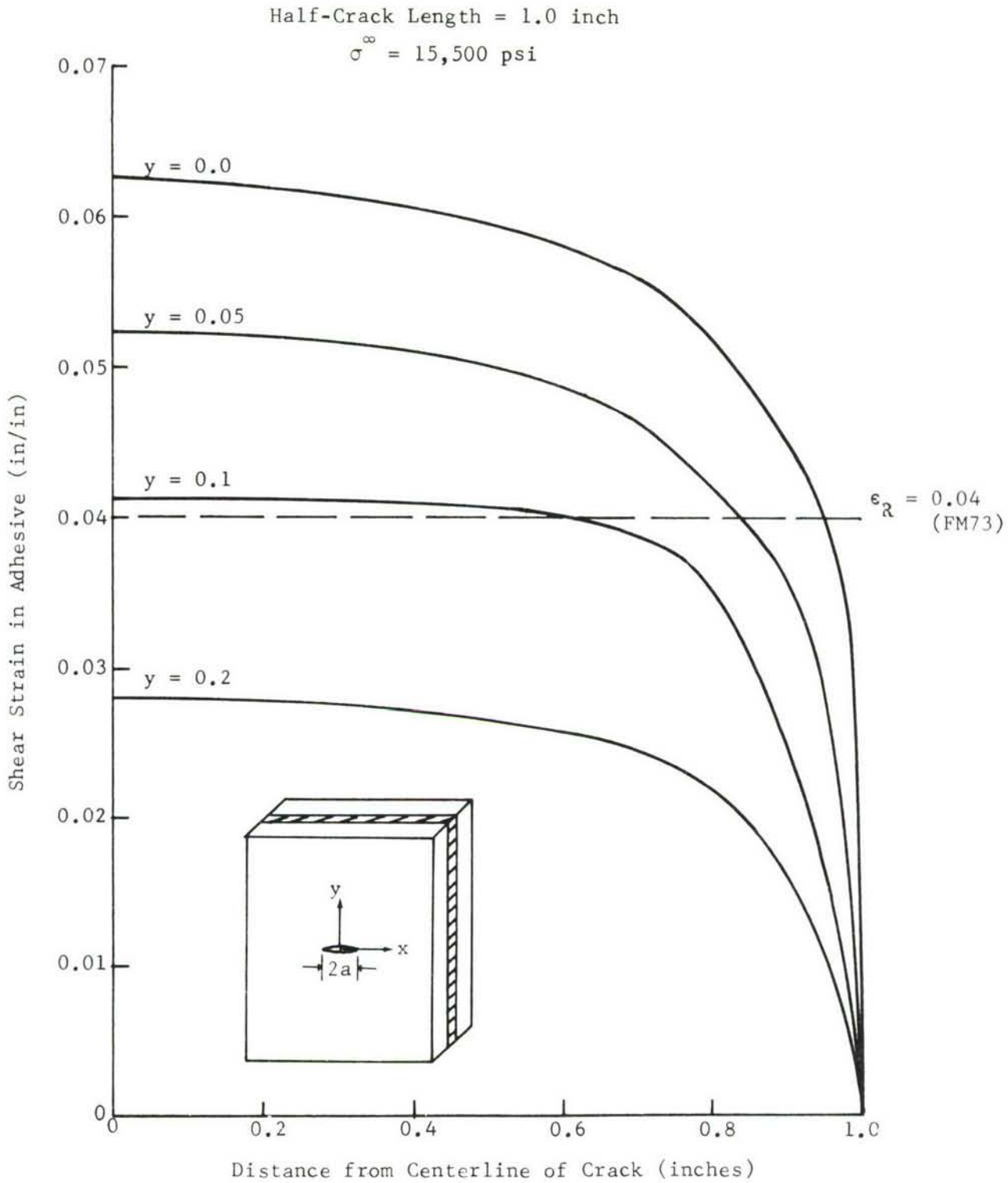

Figure 39. Variation of the Shear Strain in the Adhesive with the Distance from the Centerline of the Crack, for a Two-Ply, Bonded Structure, with a Center Crack (one-quarter of the panel considered)

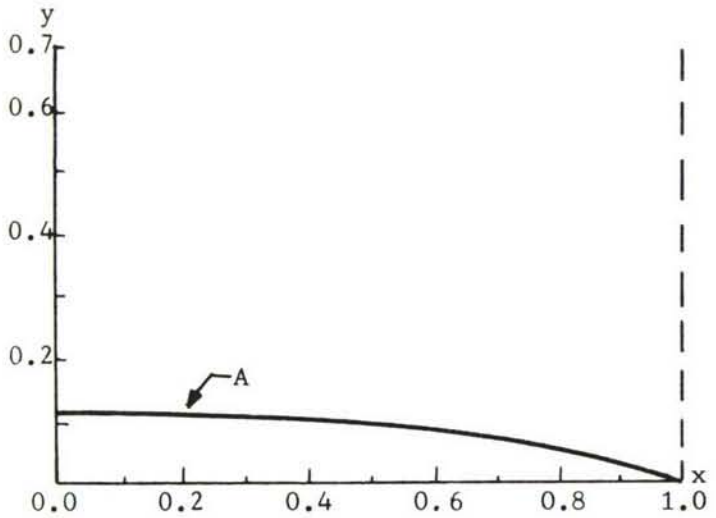

(a) Two-ply bonded panel with a center crack in one ply (one-quarter of debond shown, a = 1.0 inch)

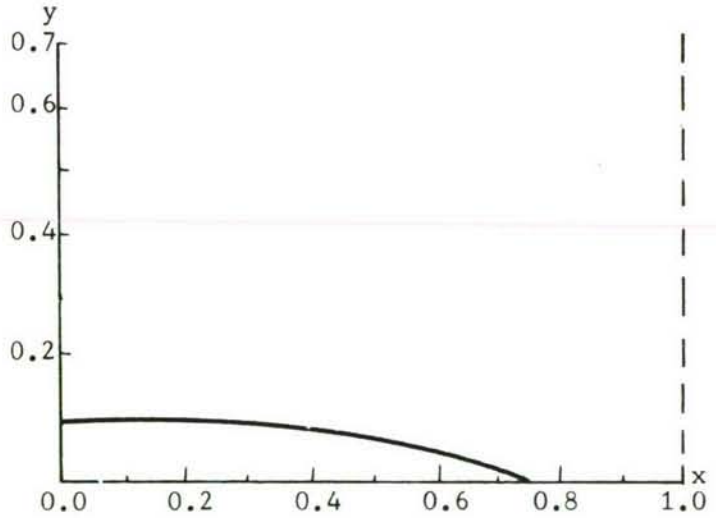

(b) Cracked plate with a bonded stiffener (one-quarter of debond shown, a = 0.75 inch)

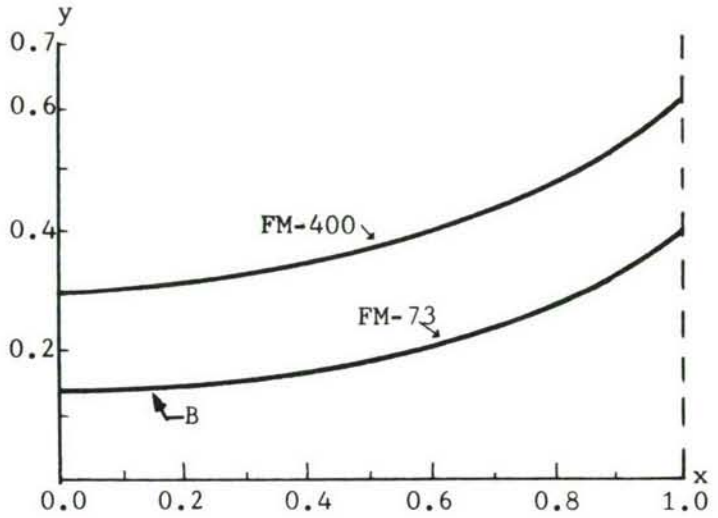

(c) Cracked plate with a bonded stiffener (one-quarter of debond shown, a = 2.0 inches)

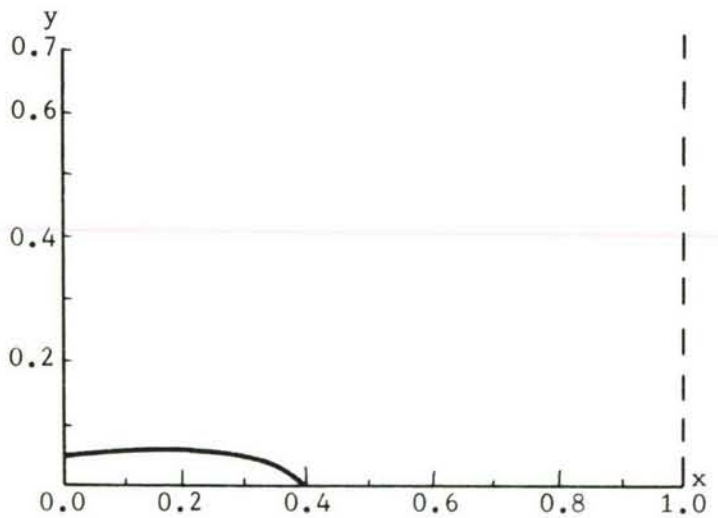

(d) Panel with a crack at a hole (one-half of debond shown, a = 0.406 inch)

Figure 40. Predicted Debond Shapes at Applied Stress of 15.5 ksi for Various Panels (all dimensions in inches)

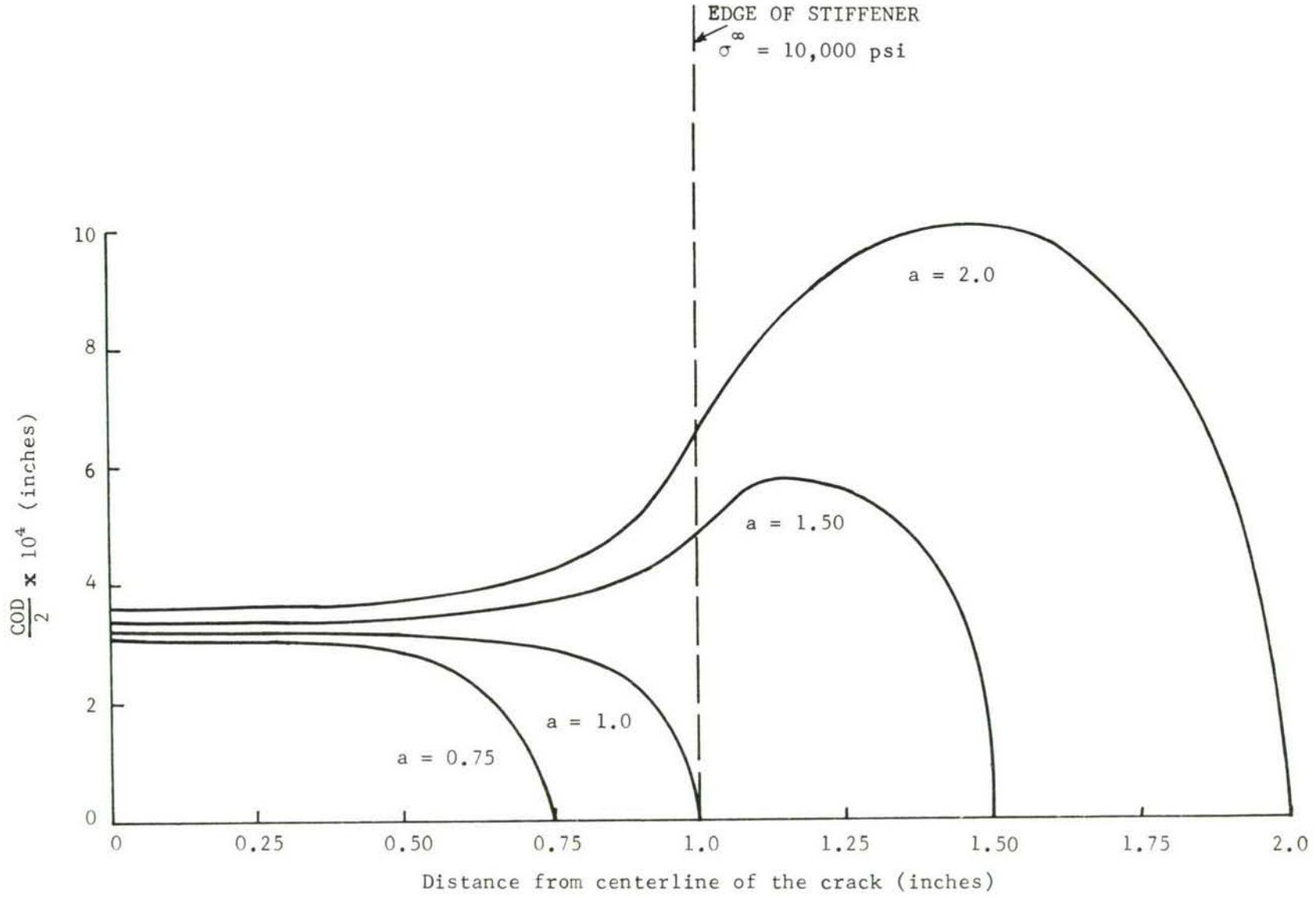

Figure 41. Variation of Crack Opening with Distance from Center of Crack (one-quarter of panel considered)

computed from the finite element analysis and from these locations, the strain in the adhesive is computed from Equation (78). The plot of strain as a function of the distance from the centerline of the crack for various values of y and a half-crack length equal to 2.0 inches is shown in Figure 42. The critical strain $\epsilon = 0.04$ (FM-73) is also shown. At $x = 0$, for the values of y larger than 0.15, the strains in the adhesive are smaller than the critical strain. Similarly, at $x = 1.0$, the strains at points farther than $y = 0.4$ are smaller than the critical strain. Other points on the boundary of the debond are obtained by interpolating between intermediate y values. The shape of the debond is plotted in Figure 39c. The actual debond for a one-quarter panel, will be the area enclosed between the x and y axes, Curve B, and the edge of the stiffener ($x = 1.0$).

For adhesive FM-400, the critical strain is about 0.02 (Reference 14), and is plotted in Figure 42. At $x = 0$, the points farther than $y = 0.3$ (approximately) will have strain smaller than 0.02. Similarly, the boundary of the debond is determined for other x locations and is shown in Figure 40c. It is seen that the size of the debond is considerably larger than that for the FM-73 adhesive.

6.5 DEBOND PREDICTION IN A TWO-PLY, ADHESIVELY BONDED STRUCTURE WITH A CRACK AT A CENTRAL HOLE

Consider the two-ply, bonded structure with a crack at a central hole shown in Figure 43. This structure has a width of six inches and an adhesive thickness of 0.008 inch. The analysis of the structure was carried out assuming no debond in the adhesive. The strains in the adhesive are computed from the displacement in the cracked and uncracked layers, and the plot of shear strain as a function of the distance from the centerline of the crack is shown in Figure 44. It is seen that the curves for y larger than 0.0 show an upward trend due to the presence of a hole. The predicted shape of debond size, corresponding to FM-73 ($\epsilon_R = 0.04$) is denoted in Figure 40d. It is seen that the debond is almost in the form of a strip.

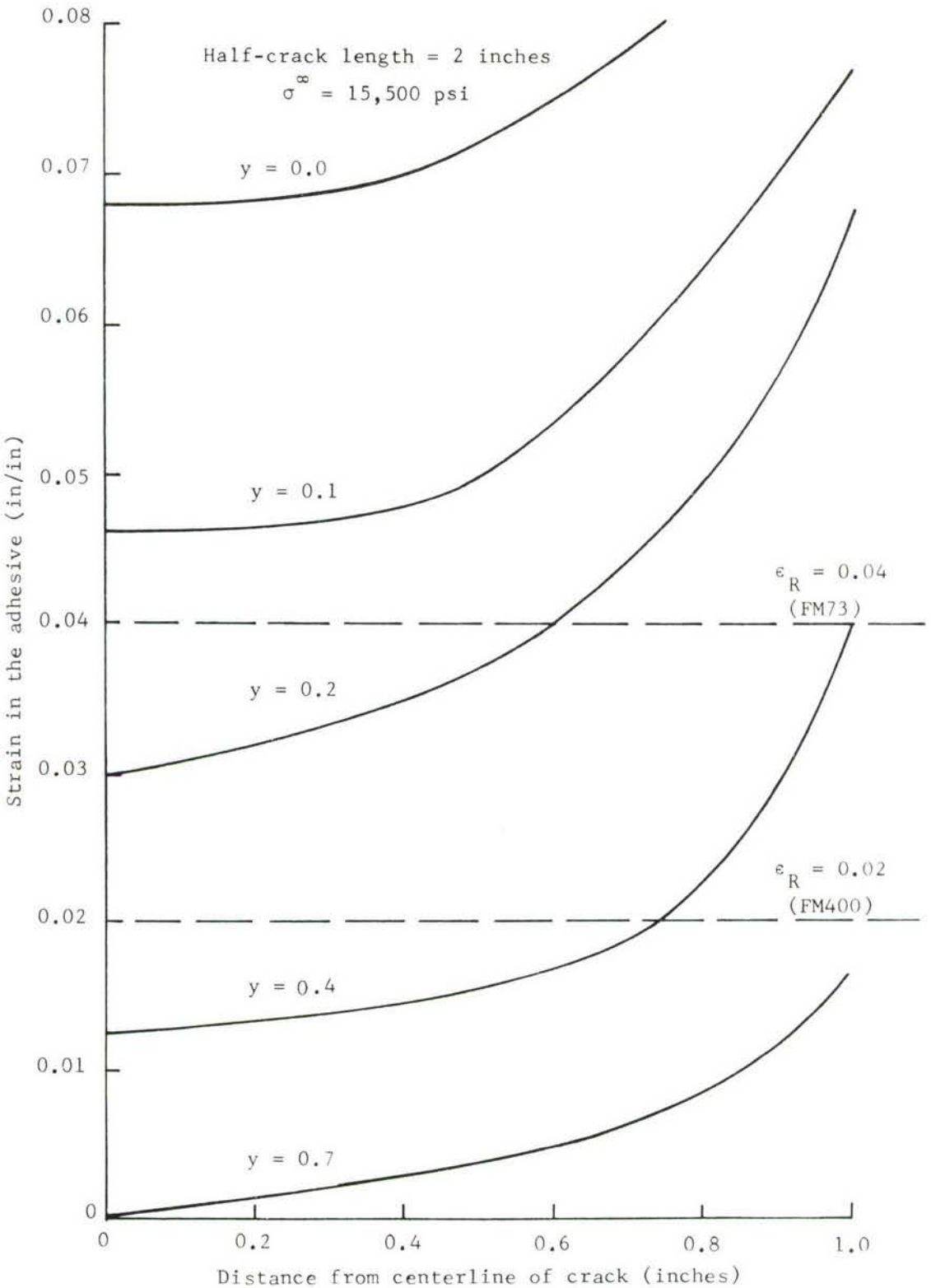

Figure 42. Variation of Strain in Adhesive with Distance from Centerline of Crack for a Cracked Plate with Bonded Stiffener (one-quarter of panel considered)

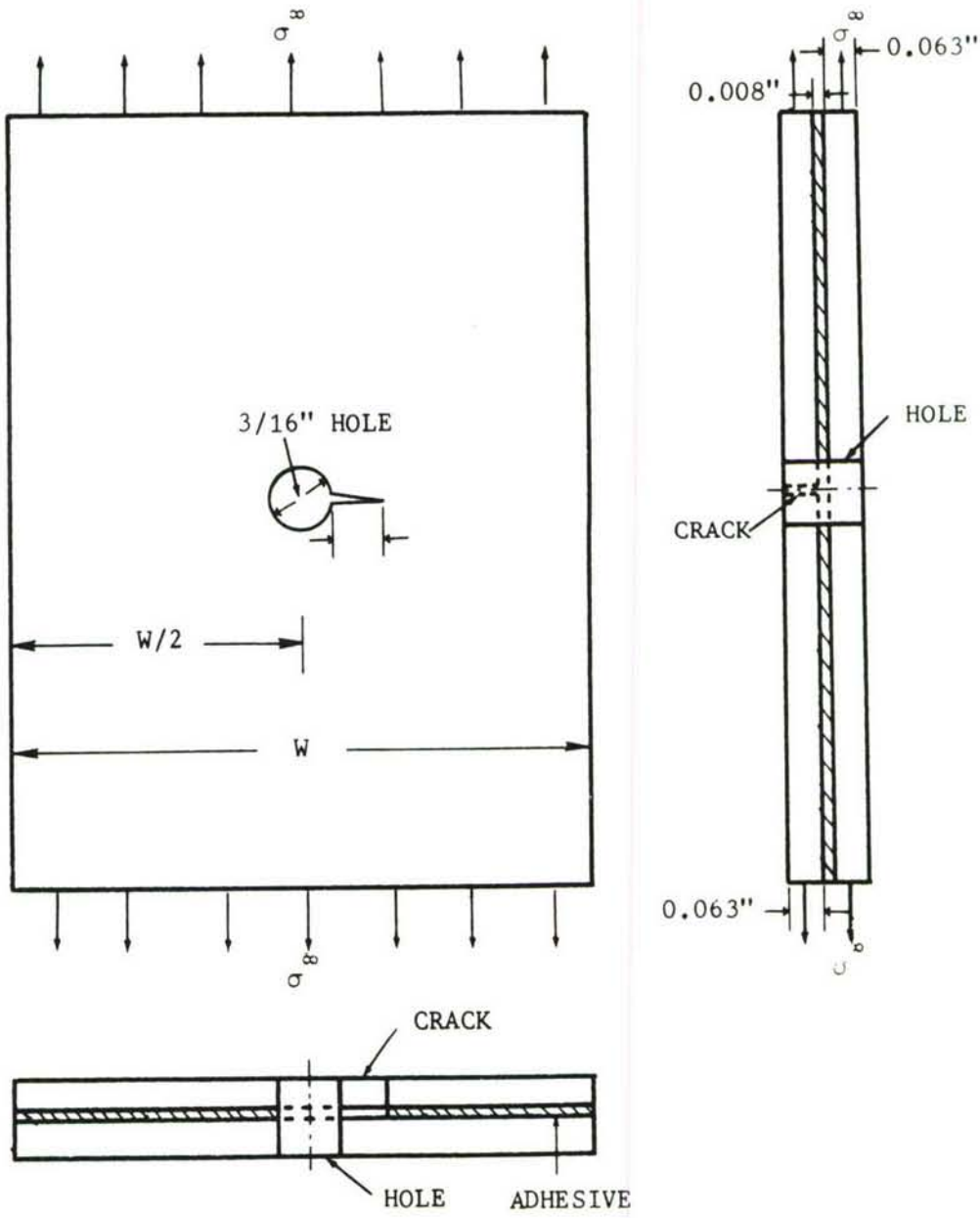

Figure 43. Two-Ply, Adhesively Bonded Structure with a Crack Emanating from a Hole

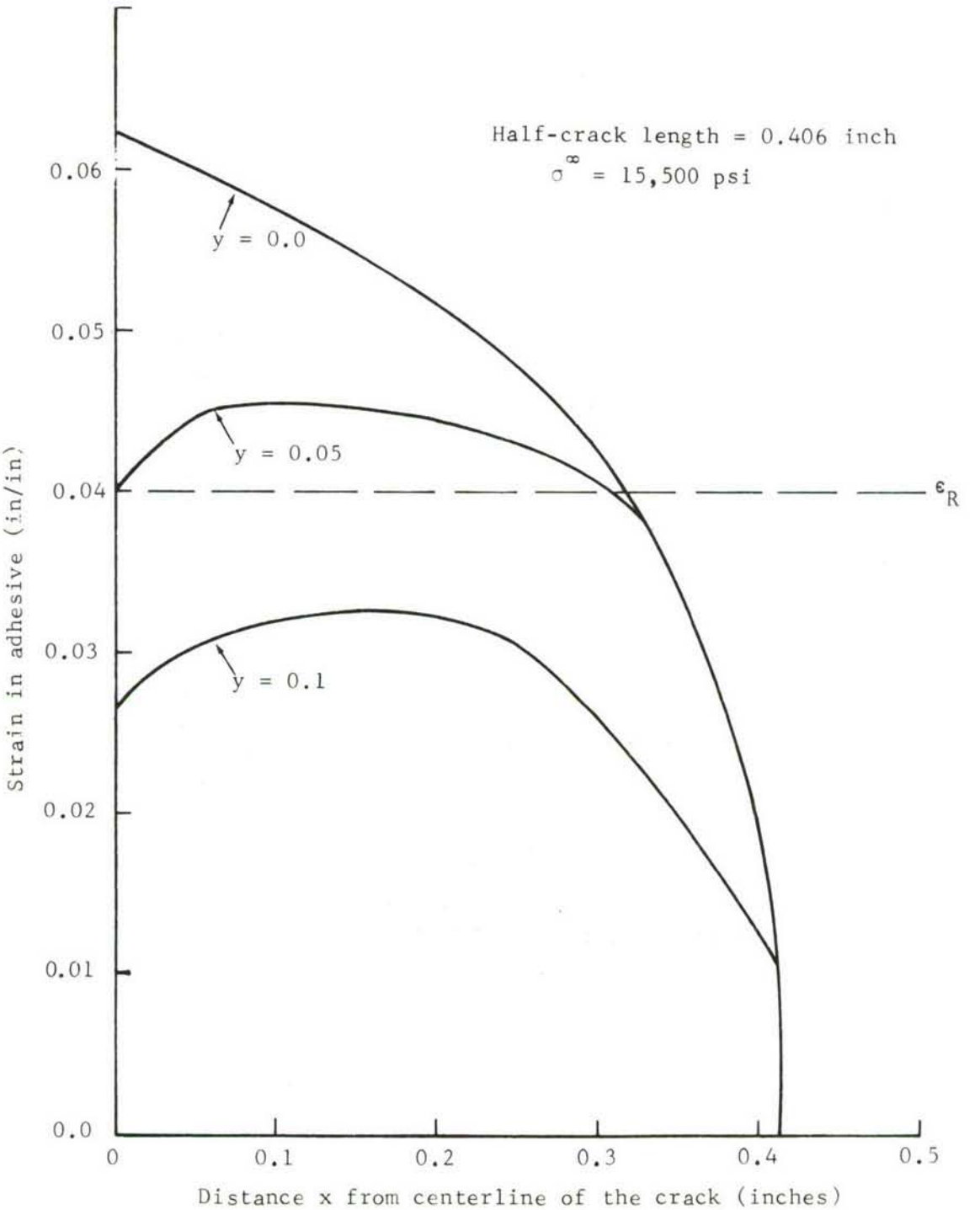

Figure 44. Variation of Strain in Adhesive with Distance from Edge of the Hole for a Two-Ply, Bonded Panel, with a Crack Emanating from a Hole (one-quarter of panel considered)

It may be noted that for predicting debond sizes here, the finite element analysis for various structures was carried out assuming no initial debond in the adhesive. The displacements in the cracked layer and sound layer will be slightly different due to the presence of a debond, and these will influence the strain in the adhesive. Hence, the size of the predicted debond will be slightly different if the initial debond present in the adhesive is taken into consideration. However, this influence will be negligible for ductile adhesives where the size of the debond is small. For brittle adhesives having a low value of ϵ_R, the size of the initial debond may have a significant influence on the debond propagation. This can be taken into consideration in the analysis, by assuming an initial debond if known or using the iteration procedure discussed in Paragraph 6.2.

SECTION 7

GUIDELINES FOR APPLYING METHODOLOGY

In Sections 2 through 6, analytical techniques were developed to study crack problems in adhesively bonded structures. In this section guidelines are provided for applying the methodology. The steps listed below are to be followed in using the techniques developed here.

1. Decide the method of analysis to be used. Mathematical methods (computer programs given in the Appendices) are recommended for parametric studies. Finite element analysis is recommended for crack growth analysis.

2. The analysis of the structure is carried out assuming no debond (if debond size not known) or known debond.

3. Using the displacements in cracked and sound layers and the failure strain of the adhesive, the size of the debond is determined by the procedure outlined in Section 6.

4. The analysis of the bonded structure is carried out once again assuming the debond size determined in Step 3. If the debond size, obtained in Step 3, is small (say elliptical with a minor-to-major axis ratio less than about 0.1) the debond size need not be recomputed. If the debond size in Step 3 is large (or significantly larger than known debond size) the debond size is recomputed with the analysis of this step. The bonded structure is analyzed once again with the new debond size.

5. Compute the stress intensity factors using the analysis of Step 4.

6. Apply bending correction to the stress intensity factors using the method outlined in Section 4.

7. Using the method described in Section 5, determine the load transfer factor or local load transfer factor (for cracks at stress concentration). If the load transfer factor is less than M_c (the critical

load transfer factor of the sound layer material), the uncracked backup layer has not cracked. The stress intensity factors obtained in Step 6 are correct.

8. The stress intensity factors are determined for various crack lengths using the procedure outlined in the above steps.

9. Obtain the crack growth data on a single monolithic layer. Using these data and a crack growth equation, say $\frac{da}{dN} = C\Delta K^n$, the constants C and n are obtained.

10. Using the stress intensity factors of Steps 8 and crack growth constants C and n, the crack growth life of a bonded structure is obtained.

11. The crack growth life in Step 10 is predicted only up to crack length a_c, at which the sound layer cracks. For crack lengths beyond sound layer cracking, the analysis can be carried out by assuming crack length a_c in the initially cracked layer, and a crack in the initially sound layer.

REFERENCES

1. Ratwani, M.M. and Wilhem, D.P., "Development and Evaluation of Methods of Plane Stress Fracture Analysis - A Technique for Predicting Residual Strength of Structures," AFFDL-TR-73-3 Part II, Volume I, April 1975.

2. Erdogan, F. and Arin K., "A Sandwich Plate with a Part-Through and a Debonding Crack," Engineering Fracture Mechanics, Volume 4, 1972 pp 449-458.

3. Arin, K., "A Plate with a Crack, Stiffened by a Partially Debonded Stringer," Engineering Fracture Mechanics, Vol. 6, 1974, pp 133-140.

4. Arin, K., "A Note on the Effect of Lateral Bending Stiffness of Stringers Attached to a Plate with a Crack," Engineering Fracture Mechanics, Volume 7, 1975, pp 173-179.

5. Alturi, S., Georgia Institute of Technology, Atlanta, Georgia, A Private Communication, May 1976.

6. Erdogan, F., and Ratwani, M.M., "Stress Distribution in Bonded Joints," Journal of Composite Materials, July 1971, pp. 378-393.

7. Tong, P., Pian, T.H.H., and Lasry, S.J., "A Hybrid Element Approach to Crack Problems in Plane Elasticity," International Journal of Numerical Methods in Engineering, Volume 7, 1973, pp. 297-308.

8. Erdogan, F., "On the Stress Distribution in Plates with Collinear Cuts Under Arbitrary Loading," Proceedings of 4th U.S. Nstional Congress of Applied Mechanics, ASME, 1962, pp. 547-553.

9. Muskhellishvilli, N.I.," Some Basic Problems of the Mathematical Theory of Elasticity," Nordhoff Publication, 1953.

10. Higdon, A., Ohlsen, E.H., and Stiles, W.B., "Mechanics of Materials," John Wiley & Sons Inc., New York, 1967.

11. Sih, G.C., "Handbook of Stress Intensity Factors." Institute of Fracture and Solid Mechanics, Lehigh University, Bethlehem, Pa. 1973.

12. Tada, H., Paris, P. and Irwin, G. "The Stress Analysis of Cracks Handbook," Del Research Corporation, Hellertown, Pa., 1973.

13. Timoshanko, S.P., and Goodier, J.N., "Theory of Elasticity," McGraw-Hill, 1951, pp. 78-81.

14. "Fatigue Behavior of Adhesively Bonded Joints," Quarterly Progress Report No. 2, Air Force Contract No. F33615-76-C-5220, prepared by General Dynamics, Fort Worth, Texas, January 1977.

APPENDICES

The computer programs for the mathematical analysis of adhesively bonded structures are outlined here. The computer programs for the solution of three different problems, as discussed in Section 2, are outlined in the following pages. All the computer programs are written in FORTRAN IV language. The programs are operational on IBM and CDC computers. The essential features of the programs for each problem are outlined in the following appendices.

APPENDIX A

A CRACKED SHEET WITH AN ADHESIVELY BONDED STRINGER AT AN ARBITRARY LOCATION

INPUT OF DEFINITIONS

The computer program has the following inputs:

1. modulus, Poisson's ratio, and thickness of the cracked sheet (EP, NUP, HP)
2. modulus, Poisson's ratio, width and thickness of the stiffener (ES, NUS, DS, TS)
3. Shear modulus and thickness of the adhesive layer (MUA, HA)
4. length of the debond (B)
5. location of the stringer, i.e., distance from centerline of sheet (D). The distance D is always positive, or zero
6. half-crack length a (A)
7. number of increments in half-crack length (NAA)
8. increment in half-crack length (DA)

DESCRIPTION OF OUTPUT

The outputs of the program are the shear stress in the adhesive, and the stress intensity factors at the right-(+A) and left-hand (-A) crack tips ($K/\sigma\sqrt{\pi a}$).

LISTING OF PROGRAM

```
C ***************************************************************************
C PROGRAM DEVELOPED BY M.M.RATWANI OF NORTHROP CORPORATION,AIRCRAFT DIVISION
C HAWTHORNE,CALIFORNIA. TELEPHONE (213) 970-5285
C PROGRAM COMPUTES STRESS INTENSITY FACTORS AND SHEAR STRESSES IN A
C CRACKED SHEET WITH ADHESIVELY BONDED STRINGER
C THE PROGRAM HAS OPTION TO PUT DEBOND OR NO DEBOND IN THE ADHESIVE
C TELESCOPIC GRID IS USED IN THE INTEGRATION OF KERNELS WHICH HAVE
C LOGARITHIMIC SINGULARITIES
C THE PROBLEM IS REDUCED TO SOLVING AN INTEGRAL EQUATION IN WHICH
C SHEAR STRESSES ARE TAKEN AS UNKNOWN QUANTITIES
C
C INPUTS ARE - EP,NUP,HP,ES,NUS,TS,DS,D,MUA,HA,B,A,DA,NAA
C N IS THE NUMBER OF COLLOCATION POINTS
C S.I.F IS THE VALUE OF STRESS INTENSITY FACTOR IN THE OUTPUT
C
C ***************************************************************************
      REAL NUP,NUS,MUP,MUS,MUA
      COMPLEX Z,Z2,ZB,ZB2,ZS,ZBS,ZZ,ZZB,ZZ2,ZZS,ZZB2,ZZBS,TH11,TH12,TH13
     3,TH14,TH41,TH42,TH31,TH32,TH33,TH34,TH51,TH52,TH61,TH62,ZP,AZZ,BZZ
     3,AZZB,BZZB,ZDM,ZPM
      DIMENSION SB(3600),AB(60),AL(60),CD(62),AT(60)
 50   FORMAT(E10.3,4F10.4)
 51   FORMAT(2F10.4,5X,I2)
 76   FORMAT(2X,8E13.4)
 85   FORMAT(X,17H S.I.F AT + A  = ,E15.7,5X,17H S.I.F AT - A  = ,E15.7)
 86   FORMAT(2X,5H Y = ,8X,7H TUY = ,10X,21H HALF-CRACK-LENGTH = ,F7.4)
 87   FORMAT(2X,7H MUA = ,E10.4,5X,6H EP = ,E10.4,5X,6H ES = ,E10.4)
 88   FORMAT(2X,19H PLATE-THICKNESS = ,F6.3,5X,18H STIFFENER-AREA = ,F6.
     33)
 89   FORMAT(2X,22H ADHESIVE-THICKNESS = ,F6.3,5X,17H DEBOND-LENGTH = ,F
     36.3)
 90   FORMAT(X,58H DISTANCE OF CENTERLINE OF STRINGER FROM CENTER OF PLA
     3TE = ,F6.3)
C
C ***************************************************************************
C     PLATE PARAMETERS
C EP= ELASTIC MODULUS OF THE PLATE
C NUP = POISSON RATIO OF PLATE MATERIAL
C HP = THICKNESS OF THE PLATE
C
      READ(5,50) EP,NUP,HP
C ***************************************************************************
C
C     STIFFENER PARAMETERS
C ES = ELASTIC MODULUS OF THE STRINGER
C NUS = POISSON RATIO OF STRINGER MATERIAL
C TS = THICKNESS OF STIFFENER
C DS = WIDTH OF THE STRINGER
C D = DISTANCE OF THE CENTERLINE OF THE STRINGER FROM CENTER OF THE PLATE
C
```

```
      READ(5,50) ES,NUS,TS,DS,D
C AS = AREA OF THE STRINGER
      AS=DS*TS
C
C ***************************************************************************
C
C     ADHESIVE PARAMETERS
C MUA = SHEAR MODULUS OF ADHESIVE
C HA = THICKNESS OF ADHESIVE LAYER
C B  = LENGTH OF DEBOND
      READ(5,50) MUA,HA,B
C
C ***************************************************************************
C
C     CRACK LENGTH PARAMETERS
C A = HALF-CRACK LENGTH
C DA = INCREMENT IN HALF-CRACK LENGTH
C NAA = NUMBER OF INCREMENTS IN HALF-CRACK LENGTH
      READ(5,51) A,DA,NAA
C
C ***************************************************************************
      PI=3.141592
       N=50
       NN3= N+2
       N1=20
       NS=35
       N2=N-N1
       N3=NS-N1
       NB=N-NS
       NB1=NB+1
      NN=N+1
      NL=N*N
       UNP=2.*(1.+NUP)
       UNS=2.*(1.+NUS)
       MUP=EP/UNP
       MUS=ES/UNS
       PK=(3.-NUP)/(1.+NUP)
      PK1=1.+PK
       PK12=PK1/2.
      PK2=PK1*PK1/2.
      PKK=1.-PK
      ASS=AS*ES
      PKR=1.-PK
      ZP1=1./(PI*4.*MUP*HP*PK1)
      ZP2=1./(4.*MUP)
      ZP3=1./(2.*PI*HP*PK1)
      YD=B
       YL=YD+0.4
       YL1=YD+1.
       YL2=YD+4.
       DEL1=(YL-YD)/N1
       DEL2=(YL1-YL)/N3
       DEL3=(YL2-YL1)/NB
       DEL4=(DEL1+DEL2)/2.
       DEL5=(DEL2+DEL3)/2.
      CD(1)=YD
C ***************************************************************************
C     DO LOOPS 139,140,141 COMPUTE Y CO-ORDINATES OF POINTS AT WHICH
C     STRESSES ARE COMPUTED. THESE CO-ORDINATES ARE THE MID-POINTS OF
C     THE TELESCOPIC GRID USED IN SOLVING INTEGRAL EQUATIONS
       DO 139 I=1,N1
```

```
 139     CD(I+1)=CD(I)+DEL1
         DO 140 I=1,N3
 140     CD(N1+1+I)=CD(N1+I)+DEL2
         DO 141 I=1,NB1
 141     CD(NS+1+I)=CD(NS+I)+DEL3
       ASD=DS*MUA/HA
       WRITE(6,90) D
       WRITE(6,87) MUA,EP,ES
       WRITE(6,88) HP,AS
       WRITE(6,89) HA,YD
       WRITE(6,86) A
C ***************************************************************************
        NAT=NAA+1
C      LOOP ON CRACK LENGTH
       DO 800 NAP=1,NAT
       A2=A*A
C
C ***************************************************************************
C      THIS LOOP COMPUTES THE RIGHT HAND SIDE OF INTEGRAL EQUATIONS(EQUAT
C      ION 20 OF SECTION 2.2.1) IN NUMERICAL ANALYSIS. IT IS ALSO LOOP
C      FOR EVALUATION OF KERNELS(EQUATION 20 OF SECTION 2.2.1)
       DO 69 I=1,N
       YI=CD(I+1)
       Z=CMPLX(D,YI)
       ZB=CONJG(Z)
       Z2=Z*Z
       ZB2=ZB*ZB
       ZS=CSQRT(Z2-A2)
       ZBS=CSQRT(ZB2-A2)
       BS=PK1*AIMAG(ZS)+PKK*YI-2.*YI*REAL(Z/ZS)
       AB(I)=ZP2*ASD*BS
        ZDM=ZB-Z
        ZP=(A+ZBS-ZB)/(A-ZB)
        ZPM=(-A+ZBS-ZB)/(-A-ZB)
       AL(I)=AIMAG(ZDM*((ZB/ZBS-1.)+ZP)/(A-ZB)-PK*ZP+(A+ZS-Z)/(A-Z))
       AT(I)=AIMAG(ZDM*((ZB/ZBS-1.)+ZPM)/(-A-ZB)-PK*ZPM+(-A+ZS-Z)/(-A-Z))
        AL(I)=-AL(I)
        AT(I)=-AT(I)
C
C ***************************************************************************
C      THIS DO LOOP EVALUATES KERNELS WHICH HAVE LOGARITHMIC SINGULARITI
C      ES AND KERNELS WHICH ARE NON-SINGULAR(EQUATION 20 OF SECTION 2.2.1)
       DO 69 J=1,N
       YJ=CD(J+1)
       ZZ=CMPLX(D,YJ)
       ZZB=CONJG(ZZ)
       ZZ2=ZZ*ZZ
       ZZS=CSQRT(ZZ2-A2)
        ZZB2=ZZB*ZZB
       ZZBS=CSQRT(ZZB2-A2)
       TH11=CLOG(ZB*ZZB-A2+ZBS*ZZBS)
       TH12=CLOG(ZB*ZZ-A2+ZBS*ZZS)
       TH13=CLOG(Z*ZZ-A2+ZZS*ZS)
       TH14=CLOG(Z*ZZB-A2+ZS*ZZBS)
       TH42=0.5*(ZBS-ZB-ZZS+ZZ)*(Z-ZB)/((ZB-ZZ)*ZBS)
       AZZ=A2-ZZ2
       AZZB=A2-ZZB2
       BZZ=(ZZ-ZZB)/(ZB-ZZ)
       TH32=0.5*(1.+ZS*ZZBS/AZZB)*(ZZB-ZZ)/(Z-ZZB)
       TH34=0.5*(1.+ZBS*ZZS/AZZ)*BZZ
       TH51=BZZ*(TH42-0.5*(Z-ZB)*(ZZ/ZZS-1.)/ZBS)
```

```
      TH62=CLOG(Z-ZZB)+CLOG(ZB-ZZ)
      IF (YI-YJ) 160,161,160
  160 TH61=CLOG(Z-ZZ)+CLOG(ZB-ZZB)
      BZZB=(ZZB-ZZ)/(ZB-ZZB)
      SP1=REAL(TH61-TH62)
      TH31=0.5*(1.+ZS*ZZS/AZZ)*(ZZ-ZZB)/(Z-ZZ)
      TH33=0.5*(1.+ZBS*ZZBS/AZZB)*BZZB
      TH41=0.5*(ZBS-ZB-ZZBS+ZZB)*(Z-ZB)/((ZB-ZZB)*ZBS)
      TH52=BZZB*(TH41-0.5*(Z-ZB)*(ZZB/ZZBS-1.)/ZBS)
      GO TO 162
  161 EP1=CD(J)
       EPR=CD(I+1)
      EP2=CD(J+2)
       ER1=EP2-EPR
       ER2=EP1-EPR
      ER3=EP2-EP1
       ER4=ER3/2.
       YLPM=2.*(ER1*ALOG(ABS(ER1))-ER2*ALOG(ABS(ER2))-ER3)
       YLPM=YLPM/ER4
      SP1=YLPM-REAL(TH62)
       TH31=-0.5*Z*(ZZ-ZZB)/(ZS*ZS)
       TH33=-0.5*ZB*(ZZB-ZZ)/(ZBS*ZBS)
       TH41=0.5*(Z-ZB)*(ZB/ZBS-1.)/ZBS
       TH52=-A2*(ZZB-ZZ)*(Z-ZB)/(4.*ZS*ZS*ZS*ZS)
  162  SP2=REAL(PK12*(TH11-TH12+PK*(TH13-TH14))+PK1*(TH41-TH42)+PK*(TH31-
     3TH32)+TH33-TH34+TH51-TH52)
      SP=PK*SP1-SP2
      IF(YI-YJ) 30,30,31
   30 SD=YI/ASS
      GO TO 32
   31 SD=YJ/ASS
    32  IL=(J-1)*N+I
       IF (J-N1) 201,202,203
  201  BIS=ASD*(SD-SP*ZP1)*DEL1
       GO TO 204
  202  BIS=ASD*(SD-SP*ZP1)*DEL4
       GO TO 204
  203   IF (J-NS) 205,206,207
  205  BIS=ASD*(SD-SP*ZP1)*DEL2
       GO TO 204
  206  BIS=ASD*(SD-SP*ZP1)*DEL5
       GO TO 204
  207  BIS=ASD*(SD-SP*ZP1)*DEL3
  204  IF(I-J) 38,39,38
  38    SB(IL)=BIS
      GO TO 69
  39    SB(IL)=1.+BIS
  69  CONTINUE
      KS=0
C
C*************************************************************************
C     THE SIMQ SOLVES FOR UNKNOWN SHEAR STRESS IN THE ADHESIVE
      CALL SIMQ(SB,AB,N,KS)
C
C*************************************************************************
C     THIS DO LOOP PRINTS OUT SHEAR STRESSES
       DO 795 I=1,N
  795 WRITE (6,76) CD(I+1),AB(I)
      SR=0.
       SR2=0.
C
```

```
C*************************************************************************
C      THIS DO LOOP COMPUTES NORMALIZED STRESS INTENSITY FACTORS
       DO 505 I=1,N
       IF (I-N1) 401,402,403
  401   SR=SR+2.*AB(I)*AL(I)*DEL1/A
       SR2=SR2-2.*AB(I)*AT(I)*DEL1/A
       GO TO 505
  402   SR=SR+2.*AB(I)*AL(I)*DEL4/A
       SR2=SR2-2.*AB(I)*AT(I)*DEL4/A
       GO TO 505
  403  IF (I-NS) 406,407,408
  406   SR=SR+2.*AB(I)*AL(I)*DEL2/A
       SR2=SR2-2.*AB(I)*AT(I)*DEL2/A
       GO TO 505
  407   SR=SR+2.*AB(I)*AL(I)*DEL5/A
       SR2=SR2-2.*AB(I)*AT(I)*DEL5/A
       GO TO 505
  408   SR=SR+2.*AB(I)*AL(I)*DEL3/A
       SR2=SR2-2.*AB(I)*AT(I)*DEL3/A
  505  CONTINUE
      SZ=SR*ZP3+1.
       SZ2=SR2*ZP3+1.
      WRITE (6,85) SZ,SZ2
  800 A=A+DA
      STOP
      END
      SUBROUTINE SIMQ(A,B,N,KS)
      DIMENSION A(1),B(1)
      TOL=0.0
      KS=0
      JJ=-N
      DO 65 J=1,N
      JY=J+1
      JJ=JJ+N+1
      BIGA=0
      IT=JJ-J
      DO 30 I=J,N
      IJ=IT+I
      IF(ABS(BIGA)-ABS(A(IJ))) 20,30,30
   20 BIGA=A(IJ)
      IMAX=I
   30 CONTINUE
      IF(ABS(BIGA)-TOL) 35,35,40
   35 KS=1
      RETURN
   40 I1=J+N*(J-2)
      IT=IMAX-J
      DO 50 K=J,N
      I1=I1+N
      I2=I1+IT
      SAVE=A(I1)
      A(I1)=A(I2)
      A(I2)=SAVE
   50 A(I1)=A(I1)/BIGA
      SAVE=B(IMAX)
      B(IMAX)=B(J)
      B(J)=SAVE/BIGA
      IF(J-N) 55,70,55
   55 IQS=N*(J-1)
      DO 65 IX=JY,N
      IXJ=IQS+IX
      IT=J-IX
      DO 60 JX=JY,N
      IXJX=N*(JX-1)+IX
```

```
      JJX=IXJX+IT
60    A(IXJX)=A(IXJX)-(A(IXJ)*A(JJX))
65    B(IX)=B(IX)-(B(J)*A(IXJ))
70    NY=N-1
      IT=N*N
      DO 80 J=1,NY
      IA=IT-J
      IB=N-J
      IC=N
      DO 80 K=1,J
      B(IB)=B(IB)-A(IA)*B(IC)
      IA=IA-N
80    IC=IC-1
      RETURN
      END
```

SAMPLE INPUT

TITLE					ENGINEER	PAGE
SINGLE STRINGER						OF
NASA SERIAL NO.	PREF	NDP JOB NO.	DASH	FOR ORGN. NO.	ANALYST	DATE

```
10.3E+6          .33          .063
10.3E+6          .33          .125          2.          .10
 0.6E+5          .008          0.0
    0.6          0.0           0
```

OUTPUT FOR SAMPLE INPUT

```
DISTANCE OF CENTERLINE OF STRINGER FROM CENTER OF PLATE = 0.100
 MUA = 0.6000E+05        EP = 0.1030E+08        ES = 0.1030E+08
 PLATE-THICKNESS =  0.063        STIFFENER-AREA =  0.250
 ADHESIVE-THICKNESS =  0.008        DEBOND-LENGTH =  0.0
 Y =              TUY =              HALF-CRACK-LENGTH =  0.6000
    0.2000E-01    0.1325E+00
    0.4000E-01    0.1150E+00
    0.6000E-01    0.1042E+00
    0.8000E-01    0.9618E-01
    0.1000E+00    0.8975E-01
    0.1200E+00    0.8428E-01
    0.1400E+00    0.7947E-01
    0.1600E+00    0.7514E-01
    0.1800E+00    0.7117E-01
    0.2000E+00    0.6751E-01
    0.2200E+00    0.6408E-01
    0.2400E+00    0.6087E-01
    0.2600E+00    0.5785E-01
    0.2800E+00    0.5501E-01
    0.3000E+00    0.5233E-01
    0.3200E+00    0.4982E-01
    0.3400E+00    0.4748E-01
    0.3600E+00    0.4529E-01
    0.3800E+00    0.4321E-01
    0.4000E+00    0.3820E-01
    0.4400E+00    0.3276E-01
    0.4800E+00    0.2991E-01
    0.5200E+00    0.2716E-01
    0.5600E+00    0.2461E-01
    0.6000E+00    0.2226E-01
    0.6400E+00    0.2013E-01
    0.6800E+00    0.1820E-01
    0.7200E+00    0.1646E-01
    0.7600E+00    0.1490E-01
    0.8000E+00    0.1351E-01
    0.8400E+00    0.1226E-01
    0.8800E+00    0.1114E-01
    0.9200E+00    0.1010E-01
    0.9600E+00    0.8977E-02
    0.1000E+01    0.6779E-02
```

0.1200E+01	0.4088E-02
0.1400E+01	0.2690E-02
0.1600E+01	0.1719E-02
0.1800E+01	0.1056E-02
0.2000E+01	0.6045E-03
0.2200E+01	0.2897E-03
0.2600E+01	-0.9730E-04
0.2800E+01	-0.2246E-03
0.3000E+01	-0.3286E-03
0.3200E+01	-0.4271E-03
0.3400E+01	-0.5323E-03
0.3600E+01	-0.6673E-03
0.3800E+01	-0.8769E-03
0.4000E+01	-0.1316E-02

S.I.F AT + A = 0.6038610E+00 S.I.F AT - A = 0.7077984E+00

APPENDIX B

CRACKED SHEET WITH TWO ADHESIVELY BONDED STRINGERS SYMMETRICALLY LOCATED ABOUT THE CENTERLINE

The inputs to this computer program are the same as for the single stringer case of Appendix A. In this case, distance D is the distance from the centerline of each stringer to the centerline of the crack. The shear stresses in the adhesive bonding each stringer to the plate are the same, also the stress intensity factors at both crack tips are equal.

INPUT OF DEFINITIONS

The computer program has the following inputs:

1. modulus, Poisson's ratio, and thickness of the cracked sheet (EP, NUP, HP)
2. modulus, Poisson's ratio, width and thickness of each stiffener (ES, NUS, DS, TS)
3. shear modulus and thickness of the adhesive layer (MUA, HA)
4. length of the debond (B)
5. location of each stringer, i.e., distance of each stringer from centerline of sheet (D). The distance D is always positive, or zero
6. half-crack length a (A)
7. number of increments in half-crack length (NAA)
8. increment in half crack length (DA)

DESCRIPTION OF OUTPUT

The outputs of the program are the shear stress in the adhesive, and the stress intensity factors at each crack tip ($K/\sigma\sqrt{\pi a}$).

LISTING OF PROGRAM

```
C ***************************************************************************
C PROGRAM DEVELOPED BY M.M.RATWANI OF NORTHROP CORPORATION,AIRCRAFT DIVISION
C HAWTHORNE,CALIFORNIA. TELEPHONE (213) 970-5285
C PROGRAM COMPUTES STRESS INTENSITY FACTORS AND SHEAR STRESSES IN A
C CRACKED SHEET WITH TWO BONDED STRINGERS SYMMETRICALLY LOCATED ABOUT
C CENTERLINE
C THE PROGRAM HAS OPTION TO PUT DEBOND OR NO DEBOND IN THE ADHESIVE
C TELESCOPIC GRID IS USED IN THE INTEGRATION OF KERNELS WHICH HAVE
C LOGARITHIMIC SINGULARITIES
C THE PROBLEM IS REDUCED TO SOLVING AN INTEGRAL EQUATION IN WHICH
C SHEAR STRESSES ARE TAKEN AS UNKNOWN QUANTITIES
C
C INPUTS ARE - EP,NUP,HP,ES,NUS,TS,DS,D,MUA,HA,B,A,DA,NAA
C N IS THE NUMBER OF COLLOCATION POINTS
C S.I.F IS THE VALUE OF STRESS INTENSITY FACTOR IN THE OUTOUT
C
C ***************************************************************************
      REAL NUP,NUS,MUP,MUS,MUA
     COMPLEX Z,Z2,ZB,ZB2,ZS,ZBS,ZZ,ZZB,ZZ2,ZZS,ZZB2,ZZBS,TH11,TH12,TH13
    3,TH14,TH41,TH42,TH31,TH32,TH33,TH34,TH51,TH52,TH61,TH62,ZP,AZZ,BZZ
    3,AZZB,BZZB,ZDM,ZPM
    3,ZI,ZBI,ZMI,ZBMI,ZJ,ZBJ,ZMJ,ZBMJ,ZPMM,ZMPM,TM11,TM12,TM13,TM14,
    3TM41,TM42,TM31,TM32,TM33,TM34,TM51,TM52,ZZMI,ZZMIB,ZZJM,ZZJBM
    3,TM61,TM62
    3,ALI
     DIMENSION SB(3600),AB(60),AL(60),CD(62),AT(60)
 50   FORMAT(E10.3,4F10.4)
 51   FORMAT(2F10.4,5X,I2)
 76   FORMAT(2X,8E13.4)
 87   FORMAT(2X,7H MUA = ,E10.4,5X,6H EP = ,E10.4,5X,6H ES = ,E10.4)
 88   FORMAT(2X,19H PLATE-THICKNESS = ,F6.3,5X,18H STIFFENER-AREA = ,F6.
    33)
 89   FORMAT(2X,22H ADHESIVE-THICKNESS = ,F6.3,5X,17H DEBOND-LENGTH = ,F
    36.3)
 86   FORMAT(2X,5H Y = ,8X,7H TUY = ,10X,21H HALF-CRACK-LENGTH = ,F7.4)
 85   FORMAT (X,9H S.I.F = ,E15.7)
 90   FORMAT(X,64H DISTANCE OF CENTERLINE OF EACH STRINGER FROM CENTER O
    3F PLATE = ,F6.3)
C
C ***************************************************************************
C     PLATE PARAMETERS
C EP= ELASTIC MODULUS OF THE PLATE
C NUP = POISSON RATIO OF PLATE MATERIAL
C HP = THICKNESS OF THE PLATE
C
      READ(5,50) EP,NUP,HP
C ***************************************************************************
C
C     STIFFENER PARAMETERS
C ES = ELASTIC MODULUS OF THE STRINGER
C NUS = POISSON RATIO OF STRINGER MATERIAL
C TS = THICKNESS OF STIFFENER
C DS = WIDTH OF EACH STRINGER
C D = DISTANCE OF THE CENTERLINE OF THE STRINGER FROM CENTER OF THE PLATE
C
      READ(5,50) ES,NUS,TS,DS,D
C AS = AREA OF EACH STRINGER
       AS=DS*TS
C
```

```
C ***************************************************************************
C
C      ADHESIVE PARAMETERS
C MUA = SHEAR MODULUS OF ADHESIVE
C HA = THICKNESS OF ADHESIVE LAYER
C B  = LENGTH OF DEBOND
       READ(5,50) MUA,HA,B
C
C ***************************************************************************
C
C      CRACK LENGTH PARAMETERS
C A = HALF-CRACK LENGTH
C DA = INCREMENT IN HALF-CRACK LENGTH
C NAA = NUMBER OF INCREMENTS IN HALF-CRACK LENGTH
       READ(5,51) A,DA,NAA
C
C ***************************************************************************
       PI=3.141592
        N=50
        NN3= N+2
        N1=20
        NS=35
        N2=N-N1
        N3=NS-N1
        NB=N-NS
        NB1=NB+1
       NN=N+1
       NL=N*N
        UNP=2.*(1.+NUP)
        UNS=2.*(1.+NUS)
        MUP=EP/UNP
        MUS=ES/UNS
        PK=(3.-NUP)/(1.+NUP)
       PK1=1.+PK
        PK12=PK1/2.
       PK2=PK1*PK1/2.
       PKK=1.-PK
       ASS=AS*FS
       PKR=1.-PK
       ZP1=1./(PI*4.*MUP*HP*PK1)
       ZP2=1./(4.*MUP)
       ZP3=1./(2.*PI*HP*PK1)
       YD=B
        YL=YD+0.4
        YL1=YD+1.
        YL2=YD+4.
        DEL1=(YL-YD)/N1
        DEL2=(YL1-YL)/N3
        DEL3=(YL2-YL1)/NB
        DEL4=(DEL1+DEL2)/2.
        DEL5=(DEL2+DEL3)/2.
      CD(1)=YD
C ***************************************************************************
C      DO LOOPS 139,140,141 COMPUTE Y CO-ORDINATES OF POINTS AT WHICH
C      STRESSES ARE COMPUTED. THESE CO-ORDINATES ARE THE MID-POINTS OF
C      THE TELESCOPIC GRID USED IN SOLVING INTEGRAL EQUATIONS
        DO 139 I=1,N1
 139     CD(I+1)=CD(I)+DEL1
        DO 140 I=1,N3
 140    CD(N1+1+I)=CD(N1+I)+DEL2
        DO 141 I=1,NB1
```

```
141    CD(NS+1+I)=CD(NS+I)+DEL3
       ASD=DS*MUA/HA
       WRITE(6,90) D
       WRITE(6,87) MUA,EP,ES
       WRITE(6,88) HP,AS
       WRITE(6,89) HA,YD
       WRITE(6,86) A
C ***************************************************************************
       NAT=NAA+1
C      LOOP ON CRACK LENGTH
       DO 800 NAP=1,NAT
       A2=A*A
C
C ***************************************************************************
C      THIS LOOP COMPUTES THE RIGHT HAND SIDE OF INTEGRAL EQUATIONS(EQUAT
C      ION 20 OF SECTION 2.2.1) IN NUMERICAL ANALYSIS. IT IS ALSO LOOP
C      FOR EVALUATION OF KERNELS(EQUATION 20 OF SECTION 2.2.1)
       DO 69 I=1,N
       YI=CD(I+1)
        Z=CMPLX(D,YI)
       ZB=CONJG(Z)
       Z2=Z*Z
       ZB2=ZB*ZB
       ZS=CSQRT(Z2-A2)
        ZBS=CONJG(ZS)
       BS=PK1*AIMAG(ZS)+PKK*YI-2.*YI*REAL(Z/ZS)
       AB(I)=ZP2*ASD*BS
        ZI=ZS-Z
        ZBI=CONJG(ZI)
        ZMI=-ZS+Z
        ZBMI=CONJG(ZMI)
        ZDM=Z-ZB
        ZJ=Z/ZS-1.
        ZBJ=CONJG(ZJ)
        ZMJ=ZJ
        ZBMJ=ZBJ
        AZZ=A-Z
        AZZB=A-ZB
        BZZ=A+Z
        BZZB=A+ZB
        ZP=(A+ZI)/AZZ
        ZPM=(A+ZBI)/AZZB
        ZMPM=(A+ZMI)/BZZ
        ZPMM=(A+ZBMI)/BZZB
         ALI=PK1*(-ZP+ZPM+ZMPM-ZPMM)+ZDM*((ZP+ZJ)/AZZ+(ZMPM+ZMJ)/BZZ+(
     3ZPMM+ZBMJ)/BZZB+(ZPM+ZBJ)/AZZB)
        AL(I)=AIMAG(ALI)
C
C ***************************************************************************
C      THIS DO LOOP EVALUATES KERNELS WHICH HAVE LOGARITHMIC SINGULARITI
C      ES AND KERNELS WHICH ARE NON-SINGULAR(EQUATION 20 OF SECTION 2.2.1)
       DO 69 J=1,N
       YJ=CD(J+1)
       ZZ=CMPLX(D,YJ)
       ZZB=CONJG(ZZ)
       ZZ2=ZZ*ZZ
       ZZS=CSQRT(ZZ2-A2)
        ZZB2=ZZB*ZZB
        ZZBS=CONJG(ZZS)
       TH11=CLOG(ZB*ZZB-A2+ZBS*ZZBS)
       TH12=CLOG(ZB*ZZ-A2+ZBS*ZZS)
```

```
      TH13=CONJG(TH11)
      TH14=CONJG(TH12)
     TH42=0.5*(ZBS-ZB-ZZS+ZZ)*(Z-ZB)/((ZB-ZZ)*ZBS)
     AZZ=A2-ZZ2
     AZZB=A2-ZZB2
     BZZ=(ZZ-ZZB)/(ZB-ZZ)
     TH32=0.5*(1.+ZS*ZZBS/AZZB)*(ZZB-ZZ)/(Z-ZZB)
      TH34=CONJG(TH32)
     TH51=BZZ*(TH42-0.5*(Z-ZB)*(ZZ/ZZS-1.)/ZBS)
     TH62=CLOG(Z-ZZB)+CLOG(ZB-ZZ)
     TM11=CLOG(-ZB*ZZ-A2-ZZS*ZBS)
      TM13=CLOG(-Z*ZZ-A2-ZZS*ZS)
      TM14=CONJG(TM11)
      TM12=CONJG(TM13)
      ZZMI=-ZZS+ZZ
      ZZMIB=CONJG(ZZMI)
      ZP=ZB+ZZB
      ZPM=ZB+ZZ
      ZMPM=Z+ZZ
      ZPMM=Z+ZZB
      BZZB=ZZ-ZZB
      TM41=0.5*ZDM*(ZBI-ZZMIB)/(ZP*ZBS)
      TM42=0.5*ZDM*(ZBI-ZZMI)/(ZPM*ZBS)
      TM31=0.5*BZZB*(1.-ZS*ZZBS/AZZB)/ZPMM
     TM32=-0.5*BZZB*(1.-ZS*ZZS/AZZ)/ZMPM
      TM34=CONJG(TM32)
      TM33=CONJG(TM31)
      ZZJM=ZZ/ZZS-1.
      ZZJBM=CONJG(ZZJM)
      TM51=BZZB*(TM41-.5*ZDM*ZZJBM/ZBS)/ZP
      TM52=-BZZB*(TM42-.5*ZDM*ZZJM/ZBS)/ZPM
      TM61=CLOG(ZPM)+CLOG(ZPMM)
      TM62=CLOG(ZMPM)+CLOG(ZP)
     IF (YI-YJ) 160,161,160
160  TH61=CLOG(Z-ZZ)+CLOG(ZB-ZZB)
     BZZB=(ZZB-ZZ)/(ZB-ZZB)
     SP1=REAL(TH61-TH62)
      SP1=SP1+REAL(TM61-TM62)
     TH31=0.5*(1.+ZS*ZZS/AZZ)*(ZZ-ZZB)/(Z-ZZ)
      TH33=CONJG(TH31)
     TH41=0.5*(ZBS-ZB-ZZBS+ZZB)*(Z-ZB)/((ZB-ZZB)*ZBS)
     TH52=BZZB*(TH41-0.5*(Z-ZB)*(ZZB/ZZBS-1.)/ZBS)
     GO TO 162
161  EP1=CD(J)
      EPP=CD(I+1)
     EP2=CD(J+2)
      ER1=EP2-EPP
      ER2=EP1-EPP
     ER3=EP2-EP1
      ER4=ER3/2.
      YLPM=2.*(ER1*ALOG(ABS(ER1))-ER2*ALOG(ABS(ER2))-ER3)
      YLPM=YLPM/ER4
     SP1=YLPM-REAL(TH62)
      SP1=SP1+REAL(TM61-TM62)
      TH31=-0.5*Z*(ZZ-ZZB)/(ZS*ZS)
      TH33=-0.5*ZB*(ZZB-ZZ)/(ZBS*ZBS)
      TH41=0.5*(Z-ZB)*(ZB/ZBS-1.)/ZBS
      TH52=-A2*(ZZB-ZZ)*(Z-ZB)/(4.*ZS*ZS*ZS*ZS)
162  SP2=REAL(PK12*(TH11-TH12+PK*(TH13-TH14))+PK1*(TH41-TH42)+PK*(TH31-
    3TH32)+TH33-TH34+TH51-TH52)
```

```
      SP2=SP2+REAL(PK12*(TM11-TM12+PK*(TM14-TM13))+PK1*(TM42-TM41)+PK*(
     3TM31-TM32)+TM33-TM34+TM51-TM52)
      SP=PK*SP1-SP2
       IF (YI-YJ) 30,30,31
 30    SD=YI/ASS
       GO TO 32
 31    SD=YJ/ASS
  32    IL=(J-1)*N+I
       IF (J-N1) 201,202,203
 201    BIS=ASD*(SD-SP*ZP1)*DEL1
       GO TO 204
 202    BIS=ASD*(SD-SP*ZP1)*DEL4
       GO TO 204
 203     IF (J-NS) 205,206,207
 205    BIS=ASD*(SD-SP*ZP1)*DEL2
       GO TO 204
 206    BIS=ASD*(SD-SP*ZP1)*DEL5
       GO TO 204
 207    BIS=ASD*(SD-SP*ZP1)*DEL3
 204    IF(I-J) 38,39,38
 38     SB(IL)=BIS
       GO TO 69
 39     SB(IL)=1.+BIS
 69    CONTINUE
       KS=0
C
C ***************************************************************************
C      THE SIMQ SOLVES FOR UNKNOWN SHEAR STRESS IN THE ADHESIVE
       CALL SIMQ(SB,AB,N,KS)
C
C***************************************************************************
C      THIS DO LOOP PRINTS OUT SHEAR STRESSES
        DO 795 I=1,N
 795   WRITE (6,76) CD(I+1),AB(I)
       SR=0.
C
C***************************************************************************
C      THIS DO LOOP COMPUTES NORMALIZED STRESS INTENSITY FACTORS
        DO 505 I=1,N
        IF (I-N1) 401,402,403
  401    SR=SR+    AB(I)*AL(I)*DEL1/A
        GO TO 505
  402    SR=SR+    AB(I)*AL(I)*DEL4/A
        GO TO 505
 403    IF (I-NS) 406,407,408
  406    SR=SR+    AB(I)*AL(I)*DEL2/A
        GO TO 505
  407    SR=SR+    AB(I)*AL(I)*DEL5/A
        GO TO 505
  408    SR=SR+    AB(I)*AL(I)*DEL3/A
 505    CONTINUE
       SZ=SR*ZP3+1.
       WRITE (6,85) SZ
 800   A=A+DA
       STOP
       SUBROUTINE SIMQ(A,B,N,KS)
       DIMENSION A(1),B(1)
       TOL=0.0
       KS=0
       JJ=-N
       DO 65 J=1,N
```

```
      JY=J+1
      JJ=JJ+N+1
      BIGA=0
      IT=JJ-J
      DO 30 I=J,N
      IJ=IT+I
      IF(ABS(BIGA)-ABS(A(IJ))) 20,30,30
20    BIGA=A(IJ)
      IMAX=I
30    CONTINUE
      IF(ABS(BIGA)-TOL) 35,35,40
35    KS=1
      RETURN
40    I1=J+N*(J-2)
      IT=IMAX-J
      DO 50 K=J,N
      I1=I1+N
      I2=I1+IT
      SAVE=A(I1)
      A(I1)=A(I2)
      A(I2)=SAVE
50    A(I1)=A(I1)/BIGA
      SAVE=B(IMAX)
      B(IMAX)=B(J)
      B(J)=SAVE/BIGA
      IF(J-N) 55,70,55
55    IQS=N*(J-1)
      DO 65 IX=JY,N
      IXJ=IQS+IX
      IT=J-IX
      DO 60 JX=JY,N
      IXJX=N*(JX-1)+IX
      JJX=IXJX+IT
60    A(IXJX)=A(IXJX)-(A(IXJ)*A(JJX))
65    B(IX)=B(IX)-(B(J)*A(IXJ))
70    NY=N-1
      IT=N*N
      DO 80 J=1,NY
      IA=IT-J
      IB=N-J
      IC=N
      DO 80 K=1,J
      B(IB)=B(IB)-A(IA)*B(IC)
      IA=IA-N
80    IC=IC-1
      RETURN
      END
```

SAMPLE INPUT

JOB TITLE: TWO STRINGER CASE | ENGINEER | PAGE ___ OF ___
CDRA SERIAL NO. | PRE. | NDP JOB NO. | DASH | FOR ORGN. NO. | ANALYST | DATE

```
10.3E+6          .33          063
10.3E+6          .33          125          1          .6
 0.6E+5          .008         0.0
    0.6          0.0          0.
```

SAMPLE OUTPUT

```
DISTANCE OF CENTERLINE OF EACH STRINGER FROM CENTER OF PLATE =  0.600
 MUA = 0.6000E+05       EP = 0.1030E+08       ES = 0.1030E+08
 PLATE-THICKNESS =  0.063       STIFFENER-AREA =  0.125
 ADHESIVE-THICKNESS =  0.008       DEBOND-LENGTH =  0.0
 Y =              TUY =              HALF-CRACK-LENGTH =  0.6000
    0.2000E-01    0.2902E-01
    0.4000E-01    0.3398E-01
    0.6000E-01    0.3602E-01
    0.8000E-01    0.3681E-01
    0.1000E+00    0.3696E-01
    0.1200E+00    0.3673E-01
    0.1400E+00    0.3627E-01
    0.1600E+00    0.3566E-01
    0.1800E+00    0.3496E-01
    0.2000E+00    0.3420E-01
    0.2200E+00    0.3340E-01
    0.2400E+00    0.3258E-01
    0.2600E+00    0.3176E-01
    0.2800E+00    0.3094E-01
    0.3000E+00    0.3012E-01
    0.3200E+00    0.2932E-01
    0.3400E+00    0.2854E-01
    0.3600E+00    0.2778E-01
    0.3800E+00    0.2700E-01
    0.4000E+00    0.2504E-01
    0.4400E+00    0.2271E-01
    0.4800E+00    0.2146E-01
    0.5200E+00    0.2022E-01
    0.5600E+00    0.1899E-01
    0.6000E+00    0.1780E-01
    0.6400E+00    0.1665E-01
    0.6800E+00    0.1556E-01
    0.7200E+00    0.1452E-01
    0.7600E+00    0.1353E-01
    0.8000E+00    0.1260E-01
    0.8400E+00    0.1171E-01
    0.8800E+00    0.1087E-01
    0.9200E+00    0.1002E-01
    0.9600E+00    0.9018E-02
    0.1000E+01    0.7685E-02
    0.1200E+01    0.5035E-02
```

```
    0.1400E+01    0.3396E-02
    0.1600E+01    0.2201E-02
    0.1800E+01    0.1362E-02
    0.2000E+01    0.7835E-03
    0.2200E+01    0.3895E-03
    0.2400E+01    0.1207E-03
    0.2600E+01   -0.6630E-04
    0.2800E+01   -0.2013E-03
    0.3000E+01   -0.3078E-03
    0.3200E+01   -0.4078E-03
    0.3400E+01   -0.5214E-03
    0.3600E+01   -0.6779E-03
    0.3800E+01   -0.9368E-03
    0.4000E+01   -0.1489E-02
S.I.F =    0.5448927E+00
```

APPENDIX C

TWO ADHESIVELY BONDED LAYERS WITH A CRACK IN ONE LAYER (SMALL CRACK LENGTHS)

A generalized computer program for this problem could not be written due to the fact that load-shedding to the sound layer is a function of crack length, as well as adhesive and adherend properties. The convergence of the solution is strongly dependent on crack length. Hence, two programs are written, one for a small crack length (half-crack length less than, or equal to 0.4 inch) and the other for a long crack length (half-crack length larger than 0.5 inch, and smaller than, or equal to one inch). Similar programs can be easily written for crack lengths larger than one inch by taking more collocation points in the numerical analysis.

The computer programs are written for the case of no debond in the adhesive, or the debond approximated as elliptical in shape. The programs have the option to input an elliptical debond with a minor-to-major axis ratio of 0.0 (no debond), 0.1, 0.2, and 0.3. Other debond shapes and sizes can easily be easily incorporated by changing the region and shape of the surface over which integration of the kernels is carried out.

INPUT DEFINITION

The computer programs have the following inputs:

1. modulus, Poisson's ratio, and thickness of the cracked layer (E1, MU1, H1)
2. modulus, Poisson's ratio, and thickness of the sound layer (E2, NU2, H2)
3. shear modulus and thickness of the adhesive layer (MUA, HA)
4. ratio of the minor-to-major axis of the elliptical debond (DEB)
5. half-crack length a (a, less than or equal to 0.4 inch)
6. number of increments in the half-crack length (NAA)
7. increments in the half-crack length (DA)

DESCRIPTION OF THE OUTPUT

The outputs of the programs are shear stress (τ_x, τ_y) at various locations in the bonded region, and the stress intensity factor ($K/\sigma\sqrt{\pi a}$).

LISTING

```
C
C*************************************************************************
C PROGRAM DEVELOPED BY M.M.RATWANI OF NORTHROP CORPORATION,AIRCRAFT DIVISION
C HAWTHORNE,CALIFORNIA. TELEPHONE (213) 970-5285
C PROGRAM COMPUTES STRESS INTENSITY FACTORS AND SHEAR STRESSES IN TWO
C PLY ADHESIVELY BONDED STRUCTURE WITH A CRACK IN ONE LAYER. THE
C PROGRAM HAS OPTION TO PUT NO DEBOND IN THE ADHESIVE OR ELLIPTICAL
C DEBOND WITH MINOR TO MAJOR AXIS RATIO OF 0.1,0.2 OR 0.3
C THIS PROGRAM GIVES CONVERGING RESULTS UPTO A = 0.4 INCH AND RATIO OF
C ADHESIVE THICKNESS TO SHEAR MODULUS = 0.1E-6
C TELESCOPIC GRID IS USED IN THE INTEGRATION OF KERNELS WHICH HAVE
C LOGARITHIMIC SINGULARITIES
C THE SIZE OF TELESCOPIC GRID DEPENDS ON CRACK LENGTH
C THE PROBLEM IS REDUCED TO SOLVING A SET OF INTEGRAL EQUATIONS IN WHICH
C SHEAR STRESSES TUX AND TUY ARE TAKEN AS UNKNOWNS
C SOLUTION OF UNKNOWN SHEAR STRESSES TUX AND TUY IS ACCOMPLISHED BY
C SOLVING A SET OF SIMULTANEOUS EQUATIONS
C X,Y ARE THE CO-ORDINATES,FROM THE CENTRE-LINE,AT WHICH SHEAR STRESSES
C ARE COMPUTED
C S.I.F IS THE STRESS INTENSITY FACTOR IN THE OUTPUT
C NX1,NX2.....,NY1,NY2.....,  ARE THE NUMBER OF COLLOCATION POINTS IN
C THE TELESCOPIC GRID FOR NUMERICAL ANALYSIS
C INPUTS ARE - E1,NU1,H1,E2,NU2,H2,MUA,HA,DEB,A,DA,NAA
C*************************************************************************
      COMPLEX Z,Z2,Z3,ZB2,ZB3,ZS,ZZZ,Z1,ZIB,ZJB,PHZ1,PHZ2,PHZ3,PH1,PH2,
     3F1,F2,TH21,TH22,ZZ,TH5,ZZB,ZZ2,ZZ2A,ZZS,ZZB2,ZZ2B,ZZB3,ZPH,ZPHB,
     3ZZZZB,ZZI,ZZIB,ZZJB,ZZJ,TH11,TH12,TH13,TH14,TH31,TH42,Z21,TH1,TH2,
     3TH32,TH41,Z1Z,Z2Z,ZL1,ZL2,Z3ZB,Z4ZB,ZPL,ZPLB,PHZ4
     3,ZXY,Z4Z,Z1Z3,Z2ZB,ZL3,ZL4
     3,ZJ,ZIM,ZIBM,ZJM,ZJBM,PH3,PH4,ZPHP,ZPHBP,ZM,ZBM,Z3BM,ZBMM,IM11,
     3IM12,IM13,IM14,ZPHPB,ZPHPP,ZBHP,ZBPP,TM31,TM32,TM33,TM34,TH33,
     3TH34,ZZIM,ZZIBM,TH43,TH44,TH51,TH52,TH53,TH54,ZZJBM,ZZJM
      REAL NU1,NU2,MUA
      DIMENSION ZXY(104),F(208),Cb(43264),F1(104),F2(104)
 45    FORMAT (2X,16,4E13.4)
 50    FORMAT(E10.3,3F10.4)
 51    FORMAT(2F10.4,5X,I2)
 76    FORMAT(2X,6E13.4)
 87    FORMAT(X,25H SOUND LAYER-THICKNESS = ,F7.4,2X,5H E = ,E9.3,3X,6H N
     3U = ,F7.4)
 88    FORMAT(X,27H CRACKED LAYER-THICKNESS = ,F7.4,2X,5H E = ,E9.3,3X,6H
     3 NU = ,F7.4)
 89    FORMAT(X,28H ADHESIVE - SHEAR MODULUS = ,E10.4,5X,13H THICKNESS =
     3,F7.4)
 100   FORMAT(2X,11E9.3)
 85    FORMAT (X,9H S.I.F. = , E15.7)
 86    FORMAT(2X,5H X = ,8X,5H Y = ,8X,7H TUX = ,6X,7H TUY = ,10X,5H A =
     3,F7.4)
 90    FORMAT(X,33H NO DEBOND IN THE ADHESIVE-DEB = ,F5.3)
 91    FORMAT(X,58H ELLIPTICAL DEBOND IN ADHESIVE-MINOR TO MAJOR AXIS RAT
     3IO= ,F4.1)
```

```
C
C*************************************************************************
C      CRACKED LAYER PARAMETERS
C  E1 = YOUNGS MODULUS OF CRACKED LAYER
C NU1 = POISSONS RATIO OF CRACKED LAYER
C  H1 = THICKNESS OF CRACKED LAYER
       READ (5,50) E1,NU1,H1
C
C*************************************************************************
C      SOUND LAYER PARAMETERS
C  E2 = YOUNGS MODULUS OF SOUND LAYER
C NU2 = POISSONS RATIO OF SOUND LAYER
C  H2 = THICKNESS OF SOUND LAYER
       READ (5,50) E2,NU2,H2
C
C*************************************************************************
C      ADHESIVE PARAMETERS
C  HA = THICKNESS OF ADHESIVE
C MUA = SHEAR MODULUS OF ADHESIVE
C DEB = RATIO OF MINOR TO MAJOR AXIS OF ELLIPTICAL SHAPE OF DEBOND
C DEB = 0., 0.1, 0.2 OR 0.3
       READ (5,50) MUA,HA,DEB
C
C*************************************************************************
C      CRACK LENGTH PARAMETERS
C  A = HALF CRACK LENGTH
C DA = INCREMENT IN HALF CRACK LENGTH
C NAA = NUMBER OF INCREMENTS IN HALF CRACK LENGTH
       READ (5,51) A,DA,NAA
C
       PI=3.141592
       PI2=2.*PI
        PI22=PI/2.
       PK1=(3.-NU1)/(1.+NU1)
       PK2=(3.-NU2)/(1.+NU2)
       PPK1=PI2*(1.+PK1)
       PPK2=PI2*(1.+PK2)
       PKS=PK1*PK1
       PK11=(PK1-1.)/2.
       PK1D=PK1/2.
        G1=E1/(2.*(1.+NU1))
        G2=E2/(2.*(1.+NU2))
        G4=4.*G1
        G12=2.*G1
        G22=2.*G2
        PKZ=PK1-1.
        PKP=PK1+1.
        H2R=H2*PPK2*G22
        HRR=H1*PPK1
        H1R=HRR*G12
        HG=HA/MUA
       PIN=1.-PI/2.
       WRITE (6,88) H1,E1,NU1
       WRITE (6,87) H2,E2,NU2
       WRITE (6,89) MUA,HA
C THE SETTING OF (X,Y) CO-ORDINATES OF TELESCOPIC GRID STARTS.
       NAB=NAA+1
C THE FOLLOWING DO LOOP VARIES THE CRACK LENGTH
```

```
      DO 370 NKJ=1,NAB
      NX1=8
      NX2=2
      NX3=4
      NX4=1
      NX5=2
      NY1=5
      NY2=4
      NY3=6
      NY4=2
      NY5=3
     A2=A*A
      DY1=A/(2*NX1)
      DY2=2.*DY1
      DY3=2.*DY2
      DY4=2.*DY3
      IF (DEB-0.1) 570,571,169
169   IF(DEB-0.2) 170,170,171
170   NR2=NX1-4
     WRITE (6,91) DEB
      NR3=1
      NPS=NX1+1-NR2
      NY1=NY1+NR3
      NXY=NX1*NY1+NPS
      EP=DY1+DY2
      DO 179 IKL=NR2,NX1
      IKP=IKL-3
      EX=(2*IKL-1)*DY1
179   ZXY(IKP)=CMPLX(EX,EP)
      GO TO 183
171   NR2=NX1-1
     WRITE (6,91) DEB
      NR3=NX1-4
      NPS=2*(NX1+1)-NR2-NR3
      NXY=NX1*NY1+NPS
      EP=DY1+DY2
      DO 180 IKL=NR2,NX1
      IKP=IKL-6
      EX=(2*IKL-1)*DY1
180   ZXY(IKP)=CMPLX(EX,EP)
      EP=EP+DY2
      DO 181 IKS=NR3,NX1
      IPP=IKP+IKS-3
      EX=(2*IKS-1)*DY1
181   ZXY(IPP)=CMPLX(EX,EP)
      GO TO 183
570   EP=DY1
      NR1=1
      NR2=1
      NR3=1
     WRITE (6,90) DEB
      GO TO 572
571   EP=DY1
      NR1=NX1-1
      NR2=1
      NR3=1
     WRITE (6,91) DEB
572   NPS=NX1+1-NR1
```

```
      NY1=NY1+NR2+NR3
      NXY=NX1*NY1+NPS
      DO 873 I=NR1,NX1
      EX=(2*I-1)*DY1
  873 ZXY(I+1-NR1)=CMPLX(EX,EP)
  183 DO 573 J=1,NY1
      NP=(J-1)*NX1+NPS
      EY=EP+J*DY2
      DO 573 I=1,NX1
      NQ=NP+I
      EX=(2*I-1)*DY1
      ZXY(NQ)=CMPLX(EX,EY)
  573 CONTINUE
      EP=EX+DY1+DY2
      DO 574 J=1,NY2
      NS=NXY+(J-1)*NX2
      EY=(2*J-1)*DY2
      DO 574 I=1,NX2
      NM=NS+I
      EX=EP+(I-1)*DY3
  574 ZXY(NM)=CMPLX(EX,EY)
      JXY=NXY+NY2*NX2
      IXY=JXY+NY3*NX3
      EP=EY+DY3
      DO 575 J=1,NY3
      EY=EP+(J-1)*DY3
      NP=JXY+(J-1)*NX3
      DO 575 I=1,NX3
      EX=(2*I-1)*DY2
      NQ=NP+I
  575 ZXY(NQ)=CMPLX(EX,EY)
      EP=EX+DY2+DY3
      DO 576 J=1,NY4
      EY=(2*J-1)*DY3
      NP=IXY+(J-1)*NX4
      DO 576 I=1,NX4
      NQ=NP+1
      EX=EP+(I-1)*DY4
  576 ZXY(NQ)=CMPLX(EX,EY)
      KXY=IXY+NX4*NY4
      EP=AIMAG(ZXY(IXY))+DY2+DY3
      KN=KXY+NX5*NY5
      DO 577 J=1,NY5
      EY=EP+(J-1)*DY4
      NP=KXY+(J-1)*NX5
      DO 577 I=1,NX5
      NQ=NP+I
      EX=(2*I-1)*DY3
  577 ZXY(NQ)=CMPLX(EX,EY)
C THE SETTING OF TELESCOPIC GRID ENDS
      NXN2=2*KN
      KNN=NXN2*KN
      KNM=KNN+KN
C     EVALUATION OF KERNELS K11,K12,K21,K22 OF INTEGRAL EQUATIONS 45 OF
C     SECTION 2.2.3 STARTS
C     FOLLOWING LOOP IS OUTER LOOP FOR EVALUATION OF KERNELS VARIES Z
      DO 69 I=1,KN
      IP=I
      IQ=KN+I
      Z=ZXY(I)
      Z2=Z*Z
```

```
      ZB=CONJG(Z)
      ZBZ=ZB*ZB
      ZS=CSQRT(Z2-A2)
       ZBS=CONJG(ZS)
      ZZZ = Z-ZB
      Z21=Z/ZS
       Z4Z=ZB/ZBS
C
C     F(IP) IS RIGHT HAND SIDE OF FIRST OF INTEGRAL EQUATIONS 45 OF
C     SECTION 2.2.3
C     F(IQ) IS RIGHT HAND SIDE OF SECOND OF INTEGRAL EQUATIONS 45 OF
C     SECTION 2.2.3
C
      F(IP)=(-PKZ*REAL(ZXY(I))+PK1*REAL(ZS)-REAL(ZBS)+2.*AIMAG(ZXY(I))*
     3AIMAG(Z4Z))/G4
      F(IQ)=(-PKZ*AIMAG(ZXY(I))+PK1*AIMAG(ZS)-AIMAG(ZBS)-2.*AIMAG(ZXY(I)
     3)*REAL(Z4Z))/G4
      ZI=ZS-Z
       ZIB=CONJG(ZI
      Z1Z=A-Z
      Z2Z=A-ZB
      ZL1=A+Z
      ZL2=A+ZB
      ZJ=Z/ZS-1.
       ZJB=CONJG(ZJ)
       ZIM=-ZS+Z
       ZIBM=CONJG(ZIM)
       ZJM=ZJ
       ZJBM=ZJB
      PHZ1=(A+ZI)/Z1Z
      PHZ2=(A+ZIB)/Z2Z
      PHZ3=(A+ZL1)/ZL1
      PHZ4=(A+ZIBM)/ZL2
      PH1=(PHZ1+ZJ)/Z1Z
      PH2=(PHZ2+ZJB)/Z2Z
      PH3=(PHZ3+ZJM)/ZL1
      PH4=(PHZ4+ZJBM)/ZL2
      ZPL=-PHZ1+PK1*PHZ2+ZZZ*PH1+PHZ3-PK1*PHZ4+ZZZ*PH3
      ZPLB=-ZZZ*PH2-PHZ2+PK1*PHZ1-ZZZ*PH4+PHZ4-PK1*PHZ3
       F1(I)=ZPL+ZPLB
       F2(I)=ZPL-ZPLB
      INNER LOOP FOR EVALUATION OF KERNELS VARIES Z0
       DO 69 I1=1,KN
       NP=(I1-1)*NXNZ+1
       NQ=KN+NP
       NS=KNN+NP
       NM=KNN+NP
       ZZ=ZXY(I1)
       IF (I1-NXY) 669,669,670
  669   DX1=DY2
       GO TO 671
  670  IF (I1-1XY) 672,672,673
  672  DX1=DY3
       GO TO 671
  673  DX1=DY4
       GO TO 671
  671  DYY=DX1
       DXY=DX1*DYY
       IO=I1
       IS=KN+I1
```

```
ZZB = CONJG(ZZ)
ZZ2 = ZZ*ZZ
ZZ2A = ZZ2-A2
ZZS =CSQRT(ZZ2A)
ZZB2 =ZZB*ZZB
ZZ2B =ZZB2-A2
 ZZBS=CONJG(ZZS)
ZPH =Z-ZZ
 ZPHB=CONJG(ZPH)
ZZZZB =ZZ-ZZB
ZZ1 = ZZS-ZZ
 ZZIB=CONJG(ZZI)
 ZZJ=ZZ/ZZS-1.
 ZZJB=CONJG(ZZJ)
ZPHP=Z+ZZ
 ZPHBP=CONJG(ZPHP)
ZPHPB=Z-ZZB
ZPHPP=Z+ZZB
 ZBHP=CONJG(ZPHPB)
 ZBPP=CONJG(ZPHPP)
ZM=Z*ZZ
 ZBM=CONJG(ZM)
ZBBM=Z*ZZB
 ZBMM=CONJG(ZBBM)
TH13=CLOG(ZM-A2+ZZS*ZS)
TH14=CLOG(ZBBM-A2+ZZBS*ZS)
 TH11=CONJG(TH13)
 TH12=CONJG(TH14)
TM12=CLOG(-ZBMM-A2-ZBS*ZZS)
TM13=CLOG(-ZM-A2-ZZS*ZS)
 TM11=CONJG(TM13)
 TM14=CONJG(TM12)
PH3=CLOG(ZPHP)
 PH4=CONJG(PH3)
PHZ1=CLOG(ZPHPB)
 PHZ2=CONJG(PHZ1)
PHZ3=CLOG(ZPHPP)
 PHZ4=CONJG(PHZ3)
ZL1=0.5*(1.-ZS*ZZBS/ZZ2B)*ZZZZB
TH31=-ZL1/ZPHPB
TM31=0.5*(1.+ZS*ZZBS/ZZ2B)*ZZZZB/ZPHPP
 TH33=CONJG(TH31)
 TM33=CONJG(TM31)
TM32= 0.5*(1.+ZBS*ZZBS/ZZ2B)*ZZZZB/ZPHBP
 TM34=CONJG(TM32)
ZL1=0.5*ZZZ
ZZI=ZZS-ZZ
 ZZIB=CONJG(ZZI)
 ZZIM=-ZZS+ZZ
 ZZIBM=CONJG(ZZIM)
TH42=ZL1*(ZIB-ZZIBM)/(ZPHBP*ZBS)
TH43=ZL1*(ZIB-ZZI)/(ZBS*ZBHP)
TH44=ZL1*(ZIB-ZZIM)/(ZBS*ZBPP)
ZL1=ZL1/ZBS
ZZJ=(ZZ/ZZS-1.)
 ZZJB=CONJG(ZZJ)
 ZZJBM=ZZJB
 ZZJM=ZZJ
TH51=(TH43-ZL1*ZZJ)*ZZZZB/ZBHP
TH52=-(TH44-ZL1*ZZJM)*ZZZZB/ZBPP
```

```
      TH54=(TH42-ZL1*ZZJBM)*ZZZZB/ZPHBP
       TH22=CLOG(Z+ZS)
       TH1=CLOG(Z-ZS)
       TH21=PK11*(PK1*TH22-CONJG(TH22)-PK1*TH1+CONJG(TH1))
       IF (I.EQ.I1) GO TO 77
      PH1=CLOG(ZPH)
       PH2=CONJG(PH1)
      TH2=ZPH/ZPHB
      TH32=-0.5*(1.-ZBS*ZZBS/ZZ2B)*ZZZZB/ZPHB
       TH34=CONJG(TH32)
       TH53=-ZZZZB*(TH41-ZL1*ZZJB)/ZPHB
       TH41=ZL1*(ZIB-ZZIB)/ZPHB
      GO TO 78
 77   TH41=0.5*ZZZ*(ZB/ZBS-1.)/ZBS
      TH32=0.5*ZB*ZZZZB/(ZBS*ZZBS)
       TH34=CONJG(TH32)
      TH53=0.25*A2*ZZZZB*ZZZ/((ZB2-A2)*(ZB2-A2))
       DX2=(DX1*DX1)/4.
       DX22=2.*DX2
       DXPI=DX22*PI
       TH2=CMPLX(DXPI,0.)
       TH2=TH2/DXY
       PH1=DX22*(ALOG(DX22)+PI22-3.)
       PH1=PH1/DXY
       PH2=PH1
 78   ZL1=-(PH1+PH2)+PH3+PH4
      ZL2=ZPHPB/ZBHP-ZPHPP/ZBPP
      ZL3=-(PHZ1+PHZ2)+PHZ3+PHZ4
      ZL4=TH2-ZPHP/ZPHBP
      Z1ZB=PK2*ZL1+ZL2
      Z2ZB=PK2*ZL3+ZL4
      Z3ZB=PK1*ZL1+ZL2+PK1D*(TH13+TH11-TM13-TM11)+0.5*(-TH12-PKS*TH14+
     3TM12+PKS*TM14)+TH51-TH52+PK1*(TH34-TM34+TH41-TH42)-TH33+TM33-TH43
     3+TH44+TH21
      Z4ZB=PK1*ZL3+ZL4+TH53-TH54+PK1D*(TH14+TH12-TM14-TM12)+0.5*(-TH11-
     3PKS*TH13+TM11+PKS*TM13)+PK1*(TH31-TM31+TH43-TH44)-TH32+TM32-TH41+
     3 TH42+TH21
      R11=REAL(Z1ZB)+REAL(Z2ZB)
      R12=-AIMAG(Z1ZB)+AIMAG(Z2ZB)
      R21=AIMAG(Z1ZB)+AIMAG(Z2ZB)
      R22=REAL(Z1ZB)-REAL(Z2ZB)
      H11=REAL(Z3ZB)+REAL(Z4ZB)
      H12=-AIMAG(Z3ZB)+AIMAG(Z4ZB)
      H21=AIMAG(Z3ZB)+AIMAG(Z4ZB)
      H22=REAL(Z3ZB)-REAL(Z4ZB)
      S11=(H11/H1R+R11/H2R)*DXY
      S12=(H12/H1R+R12/H2R)*DXY
      S21=(H21/H1R+R21/H2R)*DXY
      S22=(H22/H1R+R22/H2R)*DXY
       IF (I.EQ.I1) GO TO 789
      GO TO 790
 789  S11 = HG + S11
      S22 = HG + S22
 790   CB(NP)=S11
       CB(NQ)=S21
       CB(NS)=S12
       CB(NM)=S22
 69   CONTINUE
C EVALUATION OF KERNELS ENDS
C      SIMQ SOLVES FOR UNKNOWN SHEAR STRESSES TUX AND TUY
```

```
      CALL SIMQ(CB,F,NXN2,KS)
      WRITE (6,86) A
       DO 889 I=1,KN
  889 WRITE (6,76) ZXY(I),F(I),F(KN+I)
      SUM=0.
C     FOLLOWING LOOP COMPUTES STRESS INTENSITY FACTORS FROM EQUATION
C     48 OF SECTION 2.2.3
       DO 269 I=1,KN
       IF (I-NXY) 268,268,271
  268  DX1=DY2
       GO TO 270
  271  IF (I-IXY) 272,272,273
  272  DX1=DY3
       GO TO 270
  273    DX1=DY4
  270   DYY=DX1
       DXY=DX1*DYY
  269  SUM=SUM+(REAL(F1(I))* F(I)-AIMAG(F2(I))* F(KN+I))*DXY
       SUM1=1.-SUM/(A*HRR)
      WRITE (6,85) SUM1
  370  A=A+DA
      STOP
      END
      SUBROUTINE SIMQ(A,B,N,KS)
      DIMENSION A(1),B(1)
      TOL=0.0
      KS=0
      JJ=-N
      DO 65 J=1,N
      JY=J+1
      JJ=JJ+N+1
      BIGA=0
      IT=JJ-J
      DO 30 I=J,N
      IJ=IT+I
      IF(ABS(BIGA)-ABS(A(IJ))) 20,30,30
   20 BIGA=A(IJ)
      IMAX=I
   30 CONTINUE
      IF(ABS(BIGA)-TOL) 35,35,40
   35 KS=1
      RETURN
   40 I1=J+N*(J-2)
      IT=IMAX-J
      DO 50 K=J,N
      I1=I1+N
      I2=I1+IT
      SAVE=A(I1)
      A(I1)=A(I2)
      A(I2)=SAVE
   50 A(I1)=A(I1)/BIGA
      SAVE=B(IMAX)
      B(IMAX)=B(J)
      B(J)=SAVE/BIGA
      IF(J-N) 55,70,55
   55 IQS=N*(J-1)
      DO 65 IX=JY,N
      IXJ=IQS+IX
      IT=J-IX
      DO 60 JX=JY,N
      IXJX=N*(JX-1)+IX
```

```
      JJX=IXJX+IT
60    A(IXJX)=A(IXJX)-(A(IXJ)*A(JJX))
65    B(IX)=B(IX)-(B(J)*A(IXJ))
70    NY=N-1
      IT=N*N
      DO 80 J=1,NY
      IA=IT-J
      IB=N-J
      IC=N
      DO 80 K=1,J
      B(IB)=B(IB)-A(IA)*B(IC)
      IA=IA-N
80    IC=IC-1
      RETURN
      END
```

SAMPLE INPUT

JOB TITLE: SMALL CRACK LENGTHS | ENGINEER | PAGE

NAVA SERIAL NO. | PREF. | NOP JOB NO. | DASH | FOR ORGN. NO. | ANALYST | DATE

```
 1.0.3E+6          .33          .063
 1.0.3E+6          .33          .063
  0.6E+5          .008          0.0
     0.2           0.0           0
```

OUTPUT FOR SAMPLE INPUT

```
CRACKED LAYER-THICKNESS =  0.0630   E = 0.103E+08    NU =  0.3300
SOUND LAYER-THICKNESS =  0.0630   E = 0.103E+08    NU =  0.3300
ADHESIVE - SHEAR MODULUS = 0.6000E+05      THICKNESS =  0.0060
NO DEBOND IN THE ADHESIVE-DEB = 0.0
 X =           Y =           TUX =          TUY =              A =  0.2000
   0.1250E-01    0.1250E-01    0.2273E-02    0.1734E+00
   0.3750E-01    0.1250E-01    0.6618E-02    0.1726E+00
   0.6250E-01    0.1250E-01    0.1064E-01    0.1656E+00
   0.8750E-01    0.1250E-01    0.1218E-01    0.1560E+00
   0.1125E+00    0.1250E-01    0.1153E-01    0.1444E+00
   0.1375E+00    0.1250E-01    0.9669E-02    0.1287E+00
   0.1625E+00    0.1250E-01    0.1032E-01    0.1006E+00
   0.1875E+00    0.1250E-01    0.1267E-01    0.5847E-01
   0.1250E-01    0.3750E-01    0.1601E-02    0.1543E+00
   0.3750E-01    0.3750E-01    0.3303E-02    0.1535E+00
   0.6250E-01    0.3750E-01    0.1445E-01    0.1467E+00
   0.8750E-01    0.3750E-01    0.1913E-01    0.1371E+00
   0.1125E+00    0.3750E-01    0.2196E-01    0.1256E+00
   0.1375E+00    0.3750E-01    0.2441E-01    0.1102E+00
   0.1625E+00    0.3750E-01    0.2764E-01    0.8683E-01
   0.1875E+00    0.3750E-01    0.3096E-01    0.5028E-01
   0.1250E-01    0.6250E-01    0.1326E-02    0.1365E+00
   0.3750E-01    0.6250E-01    0.9595E-02    0.1357E+00
   0.6250E-01    0.6250E-01    0.1763E-01    0.1289E+00
   0.8750E-01    0.6250E-01    0.2358E-01    0.1201E+00
   0.1125E+00    0.6250E-01    0.2859E-01    0.1085E+00
   0.1375E+00    0.6250E-01    0.3254E-01    0.9394E-01
   0.1625E+00    0.6250E-01    0.3617E-01    0.7359E-01
   0.1875E+00    0.6250E-01    0.3785E-01    0.4638E-01
   0.1250E-01    0.8750E-01    0.2677E-03    0.1201E+00
   0.3750E-01    0.8750E-01    0.9809E-02    0.1195E+00
   0.6250E-01    0.8750E-01    0.1921E-01    0.1130E+00
   0.8750E-01    0.8750E-01    0.2568E-01    0.1047E+00
   0.1125E+00    0.8750E-01    0.3188E-01    0.9390E-01
   0.1375E+00    0.8750E-01    0.3621E-01    0.8072E-01
   0.1625E+00    0.8750E-01    0.3903E-01    0.6454E-01
   0.1875E+00    0.8750E-01    0.3842E-01    0.4658E-01
   0.1250E-01    0.1125E+00   -0.4156E-03    0.1052E+00
   0.3750E-01    0.1125E+00    0.9949E-02    0.1047E+00
   0.6250E-01    0.1125E+00    0.2011E-01    0.9844E-01
   0.8750E-01    0.1125E+00    0.2672E-01    0.9123E-01
   0.1125E+00    0.1125E+00    0.3331E-01    0.8107E-01
```

0.1375E+00	0.1125E+00	0.3754E-01	0.6985E-01
0.1625E+00	0.1125E+00	0.3868E-01	0.5696E-01
0.1875E+00	0.1125E+00	0.3924E-01	0.4280E-01
0.1250E-01	0.1375E+00	-0.1564E-02	0.9176E-01
0.3750E-01	0.1375E+00	0.9259E-02	0.9154E-01
0.6250E-01	0.1375E+00	0.1989E-01	0.8587E-01
0.8750E-01	0.1375E+00	0.2678E-01	0.7947E-01
0.1125E+00	0.1375E+00	0.3296E-01	0.7084E-01
0.1375E+00	0.1375E+00	0.3632E-01	0.6105E-01
0.1625E+00	0.1375E+00	0.3843E-01	0.5077E-01
0.1875E+00	0.1375E+00	0.3814E-01	0.4017E-01
0.1250E-01	0.1625E+00	-0.2378E-02	0.7993E-01
0.3750E-01	0.1625E+00	0.8678E-02	0.7989E-01
0.6250E-01	0.1625E+00	0.1769E-01	0.7592E-01
0.8750E-01	0.1625E+00	0.2584E-01	0.6942E-01
0.1125E+00	0.1625E+00	0.3086E-01	0.6216E-01
0.1375E+00	0.1625E+00	0.3446E-01	0.5428E-01
0.1625E+00	0.1625E+00	0.3774E-01	0.4550E-01
0.1875E+00	0.1625E+00	0.3758E-01	0.3717E-01
0.1250E-01	0.1875E+00	-0.3504E-02	0.6942E-01
0.3750E-01	0.1875E+00	0.7601E-02	0.6977E-01
0.6250E-01	0.1875E+00	0.1669E-01	0.6633E-01
0.8750E-01	0.1875E+00	0.2367E-01	0.6115E-01
0.1125E+00	0.1875E+00	0.2837E-01	0.5487E-01
0.1375E+00	0.1875E+00	0.3310E-01	0.4836E-01
0.1625E+00	0.1875E+00	0.3594E-01	0.4080E-01
0.1875E+00	0.1375E+00	0.3740E-01	0.3431E-01
0.2250E+00	0.2500E-01	0.1580E-01	0.4836E-02
0.2750E+00	0.2500E-01	0.1603E-01	-0.6329E-03
0.2250E+00	0.7500E-01	0.3320E-01	0.1022E-01
0.2750E+00	0.7500E-01	0.2576E-01	0.3299E-02
0.2250E+00	0.1250E+00	0.3552E-01	0.2397E-01
0.2750E+00	0.1250E+00	0.3156E-01	0.7547E-02
0.2250E+00	0.1750E+00	0.3663E-01	0.2428E-01
0.2750E+00	0.1750E+00	0.3380E-01	0.1092E-01
0.2500E-01	0.2250E+00	0.5324E-02	0.5734E-01
0.7500E-01	0.2250E+00	0.1783E-01	0.5280E-01
0.1250E+00	0.2250E+00	0.2890E-01	0.4259E-01
0.1750E+00	0.2250E+00	0.3445E-01	0.3255E-01
0.2500E-01	0.2750E+00	0.3357E-02	0.4369E-01
0.7500E-01	0.2750E+00	0.1468E-01	0.4076E-01
0.1250E+00	0.2750E+00	0.2460E-01	0.3405E-01
0.1750E+00	0.2750E+00	0.3191E-01	0.2640E-01
0.2500E-01	0.3250E+00	0.9759E-03	0.3334E-01
0.7500E-01	0.3250E+00	0.1208E-01	0.3206E-01
0.1250E+00	0.3250E+00	0.2200E-01	0.2686E-01
0.1750E+00	0.3250E+00	0.2813E-01	0.2141E-01
0.2500E-01	0.3750E+00	-0.3184E-02	0.2547E-01
0.7500E-01	0.3750E+00	0.7651E-02	0.2562E-01
0.1250E+00	0.3750E+00	0.1764E-01	0.2128E-01
0.1750E+00	0.3750E+00	0.2395E-01	0.1804E-01
0.2500E-01	0.4250E+00	-0.5446E-02	0.1965E-01
0.7500E-01	0.4250E+00	0.5192E-02	0.2039E-01
0.1250E+00	0.4250E+00	0.1533E-01	0.1692E-01
0.1750E+00	0.4250E+00	0.2196E-01	0.1456E-01
0.2500E-01	0.4750E+00	-0.7307E-02	0.1519E-01

```
   0.7500E-01    0.4750E+00    0.3182E-02    0.1642E-01
   0.1250E+00    0.4750E+00    0.1151E-01    0.1489E-01
   0.1750E+00    0.4750E+00    0.1933E-01    0.1244E-01
   0.2500E+00    0.5000E-01    0.2256E-01    0.3609E-02
   0.2500E+00    0.1500E+00    0.3510E-01    0.1338E-01
   0.5000E-01    0.5500E+00    0.1508E-02    0.1193E-01
   0.1500E+00    0.5500E+00    0.1235E-01    0.1020E-01
   0.5000E-01    0.6500E+00   -0.2027E-02    0.8719E-02
   0.1500E+00    0.6500E+00    0.7563E-02    0.8680E-02
   0.5000E-01    0.7500E+00   -0.3972E-02    0.6994E-02
   0.1500E+00    0.7500E+00    0.5735E-02    0.7007E-02
S.I.E. =  0.7016419E+00
```

APPENDIX D

TWO ADHESIVELY BONDED LAYERS WITH A CRACK IN ONE LAYER (LONG CRACK LENGTHS $0.5 \leq A \leq 1.0$ INCH)

INPUT PARAMETERS

The computer programs have the following inputs:

1. modulus, Poisson's ratio, and thickness of cracked layer (E1, NU1, H1)
2. modulus, Poisson's ratio and thickness of the sound layer (E2, NU2, H2)
3. shear modulus and thickness of adhesive layer (MUA, HA)
4. ratio of minor-to-major axis of the elliptical debond (DEB)
5. half-crack length A ($0.6 \leq A \leq 1.0$)
6. number of increments in half-crack length (NAA)
7. increment in half-crack length (DA)

DESCRIPTION OF OUTPUT

The outputs of the programs are shear stresses (τ_x, τ_y) at various locations in the bonded region, and the stress intensity factors ($K/\sigma\sqrt{\pi a}$).

LISTING

```
C*************************************************************************
C
C PROGRAM DEVELOPED BY M.M.RATWANI OF NORTHROP CORPORATION,AIRCRAFT DIVISION
C HAWTHORNE,CALIFORNIA,TELEPHONE (213) 970-5285
C PROGRAM COMPUTES STRESS INTENSITY FACTORS AND SHEAR STRESSES IN TWO
C PLY ADHESIVELY BONDED STRUCTURE WITH A CRACK IN ONE LAYER. THE
C PROGRAM HAS OPTION TO PUT NO DEBOND IN THE ADHESIVE OR ELLIPTICAL
C DEBOND WITH MINOR TO MAJOR AXIS RATIO OF 0.1,0.2 OR 0.3
C THIS PROGRAM GIVES CONVERGING RESULTS FOR HALF-CRACK LENGTHS BETWEEN
C 0.5 AND 1.0 INCHES
C TELESCOPIC GRID IS USED IN THE INTEGRATION OF KERNELS WHICH HAVE
C LOGARITHMIC SINGULARITIES
C THE PROBLEM IS REDUCED TO SOLVING A SET OF INTEGRAL EQUATIONS IN WHICH
```

```
C SHEAR STRESSES TUX AND TUY ARE TAKEN AS UNKNOWNS
C SOLUTION OF UNKNOWN SHEAR STRESSES TUX AND TUY IS ACCOMPLISHED BY
C SOLVING A SET OF SIMULTANEOUS EQUATIONS
C X,Y ARE THE CO-ORDINATES,FROM THE CENTRE-LINE,AT WHICH SHEAR STRESSES
C ARE COMPUTED
C S.I.F IS THE STRESS INTENSITY FACTOR IN THE OUTPUT
C NX1,NX2.....,NY1,NY2.....,ARE THE NUMBER OF COLLOCATION POINTS IN
C THE TELESCOPIC GRID FOR NUMERICAL ANALYSIS
C THE SIZE OF TELESCOPIC GRID DEPENDS ON CRACK LENGTH
C INPUTS ARE - E1,NU1,H1,E2,NU2,H2,MUA,HA,DEB,A,DA,NAA
C
      COMPLEX Z,Z2,ZB,ZB2,ZBS,ZS,ZZZ,ZI,ZIB,ZJB,PHZ1,PHZ2,PHZ3,PH1,PH2,
     3F1,F2,TH21,TH22,ZZ,ZL4,ZZB,ZZ2,ZZ2A,ZZS,ZZB2,ZZ2B,ZZBS,ZPH,ZPHB,
     3ZZZZB,ZZI,ZZIB,ZZJB,ZZJ,TH11,TH12,TH13,TH14,TH31,TH42,Z21,TH1,TH2,
     3TH32,TH41,Z1Z,Z2Z,ZL1,ZL2,Z3ZB,Z4ZB,ZFL,ZPLB,PHZ4
     3,ZXY,Z4Z,Z1ZB,Z2ZB,ZL3
     3,ZJ,ZIM,ZIBM,ZJM,ZJBM,PH3,PH4,ZPHP,ZPHBP,ZM,ZBM,ZBBM,ZBMM,TM11,
     3TM12,TM13,TM14,ZPHPB,ZPHPP,ZBHP,ZBPP,TM31,TM32,TM33,TM34,TH33,
     3TH34,ZZIM,ZZIBM,TH43,TH44,TH51,TH52,TH53,TH54,ZZJBM,ZZJM
      REAL NU1,NU2,MUA
      DIMENSION ZXY(149),F(298),CB(88804),F1(149),F2(149)
 45    FORMAT (2X,I6,4E13.4)
 50   FORMAT(E10.3,3F10.4)
 51   FORMAT(2F10.3,5X,I2)
 76   FORMAT(2X,8E13.4)
 87   FORMAT(X,25H SOUND LAYER-THICKNESS = ,F7.4,2X,5H E = ,E9.3,3X,6H N
     3U = ,F7.4)
 88   FORMAT(X,27H CRACKED LAYER-THICKNESS = ,F7.4,2X,5H E = ,E9.3,3X,6H
     3 NU = ,F7.4)
 89   FORMAT(X,28H ADHESIVE - SHEAR MODULUS = ,E10.4,5X,13H THICKNESS =
     3,F7.4)
 100   FORMAT(2X,11E9.3)
 85    FORMAT (X,9H S.I.F. = , E15.7)
 86   FORMAT(2X,5H X = ,8X,5H Y = ,8X,7H TUX = ,6X,7H TUY = ,10X,5H A =
     3,F7.4)
 90   FORMAT(X,33H NO DEBOND IN THE ADHESIVE-DEB = ,F5.3)
 91   FORMAT(X,58H ELLIPTICAL DEBOND IN ADHESIVE-MINOR TO MAJOR AXIS RAT
     3IO= ,F4.1)
C
C*****************************************************************************
C      CRACKED LAYER PARAMETERS
C E1 = YOUNGS MODULUS OF CRACKED LAYER
C NU1 = POISSONS RATIO OF CRACKED LAYER
C H1 = THICKNESS OF CRACKED LAYER
      READ (5,50) E1,NU1,H1
C
C*****************************************************************************
C      SOUND LAYER PARAMETERS
C E2 = YOUNGS MODULUS OF SOUND LAYER
C NU2 = POISSONS RATIO OF SOUND LAYER
C H2 = THICKNESS OF SOUND LAYER
      READ (5,50) E2,NU2,H2
C
C*****************************************************************************
C      ADHESIVE PARAMETERS
C MUA = SHEAR MODULUS OF ADHESIVE
C HA = THICKNESS OF ADHESIVE
C DEB = RATIO OF MINOR TO MAJOR AXIS OF ELLIPTICAL SHAPE OF DEBOND
C DEB = 0., 0.1, 0.2 OR 0.3
      READ (5,50) MUA,HA,DEB
C
```

```
C**********************************************************************
C      CRACK LENGTH PARAMETERS
C  A = HALF CRACK LENGTH
C NAA = NUMBER OF INCREMENTS IN HALF CRACK LENGTH
C  CA = INCREMENT IN HALF CRACK LENGTH
       READ (5,51) A,DA,NAA
C
       PI=3.141592
       PI2=2.*PI
        PI22=PI/2.
       PK1=(3.-NU1)/(1.+NU1)
       PK2=(3.-NU2)/(1.+NU2)
       PPK1=PI2*(1.+PK1)
       PPK2=PI2*(1.+PK2)
       PKS=PK1*PK1
       PK11=(PK1-1.)/2.
       PK10=PK1/2.
        G1=E1/(2.*(1.+NU1))
        G2=E2/(2.*(1.+NU2))
        G4=4.*G1
        G12=2.*G1
        G22=2.*G2
       PK2=PK1-1.
       PKP=PK1+1.
       H2R=H2*PPK2*G22
       HRR=H1*PPK1
       H1R=HRR*G12
       HG=HA/MUA
      PIN=1.-PI/2.
       WRITE (6,88) H1,E1,NU1
       WRITE (6,87) H2,E2,NU2
       WRITE (6,89) MUA,HA
C THE SETTING OF (X,Y) CO-ORDINATES OF TELESCOPIC GRID STARTS.
       NAB=NAA+1
C THE FOLLOWING DO LOOP VARIES THE CRACK LENGTH
        DO 370 NKJ=1,NAB
        NX1=16
        NY1=1
        NX2=1
        NY2=4
        NX3=8
        NY3=5
        NX4=1
        NY4=2
        NX5=3
        NY5=2
       A2=A*A
        DY1=A/(2*NX1)
        DY2=2.*DY1
        DY3=2.*DY2
        DY4=2.*DY3
        IF (DEB-0.1) 570,571,169
  169   IF(DEB-0.2) 170,170,171
  170   NR2=NX1-1
       WRITE (6,91) DEB
       NR3=NX1-6
       NPS=2*(NX1+1)-NR2-NR3
       NR5=1
       NR4=1
       NY1=NY1+NR4+NR5
```

```
      NXY=NX1*NY1+NPS
      EP=DY1+DY2
      DO 180 IKL=NR2,NX1
      IKP=IKL-14
      EX=(2*IKL-1)*DY1
  180 ZXY(IKP)=CMPLX(EX,EP)
      EP=EP+DY2
      DO 181 IKS=NR3,NX1
      IPP=IKP+IKS-5
      EX=(2*IKS-1)*DY1
  181 ZXY(IPP)=CMPLX(EX,EP)
      GO TO 183
  171 NR3=NX1-2
      WRITE (6,91) DEB
      EP=DY1+DY2+DY2
      NR4=NX1-4
      NR5=NX1-5
      DO 184 IKL=NR3,NX1
      IKP=IKL-13
      EX=(2*IKL-1)*DY1
  184 ZXY(IKP)=CMPLX(EX,EP)
      NPS=3*(NX1+1)-NR3-NR4-NR5
      NXY=NX1*NY1+NPS
      EP=EP+DY2
      DO 185 IKS=NR4,NX1
      IPP=IKP+IKS-11
      EX=(2*IKS-1)*DY1
  185 ZXY(IPP)=CMPLX(EX,EP)
      EP=EP+DY2
      DO 186 IKL=NR5,NX1
      IKP=IPP+IKL-6
      EX=(2*IKL-1)*DY1
  186 ZXY(IKP)=CMPLX(EX,EP)
      GO TO 183
  570  EP=DY1
       NR1=1
       NR2=1
      NR3=1
      NR4=1
      NR5=1
      WRITE (6,90) DEB
       GO TO 572
  571  EP=DY1
       NR1=NX1
       NR2=5
      NR3=1
      NR4=1
      NR5=1
      WRITE (6,91) DEB
  572  NPS=2*(NX1+1)-NR1-NR2
      NY1=NY1+NR3+NR4+NR5
       NXY=NX1*NY1+NPS
       DO 873 I=NR1,NX1
       EX=(2*I-1)*DY1
  873  ZXY(I+1-NR1)=CMPLX(EX,EP)
       EP=EP+DY2
       NR3=NX1+2-NR1-NR2
       DO 674 I=NR2,NX1
       EX=(2*I-1)*DY1
```

```
  674    ZXY(I+NR3)=CMPLX(EX,EP)
  183  DO 573 J=1,NY1
       NP=(J-1)*NX1+NPS
       EY=EP+J*DY2
       DO 573 I=1,NX1
       NQ=NP+I
       EX=(2*I-1)*DY1
       ZXY(NQ)=CMPLX(EX,EY)
  573  CONTINUE
       EP=EX+DY1+DY2
       DO 574 J=1,NY2
       NS=NXY+(J-1)*NX2
       EY=(2*J-1)*DY2
       DO 574 I=1,NX2
       NM=NS+I
       EX=EP+(I-1)*DY3
  574  ZXY(NM)=CMPLX(EX,EY)
       JXY=NXY+NY2*NX2
       IXY=JXY+NY3*NX3
       EP=EY+DY3
       DO 575 J=1,NY3
       EY=EP+(J-1)*DY3
       NP=JXY+(J-1)*NX3
       DO 575 I=1,NX3
       EX=(2*I-1)*DY2
       NQ=NP+I
  575  ZXY(NQ)=CMPLX(EX,EY)
       EP=EX+DY2+DY3
       DO 576 J=1,NY4
       EY=(2*J-1)*DY3
       NP=IXY+(J-1)*NX4
       DO 576 I=1,NX4
       NQ=NP+I
       EX=EP+(I-1)*DY4
  576  ZXY(NQ)=CMPLX(EX,EY)
       KXY=IXY+NX4*NY4
       EP=AIMAG(ZXY(IXY))+DY2+DY3
       KN=KXY+NX5*NY5
       DO 577 J=1,NY5
       EY=EP+(J-1)*DY4
       NP=KXY+(J-1)*NX5
       DO 577 I=1,NX5
       NQ=NP+I
       EX=(2*I-1)*DY3
  577  ZXY(NQ)=CMPLX(EX,EY)
C THE SETTING OF TELESCOPIC GRID ENDS
       NXN2=2*KN
       KNN=NXN2*KN
       KNM=KNN+KN
C      EVALUATION OF KERNELS K11,K12,K21,K22 OF INTEGRAL EQUATIONS 45 OF
C      SECTION 2.2.3 STARTS
C      FOLLOWING LOOP IS OUTER LOOP FOR EVALLATION OF KERNELS VARIES Z
       DO 69 I=1,KN
       IP=I
       IQ=KN+I
       Z=ZXY(I)
       Z2=Z*Z
       ZB=CONJG(Z)
       ZB2=ZB*ZB
       ZS=CSQRT(Z2-A2)
```

```
      ZBS=CONJG(ZS)
      ZZZ = Z-ZB
      Z21=Z/ZS
      Z4Z=ZB/ZBS
C
C     F(IP) IS RIGHT HAND SIDE OF FIRST OF INTEGRAL EQUATIONS 45 OF
C     SECTION 2.2.3
C     F(IQ) IS RIGHT HAND SIDE OF SECOND OF INTEGRAL EQUATIONS 45 OF
C     SECTION 2.2.3
C
      F(IP)=(-PKZ*REAL(ZXY(I))+PK1*REAL(ZS)-REAL(ZBS)+2.*AIMAG(ZXY(I))*
     3AIMAG(Z4Z))/G4
      F(IQ)=(-PKZ*AIMAG(ZXY(I))+PK1*AIMAG(ZS)-AIMAG(ZBS)-2.*AIMAG(ZXY(I)
     3)*REAL(Z4Z))/G4
      ZI=ZS-Z
      ZIB=CONJG(ZI)
      Z1Z=A-Z
      Z2Z=A-ZB
      ZL1=A+Z
      ZL2=A+ZB
      ZJ=Z/ZS-1.
      ZJB=CONJG(ZJ)
      ZIM=-ZS+Z
      ZIBM=CONJG(ZIM)
      ZJM=ZJ
      ZJBM=ZJB
      PHZ1=(A+ZI)/Z1Z
      PHZ2=(A+ZIB)/Z2Z
      PHZ3=(A+ZIM)/ZL1
      PHZ4=(A+ZIBM)/ZL2
      PH1=(PHZ1+ZJ)/Z1Z
      PH2=(PHZ2+ZJB)/Z2Z
      PH3=(PHZ3+ZJM)/ZL1
      PH4=(PHZ4+ZJBM)/ZL2
      ZPL=-PHZ1+PK1*PHZ2+ZZZ*PH1+PHZ3-PK1*PHZ4+ZZZ*PH3
      ZPLB=-ZZZ*PH2-PHZ2+PK1*PHZ1-ZZZ*PH4+PHZ4-PK1*PHZ3
      F1(I)=ZPL+ZPLB
      F2(I)=ZPL-ZPLB
C     INNER LOOP FOR EVALUATION OF KERNELS VARIES ZO
      DO 69 I1=1,KA
      NP=(I1-1)*NXN2+I
      NC=KA+NP
      NS=KAN+NP
      NM=KAM+NP
      ZZ=ZXY(I1)
      IF (I1-NXY) 669,669,670
669   DX1=DY2
      GO TO 671
670   IF (I1-IXY) 672,672,673
672   DX1=DY3
      GO TO 671
673   DX1=DY4
      GO TO 671
671   DYY=DX1
      DXY=DX1*DYY
      ID=I1
      IS=KA+I1
      ZZB = CONJG(ZZ)
      ZZ2 = ZZ*ZZ
      ZZ2A = ZZ2-A2
```

```
      ZZS =CSQRT(ZZ2A)
      ZZB2 =ZZB*ZZB
      ZZ2B =ZZB2-A2
       ZZBS=CONJG(ZZS)
      ZPH =Z-ZZ
       ZPHB=CONJG(ZPH)
      ZZZZB =ZZ-ZZB
      ZZI = ZZS-ZZ
       ZZIB=CONJG(ZZI)
       ZZJ=ZZ/ZZS-1.
       ZZJB=CONJG(ZZJ)
      ZPHP=Z+ZZ
       ZPHBP=CONJG(ZPHP)
      ZPHPB=Z-ZZB
      ZPHPP=Z+ZZB
       ZBHP=CONJG(ZPHPB)
       ZBPP=CONJG(ZPHPP)
      ZM=Z*ZZ
       ZBM=CONJG(ZM)
      ZBBM=Z*ZZB
       ZBMM=CONJG(ZBBM)
      TH13=CLOG(ZM-A2+ZZS*ZS)
      TH14=CLOG(ZBBM-A2+ZZBS*ZS)
       TH11=CONJG(TH13)
       TH12=CONJG(TH14)
      TM12=CLOG(-ZBMM-A2-ZBS*ZZS)
      TM13=CLOG(-ZM-A2-ZZS*ZS)
       TM11=CONJG(TM13)
       TM14=CONJG(TM12)
      PH3=CLOG(ZPHP)
       PH4=CONJG(PH3)
      PHZ1=CLOG(ZPHPB)
       PHZ2=CONJG(PHZ1)
      PHZ3=CLOG(ZPHPP)
       PHZ4=CONJG(PHZ3)
      ZL1=0.5*(1.-ZS*ZZBS/ZZ2B)*ZZZZB
      TH31=-ZL1/ZPHPB
      TM31=0.5*(1.+ZS*ZZBS/ZZ2B)*ZZZZB/ZPHPP
       TH33=CONJG(TH31)
       TM33=CONJG(TM31)
      TM32= 0.5*(1.+ZBS*ZZBS/ZZ2B)*ZZZZB/ZPHBP
       TM34=CONJG(TM32)
      ZL1=0.5*ZZZ
      ZZI=ZZS-ZZ
       ZZIB=CONJG(ZZI)
       ZZIM=-ZZS+ZZ
       ZZIBM=CONJG(ZZIM)
      TH42=ZL1*(ZIB-ZZIBM)/(ZPHBP*ZBS)
      TH43=ZL1*(ZIB-ZZI)/(ZBS*ZBHP)
      TH44=ZL1*(ZIB-ZZIM)/(ZBS*ZBPP)
      ZL1=ZL1/ZBS
      ZZJ=(ZZ/ZZS-1.)
       ZZJB=CONJG(ZZJ)
       ZZJBM=ZZJB
       ZZJM=ZZJ
      TH51=(TH43-ZL1*ZZJ)*ZZZZB/ZBHP
      TH52=-(TH44-ZL1*ZZJM)*ZZZZB/ZBPP
      TH54=(TH42-ZL1*ZZJBM)*ZZZZB/ZPHBP
       TH22=CLOG(Z+ZS)
       TH1=CLOG(Z-ZS)
```

```
      TH21=PK11*(PK1*TH22-CONJG(TH22)-PK1*TH1+CONJG(TH1))
       IF (I.EQ.11) GO TO 77
      PH1=CLOG(ZPH)
       PH2=CONJG(PH1)
      TH2=ZPH/ZPHB
      TH32=-0.5*(1.-ZBS*ZZBS/ZZ2B)*ZZZZB/ZPHB
       TH34=CONJG(TH32)
       TH53=-ZZZZB*(TH41-ZL1*ZZJB)/ZPHB
       TH41=ZL1*(ZIB-ZZIB)/ZPHB
      GO TO 78
 77   TH41=C.5*ZZZ*(ZE/ZBS-1.)/ZBS
      TH32=C.5*ZB*ZZZZB/(ZBS*ZZBS)
       TH34=CONJG(TH32)
      TH53=C.25*A2*ZZZZB*ZZZ/((ZB2-A2)*(ZB2-A2))
       DX2=(DX1*DX1)/4.
       DX22=2.*DX2
       DXPI=DX22*PI
       TH2=CMPLX(DXPI,C.)
       TH2=TH2/DXY
       PH1=DX22*(ALOG(DX22)+PI22-3.)
       PH1=PH1/DXY
       PH2=PH1
 78   ZL1=-(PH1+PH2)+PH3+PH4
      ZL2=ZPHPB/ZBHP-ZPHPP/ZBPP
      ZL3=-(PHZ1+PHZ2)+PHZ3+PHZ4
      ZL4=TH2-ZPHP/ZPHBP
      Z1ZB=PK2*ZL1+ZL2
      Z2ZB=PK2*ZL3+ZL4
      Z3ZB=PK1*ZL1+ZL2+PK1D*(TH13+TH11-TM13-TM11)+0.5*(-TH12-PKS*TH14+
     3TM12+PKS*TM14)+TH51-TH52+PK1*(TH34-TM34+TH41-TH42)-TH33+TM33-TH43
     3+TH44+TH21
      Z4ZB=PK1*ZL3+ZL4+TH53-TH54+PK1D*(TH14+TH12-TM14-TM12)+0.5*(-TH11-
     3PKS*TH13+TM11+PKS*TM13)+PK1*(TH31-TM31+TH43-TH44)-TH32+TM32-TH41+
     3 TH42+TH21
      R11=REAL(Z1ZB)+REAL(Z2ZB)
      R12=-AIMAG(Z1ZB)+AIMAG(Z2ZB)
      R21=AIMAG(Z1ZB)+AIMAG(Z2ZB)
      R22=REAL(Z1ZB)-REAL(Z2ZB)
      H11=REAL(Z3ZB)+REAL(Z4ZB)
      H12=-AIMAG(Z3ZB)+AIMAG(Z4ZB)
      H21=AIMAG(Z3ZB)+AIMAG(Z4ZB)
      H22=REAL(Z3ZB)-REAL(Z4ZB)
      S11=(H11/H1R+R11/H2R)*DXY
      S12=(H12/H1R+R12/H2R)*DXY
      S21=(H21/H1R+R21/H2R)*DXY
      S22=(H22/H1R+R22/H2R)*DXY
       IF (I.EQ.11) GO TO 789
      GO TO 790
 789  S11 = HG + S11
      S22 = HG + S22
 790   CB(NP)=S11
       CB(NQ)=S21
       CB(NS)=S12
       CB(NM)=S22
 69   CONTINUE
C EVALUATION OF KERNELS ENDS
C     SIMQ SOLVES FOR UNKNOWN SHEAR STRESSES TUX AND TUY
      CALL SIMQ(CB,F,NN2,KS)
      WRITE (6,86) A
       DO 889 I=1,KN
```

```
  889  WRITE (6,76) ZXY(I),F(I),F(KN+I)
       SUM=0.
C      FOLLOWING LOOP COMPUTES STRESS INTENSITY FACTORS FROM EQUATION
C      48 OF SECTION 2.2.3
       DO 269 I=1,KN
       IF (I-NXY) 268,268,271
  268  DX1=DY2
       GO TO 270
  271  IF (I-IXY) 272,272,273
  272  DX1=DY3
       GO TO 270
  273    DX1=DY4
  270   DYY=DX1
       DXY=DX1*DYY
  269  SUM=SUM+(REAL(F1(I))* F(I)-AIMAG(F2(I))* F(KN+I))*DXY
       SUM1=1.-SUM/(A*HRR)
       WRITE (6,85) SUM1
  370  A=A+CA
       STOP
       END
       SUBROUTINE SIMQ(A,B,N,KS)
       DIMENSION A(1),B(1)
       TOL=0.0
       KS=0
       JJ=-N
       DO 65 J=1,N
       JY=J+1
       JJ=JJ+N+1
       BIGA=0
       IT=JJ-J
       DO 30 I=J,N
       IJ=IT+I
       IF(ABS(BIGA)-ABS(A(IJ))) 20,30,30
  20   BIGA=A(IJ)
       IMAX=I
  30   CONTINUE
       IF(ABS(BIGA)-TOL) 35,35,40
  35   KS=1
       RETURN
  40   I1=J+N*(J-2)
       IT=IMAX-J
       DO 50 K=J,N
       I1=I1+N
       I2=I1+IT
       SAVE=A(I1)
       A(I1)=A(I2)
       A(I2)=SAVE
  50   A(I1)=A(I1)/BIGA
       SAVE=B(IMAX)
       B(IMAX)=B(J)
       B(J)=SAVE/BIGA
       IF(J-N) 55,70,55
  55   IQS=N*(J-1)
       DO 65 IX=JY,N
       IXJ=IQS+IX
       IT=J-IX
       DO 60 JX=JY,N
       IXJX=N*(JX-1)+IX
```

```
      JJX=IXJX+IT
   60 A(IXJX)=A(IXJX)-(A(IXJ)*A(JJX))
   65 B(IX)=B(IX)-(B(J)*A(IXJ))
   70 NY=N-1
      IT=N*N
      DO 80 J=1,NY
      IA=IT-J
      IB=N-J
      IC=N
      DO 80 K=1,J
      B(IB)=B(IB)-A(IA)*B(IC)
      IA=IA-N
   80 IC=IC-1
      RETURN
      END
```

SAMPLE INPUT

JOB TITLE	ENGINEER	PAGE
LONG CRACK LENGTHS		
OPWA SERIAL NO. / PRE. / NCP JOB NO. / DASH / FOR ORGN. NO.	ANALYST	DATE

10.3E+6	.33	.063
10.3E+6	.33	.063
0.6E+5	.008	0.0
0.6	0.0	0

OUTPUT FOR SAMPLE INPUT

```
CRACKED LAYER-THICKNESS =  0.0630    E = 0.103E+08    NU =  0.3300
SOUND LAYER-THICKNESS =  0.0630    E = 0.103E+08     NU =  0.3300
ADHESIVE - SHEAR MODULUS = 0.6000E+05        THICKNESS =  0.0080
ELLIPTICAL DEBOND IN ADHESIVE-MINOR TO MAJOR AXIS RATIO=  0.1
 X =               Y =               TUX =              TUY =                A =  0.6000
   0.5813E+00    0.1875E-01    0.4488E-01    0.7451E-01
   0.1687E+00    0.5625E-01    0.2974E-01    0.2487E+00
   0.2062E+00    0.5625E-01    0.3737E-01    0.2396E+00
   0.2437E+00    0.5625E-01    0.4735E-01    0.2273E+00
   0.2813E+00    0.5625E-01    0.5018E-01    0.2222E+00
   0.3187E+00    0.5625E-01    0.5460E-01    0.2133E+00
   0.3562E+00    0.5625E-01    0.5920E-01    0.1993E+00
   0.3938E+00    0.5625E-01    0.5972E-01    0.1877E+00
   0.4312E+00    0.5625E-01    0.6161E-01    0.1747E+00
   0.4688E+00    0.5625E-01    0.6298E-01    0.1602E+00
   0.5062E+00    0.5625E-01    0.6410E-01    0.1426E+00
   0.5437E+00    0.5625E-01    0.6756E-01    0.9777E-01
   0.5813E+00    0.5625E-01    0.6619E-01    0.5842E-01
   0.1875E-01    0.9375E-01   -0.3756E-02    0.2070E+00
   0.5625E-01    0.9375E-01    0.7876E-02    0.2188E+00
   0.9375E-01    0.9375E-01    0.1143E-01    0.2219E+00
   0.1312E+00    0.9375E-01    0.1754E-01    0.2215E+00
   0.1687E+00    0.9375E-01    0.2890E-01    0.2159E+00
   0.2062E+00    0.9375E-01    0.3627E-01    0.2073E+00
   0.2437E+00    0.9375E-01    0.4620E-01    0.1954E+00
   0.2813E+00    0.9375E-01    0.4923E-01    0.1905E+00
   0.3187E+00    0.9375E-01    0.5426E-01    0.1820E+00
   0.3562E+00    0.9375E-01    0.5998E-01    0.1682E+00
   0.3938E+00    0.9375E-01    0.6151E-01    0.1600E+00
   0.4312E+00    0.9375E-01    0.6507E-01    0.1452E+00
   0.4688E+00    0.9375E-01    0.6856E-01    0.1312E+00
   0.5062E+00    0.9375E-01    0.7104E-01    0.1155E+00
   0.5437E+00    0.9375E-01    0.7456E-01    0.8859E-01
   0.5813E+00    0.9375E-01    0.7244E-01    0.4694E-01
   0.1875E-01    0.1312E+00   -0.7111E-02    0.1765E+00
   0.5625E-01    0.1312E+00    0.5077E-02    0.1882E+00
   0.9375E-01    0.1312E+00    0.6245E-02    0.1915E+00
   0.1312E+00    0.1312E+00    0.1556E-01    0.1919E+00
   0.1687E+00    0.1312E+00    0.2737E-01    0.1881E+00
   0.2062E+00    0.1312E+00    0.3545E-01    0.1804E+00
   0.2437E+00    0.1312E+00    0.4592E-01    0.1688E+00
   0.2813E+00    0.1312E+00    0.4940E-01    0.1640E+00
   0.3187E+00    0.1312E+00    0.5504E-01    0.1555E+00
   0.3562E+00    0.1312E+00    0.6070E-01    0.1445E+00
```

0.3938E+00	0.1312E+00	0.6359E-01	0.1338E+00
0.4312E+00	0.1312E+00	0.6844E-01	0.1154E+00
0.4688E+00	0.1312E+00	0.7179E-01	0.1071E+00
0.5062E+00	0.1312E+00	0.7474E-01	0.9277E-01
0.5437E+00	0.1312E+00	0.7684E-01	0.7139E-01
0.5813E+00	0.1312E+00	0.7377E-01	0.5199E-01
0.1875E-01	0.1687E+00	0.1014E-01	0.1512E+00
0.5625E-01	0.1687E+00	0.2504E-02	0.1631E+00
0.9375E-01	0.1687E+00	0.4126E-02	0.1666E+00
0.1312E+00	0.1687E+00	0.1229E-01	0.1678E+00
0.1687E+00	0.1687E+00	0.2623E-01	0.1650E+00
0.2062E+00	0.1687E+00	0.2844E-01	0.1641E+00
0.2437E+00	0.1687E+00	0.4501E-01	0.1481E+00
0.2813E+00	0.1687E+00	0.5041E-01	0.1419E+00
0.3187E+00	0.1687E+00	0.5590E-01	0.1357E+00
0.3562E+00	0.1687E+00	0.6007E-01	0.1279E+00
0.3938E+00	0.1687E+00	0.6674E-01	0.1119E+00
0.4312E+00	0.1687E+00	0.7078E-01	0.1012E+00
0.4688E+00	0.1687E+00	0.7364E-01	0.9040E-01
0.5062E+00	0.1687E+00	0.7482E-01	0.7656E-01
0.5437E+00	0.1687E+00	0.7558E-01	0.6219E-01
0.5813E+00	0.1687E+00	0.7411E-01	0.4364E-01
0.1875E-01	0.2062E+00	0.1286E-01	0.1304E+00
0.5625E-01	0.2062E+00	0.1001E-03	0.1426E+00
0.9375E-01	0.2062E+00	0.2163E-02	0.1465E+00
0.1312E+00	0.2062E+00	0.1090E-01	0.1482E+00
0.1687E+00	0.2062E+00	0.2161E-01	0.1468E+00
0.2062E+00	0.2062E+00	0.2859E-01	0.1454E+00
0.2437E+00	0.2062E+00	0.4613E-01	0.1297E+00
0.2813E+00	0.2062E+00	0.4905E-01	0.1272E+00
0.3187E+00	0.2062E+00	0.5705E-01	0.1194E+00
0.3562E+00	0.2062E+00	0.6219E-01	0.1096E+00
0.3938E+00	0.2062E+00	0.6869E-01	0.9951E-01
0.4312E+00	0.2062E+00	0.7453E-01	0.8386E-01
0.4688E+00	0.2062E+00	0.7536E-01	0.7509E-01
0.5062E+00	0.2062E+00	0.7659E-01	0.6356E-01
0.5437E+00	0.2062E+00	0.7589E-01	0.5317E-01
0.5813E+00	0.2062E+00	0.7280E-01	0.4126E-01
0.6375E+00	0.3750E-01	0.4003E-01	0.2722E-02
0.6375E+00	0.1125E+00	0.6173E-01	0.1263E-01
0.6375E+00	0.1875E+00	0.6603E-01	0.8376E-02
0.6375E+00	0.2625E+00	0.7303E-01	0.1988E-01
0.3750E-01	0.3375E+00	0.7403E-02	0.8058E-01
0.1125E+00	0.3375E+00	0.7224E-02	0.9115E-01
0.1875E+00	0.3375E+00	0.2036E-01	0.9159E-01
0.2625E+00	0.3375E+00	0.4237E-01	0.7724E-01
0.3375E+00	0.3375E+00	0.5583E-01	0.6780E-01
0.4125E+00	0.3375E+00	0.6256E-01	0.5744E-01
0.4875E+00	0.3375E+00	0.7197E-01	0.3828E-01
0.5625E+00	0.3375E+00	0.7720E-01	0.2624E-01
0.3750E-01	0.4125E+00	0.1251E-01	0.5667E-01
0.1125E+00	0.4125E+00	0.9130E-04	0.6769E-01
0.1875E+00	0.4125E+00	0.1406E-01	0.6912E-01
0.2625E+00	0.4125E+00	0.3339E-01	0.6260E-01
0.3375E+00	0.4125E+00	0.4355E-01	0.5130E-01
0.4125E+00	0.4125E+00	0.5606E-01	0.4238E-01
0.4875E+00	0.4125E+00	0.6367E-01	0.2807E-01
0.5625E+00	0.4125E+00	0.7223E-01	0.1732E-01
0.3750E-01	0.4875E+00	0.1665E-01	0.3997E-01

```
  0.1125E+00   0.4875E+00  -0.8542E-02   0.5148E-01
  0.1875E+00   0.4875E+00   0.1186E-01   0.5299E-01
  0.2625E+00   0.4875E+00   0.2119E-01   0.5351E-01
  0.3375E+00   0.4875E+00   0.4061E-01   0.3889E-01
  0.4125E+00   0.4875E+00   0.4806E-01   0.3356E-01
  0.4875E+00   0.4875E+00   0.5931E-01   0.2081E-01
  0.5625E+00   0.4875E+00   0.6873E-01   0.1255E-01
  0.3750E-01   0.5625E+00  -0.2008E-01   0.2805E-01
  0.1125E+00   0.5625E+00  -0.1071E-01   0.3985E-01
  0.1875E+00   0.5625E+00   0.5964E-02   0.4328E-01
  0.2625E+00   0.5625E+00   0.1806E-01   0.4305E-01
  0.3375E+00   0.5625E+00   0.3592E-01   0.3017E-01
  0.4125E+00   0.5625E+00   0.4629E-01   0.2700E-01
  0.4875E+00   0.5625E+00   0.5551E-01   0.1960E-01
  0.5625E+00   0.5625E+00   0.6673E-01   0.9615E-02
  0.3750E-01   0.6375E+00  -0.2306E-01   0.1955E-01
  0.1125E+00   0.6375E+00  -0.1254E-01   0.3169E-01
  0.1875E+00   0.6375E+00   0.1166E-02   0.3571E-01
  0.2625E+00   0.6375E+00   0.1929E-01   0.3535E-01
  0.3375E+00   0.6375E+00   0.2939E-01   0.3183E-01
  0.4125E+00   0.6375E+00   0.4157E-01   0.2483E-01
  0.4875E+00   0.6375E+00   0.5376E-01   0.1820E-01
  0.5625E+00   0.6375E+00   0.6550E-01   0.9243E-02
  0.6750E+00   0.7500E-01   0.4657E-01  -0.6000E-02
  0.6750E+00   0.2250E+00   0.6529E-01   0.7101E-03
  0.7500E-01   0.7500E+00  -0.1413E-01   0.2330E-01
  0.2250E+00   0.7500E+00   0.8552E-02   0.2977E-01
  0.3750E+00   0.7500E+00   0.3526E-01   0.2177E-01
  0.7500E-01   0.9000E+00  -0.1758E-01   0.1740E-01
  0.2250E+00   0.9000E+00  -0.5133E-03   0.2915E-01
  0.3750E+00   0.9000E+00   0.3065E-01   0.2509E-01
S.I.F. =  0.4773804E+00
```


☆U.S.Government Printing Office: 1977 — 757-001/120